Hydrological and hydrochemical controls on mobility of natural organic matter, iron and arsenic

A thesis submitted to The University of Manchester for the degree of Doctor of Philosophy (PhD) in the Faculty of Science and Engineering

2021

Tianming Wang

School of Natural Sciences

List of Contents

Chapter 1. Introduction 21

1.1 Iron 24

1.2 Natural Organic matter 27

1.2.1 Climate change and changing NOM 35

1.3 Interaction of Fe and NOM 37

1.4 Arsenic 39

1.5 Aim 42

Chapter 2. Methodologies 45

General reasons for methods 45

Study area 45

Flux calculation 49

Discharge measurement 50

Stage measurement 50

Stage-discharge relationship 51

Sample collection 55

Sample analysis 57

Filtration 58

[NOM] measurement 62

[Fe] and [As] measurements 63

Continuous [NOM] and [As] measurements 64

Pyrolysis gas chromatography mass spectroscopy (Py GC/MS) 66

Chapter 3. Quantity of OC flux from an upland peat catchment 68

3.1 Introduction 68

3.2 Materials and methods 77

Sampling and sample analysis 77

Continuous [OC] measurement and calculation of OC flux 78

3.3 Results and Discussion 80

Quantification of OC flux by using interpolation 80

Comparison of fluxes by interpolation and rating relationships 85

Comparison of OC flux with previous estimation 87

Relationship between [OC] and Q 88

Mobilisation of OC within a discharge event 91

3.4 Conclusions 96

Chapter 4. Effect of NOM on speciation and size of Fe change with flow path, pH, temperature and daylight in natural waters 99

4.1 Introduction 99

Fe in natural waters 99

Fe NOM interaction 100

Importance of anoxic interaction of Fe and NOM 101

Limitations of previous work on anoxic binding of FeII. 102

Daylight exposure and temperature 103

Selection of NOM 104

Aim and objectives 106

4.2 Materials and methods 107

Collection of NOM 107

Size separation of NOM 107

Selection of appropriate size class of NOM 109

Chemical characterisation of selected NOM 111

Preparation of FeII stock solution 113

Fe speciation, total Fe and total OC 113

Type A interaction 116

Type B interaction 117

Conditions under which Type A and Type B were compared 118

4.3 Results and Discussion 119

Fe speciation in the absence of NOM 119

Anoxic interaction of FeII and NOM 119

Anoxic binding of Fe to NOM 119

Anoxic coagulation of NOM by Fe 121

The effect of mixing order 124

Effects of increased pH 127

Effects of temperature 128

Effects of darkness 131

4.4 Conclusions 133

Chapter 5. Controls on the mobility of As in natural waters: The role of NOM, Fe and changing hydrological conditions 137

5.1 Introduction 137
5.2 Materials and methods 148
Sampling and sample analysis 148
Continuous [As] Measurement and calculation of As flux 149
5.3 Results and Discussion 150
As concentrations of stream waters 150
Quantification of As flux by using interpolation 156
Comparison of fluxes by interpolation and rating relationships 158
Relationship between [As] and Q, [Fe] or [NOM] 159
Mobilisation of As within a discharge event 164
Changes in PSD of As, Fe and NOM 172
5.4 Conclusions 175
Chapter 6. Conclusions 177
6.1 Quantity of OC flux from an upland peat catchment 177
6.2 Effect of NOM on speciation and size of Fe change with flow path, pH, temperature and daylight in natural waters 178
6.3 Controls on the mobility of As in natural water: The role of NOM, Fe and changing hydrological conditions 179
Reference 182

List of Figures

Figure 1 Fe-Fe cycle from minerals to aquatic environment and back. ... 26

Figure 2 The interaction of NOM and Fe in natural water. Part of Fe(II) reacted with NOM is retained after entering the oxic environment (Jackson et al., 2012). 37

Figure 3 The occurrence and mobilisation path of As during As cycle in environment (Wang and Mulligan, 2006). 42

Figure 4 Relative location of the study site (Parra, 2019). 46

Figure 5 Location of Crowden Great Brook in UK and location of sampling sites in eroded and uneroded sub-catchments at the Crowden Great Brook. Figure adapted from Do (2013), Hegan (2012), Parra (2019) and Todman (2005). It reproduced from Ordnance Survey map date by permission of Ordnance Map, ©Crown copyright. 48

Figure 6 A dilution gauging curve on 16/10/2019. 53

Figure 7 The relationship between stage and Q for (A) uneroded sub-catchment (site 30) and (B) eroded sub-catchment (site 50). 54

Figure 8 Flow duration curve under 3 years (2017-2019) for uneroded sub-catchment (U) and eroded sub-catchment (E). 55

Figure 9 Sigma SD900 auto sampler with collected samples. 57

Figure 10 The mechanism and process of TFU (Schwartz and Seeley, 2002). 59

Figure 11 Mass balance of NOM (OC) during TFU process, TFU is

completed when mass of retentate and filtrate is constant. 61
Figure 12 The occurrence and pathways of direct carbon flux and indirect carbon flux from upland peat catchment (Do, 2013; Tranvik et al., 2009). 72
Figure 13 OC sampling and discharge (Q) monitoring for A) site 30 and B) site 50 during study period. 83
Figure 14 Estimation of OC flux at site 30 (A) and site 50 (B) by interpolation for each daily sampling period. 85
Figure 15 Relationship between [OC] and Q for A) UF and B) <0.2 µm at site 30. Each point represents a Q and [OC] measurement caught at the same time. 89
Figure 16 Relationship between [OC] and Q for A) UF and B) <0.2 µm at site 50. Each point represents a Q and [OC] measurement caught at the same time. 89
Figure 17 Relationship between Log ([OC]) and Log (Q) for A) UF and B) <0.2 µm at site 30. 91
Figure 18 Relationship between Log ([OC]) and Log (Q) for A) UF and B) <0.2 µm at site 50. 91
Figure 19 DOC concentration and discharge (Q) for A) site 30 and B) site 50 during discharge event. 95
Figure 20 Relationship between [OC] and Q and the high-resolution time series of [OC] v Q during discharge event for A) site 30 and B) site 50.

The time series direction is shown by arrows. 96
Figure 21 Schematic of A) typical simulation conditions under which transformations of FeII to FeIII(hydr)oxides are studied; coincident mixing [(FeII+NOM+D.O.)] and B) conditions which simulate more generally applicable conditions; sequential mixing [(FeII+NOM) + D.O.]. 102
Figure 22 Proportions of total mass of OC within particular size classes in runoff from Crowden Great Brook. Calculated from measurements of concentration and discharge made over 3 years. 110
Figure 23 Relative abundance of compounds in terms of degree of oxidation in different size classes of NOM collected from Crowden Great Brook (only size classes in which enough solid could be isolated were analysed). 112
Figure 24 Base addition on oxidation of FeII in DIW in order to maintain pH 6.5, 0.0366 mmol of base for 0.012 mmol of FeII. 115
Figure 25 Fe speciation over time under 25 degrees, full daylight and anoxic conditions. (A) Fe:NOM ratio is 1:5 at pH 7.5; (B) Fe:NOM ratio is 1:10 at pH 7.5 and PSD of Fe and NOM at the end point are shown beside; (C) Fe:NOM ratio is 1:10 at pH 6.5 and PSD of Fe and NOM at the end point are shown beside; (D) Fe:NOM ratio is 1:15 at pH 7.5; (E) Fe:NOM ratio is 1:30 at pH 7.5. 122
Figure 26 Fe speciation over time under 25 degrees, pH 6.5 and full

daylight conditions. PSD of Fe and NOM at the end point are shown beside. (A) Anoxic control and (B) Oxic control; (C) Type B and full Fe speciation at the end point are shown beside; (D) Type A and full Fe speciation at the end point are shown beside. 126

Figure 27 Fe speciation over time under 25 degrees, pH 7.5 and full daylight conditions. PSD of Fe and NOM at the end point are shown beside. (A) Anoxic control and (B) Oxic control; (C) Type B and (D) Type A simulation. 128

Figure 28 Fe speciation over time under 10 degrees, pH 6.5 and full daylight conditions. PSD of Fe and NOM at the end point are shown beside. (A) Anoxic control and (B) Oxic control; (C) Type B and full Fe speciation at the end point are shown beside; (D) Type A and full Fe speciation at the end point are shown beside. 130

Figure 29 Fe speciation over time under 25 degrees, pH 6.5 and dark conditions. PSD of Fe and NOM at the end point are shown beside. (A) Anoxic control and (B) Oxic control; (C) Type B and full Fe speciation at the end point are shown beside; (D) Type A and full Fe speciation at the end point are shown besides. 133

Figure 30 The occurrence and mobilisation path of As during As cycle in environment (Wang and Mulligan, 2006). 139

Figure 31 Dissolved NOM, As, Fe concentrations and discharge (Q) for A) site 30 and B) site 50 during study period. 155

Figure 32 Estimation of As flux by interpolation for each daily sampling period. 157

Figure 33 Relationship between [As] and Q for A) site 30 and B) site 50. 160

Figure 34 Relationship between Log ([As]) and Log (Q) for A) site 30 and B) site 50. 161

Figure 35 Relationship between [As] and [Fe] for A) site 30 and B) site 50. 163

Figure 36 Relationship between [As] and [NOM] for A) site 30 and B) site 50. 163

Figure 37 Dissolved NOM (C and D), As, Fe (E and F) concentrations and discharge (Q) (A and B) for site 30 and site 50 during discharge event. 168

Figure 38 Relationship between [As] and [Fe] for A) site 30 and B) site 50 during discharge event. 169

Figure 39 Relationship between [As] and [NOM] for A) site 30 and B) site 50 during discharge event. 170

Figure 40 Relationship between Log ([As]) and Log (Q) for A) site 30 and B) site 50 during discharge event. The trajectory of site 30 is clockwise. 171

Figure 41High-resolution time series of [As] v Q during discharge event for A) site 30 and B) site 50. The time series direction is shown by arrows.

..... 171

Figure 42 PSD of As, Fe and NOM for each site. 174

List of Tables

Table 1 Some of the acronyms used in NOM-related studies and their meaning in relation NOM origin (References are given only to illustrate the use of the term. They are not necessarily the oldest nor the most representative). 28

Table 2 Estimation of OC flux in different forms by interpolation for each site. 82

Table 3 Estimation of OC flux in different forms by rating relationship for each site and compare with the values estimated through the interpolation *(Italic values in brackets).* 87

Table 4 Listing of variables and their ranges across which anoxic mixing (Exp. 1) and Type A and Type B mixing of Fe, NOM and D.O. were simulated. Cells in bold highlight the parameters being compared. 118

Table 5 Speciation and size of FeII and NOM in mass and % of total in an anoxic suspension of 1.7 mg/L Fe and 17 mg/L OC. 123

Table 6 Summary of As, Fe, NOM concentrations and discharge over study sites. 153

Table 7 Estimation of As flux by interpolation for each site. 157

Table 8 Comparison of As Flux (kg/year/km^2) between interpolation and rating relationship for each study site. 159

Table 9 Correlation coefficients of Fe and NOM with As for each size within both sites. 173

Abstract

The University of Manchester

Tianming Wang

PhD

Hydrological and hydrochemical controls on mobility of natural organic matter, iron and arsenic

2021

This project reviewed several recent studies conducted by the author that investigated the important role of hydrological and hydrochemical conditions in natural water in the mobility and fate of natural organic matter (NOM), iron (Fe) and arsenic (As). NOM is a critical component in aquatic water as it has a strong control on water chemistry and close association with global carbon (C) cycle, mobility of nutrients (Fe)/pollutants (As) and water treatment. Thus, this study aimed to investigate NOM in quantity and quality from peatland runoff and explore how it was changed. Organic carbon (OC) fluxes were monitored under baseflow and stormflow in uneroded and eroded sites during study period. The data showed that OC flux was higher in the eroded site compared to the uneroded site. NOM export from peatland was increased at a great rate under stormflow with higher discharge (Q) in the eroded site. These demonstrated that the loss and mobility of NOM in peatland is expected to be aggravated by changed rainfall patterns and erosion. Considering that increased aquatic NOM flux is the dominant driver of global warming through greenhouse gas emissions (CO_2), therefore, this study suggests that increased NOM release have exacerbated the release of CO_2 to the environment posing continuous degradation of global warming. In order to reduce the loss of NOM and mitigate its negative impact on global C cycle, a series of management practices should be considered.

Fe is found naturally in aquatic environments in diverse forms and is an essential nutrient. The mobility and speciation of Fe relies on oxygen (D.O.) and NOM. This project simulated the interaction between Fe and NOM under

different conditions in natural water (such as NOM content, pH, light, temperature and mixing order of Fe, NOM and D.O.) to understand the controls on Fe mobility in natural water. The results of this study showed that NOM mainly affects the mobility of Fe by controlling size and oxidation state of Fe. The mobility of Fe cannot be assumed to be that of a free aqueous ion due to the generation of Fe particulates with multiple speciation (FeII or FeIII bound to NOM or FeIII(hydr)oxide) by association with NOM. The mobility of particulate Fe will be reduced and the extent of which is controlled by the simulation conditions. The association of Fe with NOM is not low, which affects Fe lability, specific surface area, speciation and therefore its evolution, having important implications in nutrient availability.

Both NOM and Fe can play an important role in the mobility and fate of As in upland peat catchment, but there is a lack of data on the reliable quantitative As mobilisation and how As mobilisation affected by NOM or Fe. Considering that As is a toxic element, elevated levels of As in water will have a serious negative impact on human health and environment. Therefore, this project investigated the release and mobility of As in upland peat catchments. The results of this study preliminarily determined the release mechanism of As. Detailed stream water sampling indicated that the As release and mobility from peat soil into stream is strongly correlated to NOM and/or Fe. Fe and NOM mainly affect the transport of As in particulate form and dissolved form respectively. In the eroded site, stormflow with high Q was more likely to cause the export of NOM and Fe in peat soil, which indirectly leads to an increase in As concentration in stream. However, the concentration of As was reduced in the uneroded stie, because its dominant factor, Fe, is diluted by the influence of high Q. Understanding release factors of As provides useful conditions for As monitoring and control in upland peat catchment and therefore it is benefit for managing and predicting As.

Declaration

No portion of this work referred to in the thesis has been submitted in support of an application for another degree or qualification, of this, or any other university or other institute of learning.

Copyright Statement

i. The author of this thesis (including any appendices and/or schedules to this thesis) owns certain copyright or related rights in it (the “Copyright”) and s/he has given The University of Manchester certain rights to use such Copyright, including for administrative purposes.

ii. Copies of this thesis, either in full or in extracts and whether in hard or electronic copy, may be made only in accordance with the Copyright, Designs and Patents Act 1988 (as amended) and regulations issued under it or, where appropriate, in accordance with licensing agreements which the University has from time to time. This page must form part of any such copies made.

iii. The ownership of certain Copyright, patents, designs, trademarks and other intellectual property (the “Intellectual Property”) and any reproductions of copyright works in the thesis, for example graphs and tables (“Reproductions”), which may be described in this thesis, may not be owned by the author and may be owned by third parties. Such Intellectual Property and Reproductions cannot and must not be made available for use without the prior written permission of the owner(s) of the relevant Intellectual Property and/or Reproductions.

iv. Further information on the conditions under which disclosure,

publication and commercialisation of this thesis, the Copyright and any Intellectual Property and/or Reproductions described in it may take place is available in the University IP Policy (see http://documents.manchester.ac.uk/display.aspx?DocID=24420), in any relevant Thesis restriction declarations deposited in the University Library, The University Library's regulations (see http://www.manchester.ac.uk/library/aboutus/regulations) and in The University's policy on presentation of Theses.

Acknowledgment

First and foremost, I would like to thank Dr. Stephen Boult. With his guidance and support, I conducted a series of research for this project. Without his assistance, I am not able to finish my work. Also, I would like to thank Dr. Bart van Dongen for his assistance, motivation and humour throughout this time.

I would like to thank as well Abby Ragazzon-Smith, Rosie Byrne, Ilya Strashnov, Paul Lythgoe and Alastair Bewsher as well as to the other staff in the Departure of Earth, Atmospheric and Environmental Sciences for their practical help and advice in the laboratory.

Thanks also go to my colleague Wei Li who is closely associated with me at work and life. The finished project successfully is inseparable from the tacit cooperation between each other. Without her help this will not be possible. Meanwhile, I also thank my other colleagues, KaKi Wong and Felipe Rojas Parra for their suggestion and assistance.

Finally, I would like to thank my parents and my wife for their financial and morale support during the PhD period. These are important prerequisites for my successful completion of the work.

Abbreviations

DBPs	Disinfection by-products
DIW	Deionised water
D.O.	Dissolved oxygen
DOC	Dissolved organic carbon
EC	Electrical conductivity
Eh	Redox potential
FA	Fulvic acid
GHG	Greenhouse gases
HA	Humic acid
ICP-AES	Inductively coupled plasma-atomic emission spectrometry
ICP-MS	Inductively coupled plasma mass spectrometry
IR	Infrared spectroscopy
MS	Mass spectrometry
MW	Molecular weight
NOM	Natural organic carbon
OC	Organic carbon
POC	Particulate organic carbon
ppb	Parts per billion
ppm	Parts per million
ppt	Parts per trillion
PSD	Particle size distribution
Py GC/MS	Pyrolysis gas chromatography mass spectroscopy
SSA	Specific surface area
TC	Total carbon

TFU	Tangential flow ultrafiltration
TIC	Total inorganic carbon
TOC	Total organic carbon
UV-Vis	Ultraviolet-visible spectroscopy
WHO	World Health Organization

Chapter 1. Introduction

Undoubtedly, water resource plays an important role in our lives. For sustaining human life, water is one of the basic necessities and life is not possible without water (Fu et al., 2014; Science.uwaterloo.ca, 2017). As a normal and basic human right, access to high quality of water resources and good water environment is essential to human health. Meanwhile, it can be a component of policy to project human lives and activities efficiently (World Health Organization, 2011). However, water pollution, which is the most significant water issue, causes growing lack of fresh and clean water resources (Pimentel et al., 2004). Besides, it is becoming globally worse and currently it is at dangerous levels. According to the data of World Health Organization (WHO), large number of population (more than 2 billion) cannot receive fresh and clean water resources (Fu et al., 2014; Simonvic, 2002).

With the growth of the human population globally, human activities have increasingly led to environmental degradation and associated pollution (Owa, 2013). Agricultural manufacturing, mining, waste disposal and other human activities (industrialization and urbanization) can release metals to water environment, leading to a rise in toxic levels of metals in water. This aggravates natural water pollution and seriously impacts on water quality. Because heavy metals are difficult to be degraded or destroyed, once water resources are contaminated by heavy metals, they are very hard to be

remediated and treated (Choudhary et al., 2007; Gallego et al.,1996). In addition to heavy metals, organic pollutants, acidic atmospheric deposition and runoff, nutrients (mainly nitrogen and phosphorus) suspended sediments and so on will also have a negative impact on water environment. As a consequence, in order to avoid this serious threat to humanity and also achieve fresh and clean water resources, some necessary measures, which are used for controlling and improving water pollution including water remediation and treatment, should be taken.

Sorption can adjust the concentration of pollutants (organic pollutants, trace metals, etc.) in natural water by various ways, such as controlling the degradation, distribution or migration of pollutions (Davis,1984). Generally, pollutants in water can be controlled or reduced by other present substances such as iron (Fe), organic matter, organic metal complexes, etc. (Vosyliene and Mikalajune, 2006). As one of the most reactive elements in natural water, Iron (Fe) can be used in controlling behaviour of pollutants/nutrients, especially in the form of Fe oxides and hydroxide. Fe oxides and hydroxide can efficiently control the solubility and mobility of toxic metals by sorption (Gaffney et al., 2008; Lee et al.,2003; Viollier et al., 2000). In addition, an *in situ* formed suspended Fe colloid is produced during oxidation of Fe(II) and it can be considered as mobile potentially and move with water flow (Wolthoorn, 2004). After forming the colloidal fraction, their reactivity, their high specific

surface area (SSA) and ubiquity at the Earth's surface enable colloidal Fe oxides or Fe colloids to have abilities of absorption and high mobility. Thus, this means that Fe will be able to limit the behaviour of contaminants in water (Accardi-Dey and Gschwend, 2002). Besides, as one of the important components in aquatic system, Natural Organic Matter (NOM) can also control the behaviour of pollutants (containing apparent solubility, mobility, adsorption-desorption equilibrium, hydrolysis, photogradation and so on) in natural water through sorption, especially for organic pollutants and heavy metals (Ling et al., 2004). The type (specific chemical composition or physical size) of NOM can decide its specific property (capacity and strength of sorption). Many reports indicated that size and chemical characteristics of NOM are two major factors to affect its role of sorption. Secondly, due to its polydisperse nature, the sorption capacity of NOM will also change according to the different fraction or amount of NOM in water. Meanwhile, the parameters of water quality such as pH and ionic strength will influence NOM sorption by changing and adjusting the charge and configuration of NOM (Hyung and Kim, 2008). NOM can not only impact on the behaviour of Fe, but also produce complexes by the interaction and combination with Fe (Matilainen et al., 2010; Theis and Singer, 1974). These complexes can be a useful material to play a role in controlling heavy metal pollution.

1.1 Iron

Iron (Fe) is ubiquitous. As one of the most common metallic elements on the earth, Fe exists in natural water, soil, rocks, minerals and so on. Many studies have shown that Fe is abundant in natural water (Vuori, 1995; Tufekci et al., 2003). When groundwater comes in contact with the underlying Fe-rich soils, rocks and minerals in the aquifer, Fe will be dissolved and released to water. Also, both weathering of those solid materials and erosion cause Fe into water environment (Wolthoorn et al., 2004; World Health Organization, 2011; Oregon.gov, 2017).

Fe(II) and Fe(III) are two main oxidation states of Fe in water and they are thermodynamically stable under their respective conditions (Viollier, E et al., 2000). Generally, Fe is mainly dissolved in the form of Fe(II) when the dissolved oxygen (D.O.) content is insufficient and it will particulate in oxic condition as suspended insoluble FeIII(hydr)oxides which may coagulate and be deposited. Deep aquifers in groundwater have low dissolved oxygen content, especially if organic matters exist in aquifer. The organic matter will exhaust most of oxygen in water during its decomposition. Therefore, Fe will dissolve in the form of Fe(II) after entering the groundwater (Wolthoorn et al., 2004; World Health Organization, 2011; Oregon.gov, 2017).

Unlike groundwater, surface water usually has a higher D.O. content, so when

Fe enter surface water from groundwater, D.O. will oxidize Fe from Fe(II) to Fe(III) with consequent rise in precipitation of Fe(III) and decrease in concentration of dissolved Fe(II), and then insoluble oxides and hydroxides of Fe(III) will be generated by hydrolysis of Fe(III) (Baalousha, et al., 2006; Deng, 1997; Vignati, 2003; Weber et al., 2006; Wolthoorn et al., 2004). It is precisely because of the combination of Fe(II) and D.O. that it is easy to form the two most common elements--Fe oxides and hydroxides in surface water (World Health Organization, 2011). This results in the constant changes of Fe speciation which in turn effects the mobility of Fe and other elements such as heavy metals, sulphur, carbon and hydrogen. A large number of the colloidal Fe oxyhydroxides are formed because of the oxidation of Fe(II) to Fe(III) and therefore their coagulation results in the formation of particulate Fe. By coagulation and flocculation of particulate Fe, their size and mass are increased, which cause sedimentation by gravity. As a result, after Fe precipitates and then accumulates in the subsurface, it combines with subsurface soils, rocks or minerals again and then is re-mineralized (Croot and Heller, 2012; Wolthoorn et al., 2004). Figure 1 shows the whole process of Fe-Fe cycle from minerals to aquatic environment and then back to minerals.

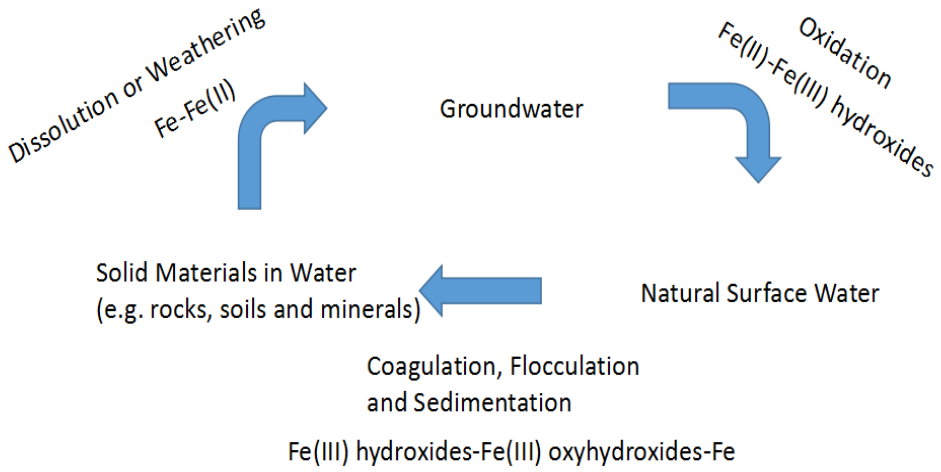

Figure 1 Fe-Fe cycle from minerals to aquatic environment and back.

Fe is one of the vital components to control metal pollutants in natural water, particularly it is in the form of Fe(III) including Fe(III)hydroxides, oxides, oxyhydroxides and so on. The source of Fe(III) are usually from the oxidation of Fe(II). Generally, Fe(III)(hydr)oxides can sorb and coprecipitate ions in natural water so that the ions will not dissolve. Therefore, the sorption/coprecipitation of Fe(oxy)(hydr)oxides significantly affects the enrichment of metal pollutants and controls the concentration of metal pollutants in natural water. Small particles of Fe(III) (hydr)oxides with high SSA is the most important because high SSA promote their ability of sorption and therefore they will be the powerful sorbents for dissolved species (e.g. heavy metal contaminants) and have great effects on sorption of toxic metals. As a result, the measurement and determination of the concentration of Fe

(hydro)xides plays an important role in the prediction of solubility mobility and bioavailability of several toxic metals (Jackson et al., 2012; Jones et al., 2009).

1.2 Natural Organic matter

Natural organic matter (NOM) is one of the most abundant materials on earth, which originates from soil erosion and biological decomposition. NOM exists not only in soil and sediments, but also in almost natural water bodies, including surface water, groundwater, etc (the range is between a few mg/L to a few hundred mg/L C) (Chen et al., 2011). This is the result of the interactions of the hydrological cycle with the biosphere and geosphere.

The specific conditions of biogeochemical cycles in waters from different sources are not the same and therefore they cause the considerable different in the amount, character, quality and properties of NOM in different aquatic environments (Matilainen et al., 2010). In addition, other environmental factors such as climate (e.g. rain, snow, snowmelt or flood) and the hydrological regime impact on the amount of NOM, so the amount, character and properties of NOM also depend on time (season) (Matilainen and Sillanpää, 2010). Because of the difference in origin, there are many types of NOM and various types of NOM have appreciably different properties. Table 1 shows the different types of NOM named according to its origin (Filella, 2009). In addition, through a lot of research on the properties of aquatic systems (e.g.

small streams vs large rivers, rivers vs lakes, pristine vs populated areas), NOM can include pedogenic organic matter and aquogenic organic matter. The former is the organic matter produced by bacteria and fungi decomposing higher plants and being leached from the soil in the basin by rainwater. NOM derived from peat can also be immersed in water environments in peat-rich areas. The latter comes from the water itself or the water in the upstream, mainly from the excrement and decomposition of plankton and aquatic bacteria (Filella, 2009).

Table 1 Some of the acronyms used in NOM-related studies and their meaning in relation NOM origin (References are given only to illustrate the use of the term. They are not necessarily the oldest nor the most representative).

Acronym	Meaning	Origin	Reference
AOM	Aquogenic organic carbon	Formed in the water mass itself from plankton and bacteria metabolism and degradation	Buffle (1988)
AOM	Algogenic organic matter	Organic matter formed by metabolic	Sehmidt et al. (1998)

		processes of microorganisms like cyanobacteria and green algac	
AROM	Aquogenic refractory organic matter	Non-easily degradable fraction of AOM	Buffle (1988)
AntOM	Anthropogenic organic matter	Organic compounds resulting from human activity	Buffle (1988)
EDOC	Excreted DOC		Hama and Handa (1987)
EOC	Excreted organic carbon		Munster (1993)
EOC	Extracellular organic carbon		Sondergaard and Schierup (1982)
EOM	Extracellular organic matter		Hoyer et al. (1985)
EPS	Exopolymeric substances		Hoagland et al. (1993)
IOM	Intracellular organic matter		Pivokonsky et al. (2006)

PDOC	Phytoplankton extracellular products	Compounds produced by ‘excretion’, ‘exudation’ or ‘extracellular release’ of photosynthetically produced organic carbon	Sundh (1989)
PDOC	Photosynthetically produced dissolved organic carbon		Cole et al. (1984)
POM	Pedogenic organic matter	Originated from leaching of soil organic matter	Buffle (1988)
PROM	Pedogenic refractory organic matter	Non-easily degradable fraction of POM	Buffle (1988)
SedOM	Sediment organic matter	Compounds resulting from accumulation and transformation of AOM, POM and organic debris in	Buffle (1988)

		sediments	
SOM	Soil organic matter	Compounds produced in soil, essentially by decomposition of higher plants	Buffle (1988)
TOM	Peat organic matter	Compounds resulting from degradation less advanced than soil organic matter	Buffle (1988)
TOM	Terrestrial organic matter, terrigenous organic matter	Term usually used in ocean studies; terrestrial, terrigenous	Hedges et al. (1997); Mannino and Harvey (2000)

As a complex matrix of organic materials, and a mixture of chemically complex polyelectrolytes (Hyung and Kim, 2008), NOM has heterogeneity. Due to different physical structure, chemical composition and properties in NOM, it is also considered to be complex mixture with unclear definition. The chemical composition and functional groups of NOM closely affect its structure. The molecular size, shape and aggregation state are considered to

be the key factors affecting physical and chemical reactions. In addition, the surface charge and spectroscopic/photochemical properties of NOM in solutions will be controlled by electrolyte and pH. Interactions such as complexation/cation bridging effects between functional groups in NOM and divalent and multivalent cations may also cause significant changes in the structure of NOM (Shen et al., 2015). Currently, there is no effective method that allows for the quantification of different types of NOM depending on their origin in Table 1. However, measurement of bulk parameters (see next paragraph) is benefit for providing an insight into the sources of NOM present in a given system. Many structurally unique compounds generated only in specific organisms and/or environmental conditions can be used as ‘‘biomarkers’’ to study NOM origin, because they can be used to trace the remains of different sources back by space, time and variable degrees of degradation (Filella, 2009).

Generally, hydrophobic (humic substances), hydrophilic and transphilic fractions have been found as three segments of the fraction in NOM. Among them, hydrophobic fraction with phenolic structures and conjugated double bonds has abundant content of aromatic carbon and almost 50% of dissolved organic carbon (DOC), which are larger molecular weight (MW), can be represented in the hydrophobic fraction. 25-40% of DOC with lower MW (polysaccharides, amino acids, protein and so on) makes up of hydrophilic

NOM which is also defined as a non-humic fraction operationally. Besides, the proportion of aliphatic carbon and nitrogenous compounds (carbohydrates, sugars, proteins, amino acids and so on) are higher in hydrophilic NOM. For another, in natural water, the transphilic fraction is composed of approximately 25% DOC and the MW of DOC is between hydrophobic and hydrophilic fractions (Matilainen et al., 2011, Zularisam et al., 2006).

NOM can be also fractionated into two parts: humic substances and non-humic fractions. Humic substance is the main reason to effect on the colour of natural water and accounting for over 50% of DOC in water (Matilainen et al., 2011). Meanwhile, humic substances, which comprise both aromatic and aliphatic components with mainly carboxylic and phenolic functional groups, are complex mixtures. They are more hydrophobic than non-humic fractions. As regards the non-humic fractions of NOM, generally, they consist of transphilc acids, proteins amino acids and carbohydrates and their amount of DOC is lower that is between 20% to 40% (Aiken et al., 1992, Fan et al., 2001). Next, as the predominant fraction of NOM, the humic substances comprise three categories based on solubility: humic acid (HA), fulvic acid (FA) and humin. For instance, when the pH is lower than 2, the HA with relatively high molecular weight will precipitate. In terms of FA (lower molecular weight), it is soluble at any pH (Fan et al., 2001).

Basically, the dissolved fraction of NOM is the size fraction that going through a 0.45 μm filter and it can be an important component on the earth, especially in aquatic environments, because its existence has significant effect on acidity, nutrient availability and toxicity of ecosystems (Aiken et al., 2011; Zhang et al., 2009). Except dissolved NOM, the particulate matter of NOM, which is composed of aggregates, also exist in natural water. The crossflow ultrafiltration (at about 0.5 μm) can separate the dissolved matter (including truly dissolved matter and some parts of colloidal) and particulate (including colloidal). By gravity, the particulate matter will settle down (Macrellis et al., 2001). However, some parts of colloidal matter with smaller aggregates in NOM will not settle down (Baborowski et al., 2003). In order to understand the role of NOM in water chemistry, it is necessary to separate and obtain different fraction of NOM, so the specific size of filter should be used correctly. Generally, the size of NOM less than 0.22 μm is truly dissolved matter, between 1 μm and 0.22 μm is colloidal, and greater than 1 μm is particulate (Krachler et al., 2016). Thus, it can be seen that the particle size of NOM is related to its mobility and solubility. The mobility of larger particles will be limited, but smaller particles are easier to spread to further place (Barber et al., 2001). Much research mentioned the importance of NOM in controlling and impacting the aggregation of colloids and behaviours of organic pollutants and metals. In recent decades, it is well known that the dissolved NOM plays a key role on the stability and mobility of particles including colloidal particles in

aquatic environments and it also impacts on the biogeochemical cycling of trace metals. Generally, the stability of particles can be improved by dissolved NOM (Aiken et al., 2011; Zhang et al., 2009). For example, the content of heavy metals will be diluted or effected by NOM when they enter to water. In addition, due to the interaction between NOM and heavy metals, their insoluble salts or complexes will be generated and these salts and complexes are not harmful to aquatic environment which have been proved (Vosyliene and Mikalajune, 2006). Overall, NOM is responsible for mobility and stability properties of colloids and particles in natural water and can control the fate and transport of pollutants. Many inorganic and organic pollutants can interact with NOM and therefore their toxicities will reduce (Kim and Yu, 2005). Meanwhile, particle size distribution has significant effect on the chemical and physical properties of NOM. The behaviour (not only about its own performance, but also on other material effects) of NOM in natural water depends on its particle size.

1.2.1 Climate change and changing NOM

Many studies have shown that different climatic conditions (temperature, precipitation) and hydrology (runoff and its composition) affect NOM in natural water (Hejzlar et al., 2003). With global warming, climate patterns will change and this will bring an increase in the frequency of extreme weather events (floods and droughts) (Ritson et al., 2014). Temperature and precipitation

pattens are two crucial climate-related factors that can cause changes in the quantity and quality of NOM. It has been proven that the content of NOM increases with increasing temperature (decomposition of NOM). On the other hand, a large amount of NOM will be flushed out from the soil (peatlands) and entered in water due to rainfall events, resulting in a high NOM concentration. These changes affect water quality (Chang et al., 2020).

Due to the influence of climate, the composition and stability of NOM released from soil to water will change and this could probably affect the fluxes of greenhouse gases from water to atmosphere (Wu et al., 2020). Peatlands accumulate a large amount of NOM (organic carbon), and once they are destabilized, it will cause an increase in the amount of dissolved organic matter in water (Freeman et al., 2004). The greenhouse gases (GHG) flux in water, especially CO_2, is regulated by the concentration of NOM, and also affected by quality, chemical composition and properties of NOM. Both rivers and streams are important channels for carbon (C) transportation and circulation. A large amount of carbon dioxide (CO_2) will be released from water to atmosphere, which is derived from the input of terrestrial C and the *in-situ* respiration of NOM. In addition, the mineralization of NOM will also affect CO_2 emissions from water. Therefore, once the NOM in water changes such as the content increases, the GHG flux will be severely affected (Ni et al., 2020; Wu et al., 2020).

1.3 Interaction of Fe and NOM

NOM can influence the properties of particles in water. Lots of research indicated that NOM has significant effects (promoting or obstructing) on Fe oxidation and the specific effect depends on its type, concentration or different environmental conditions such as pH. The interaction of NOM and Fe(II) with oxygen in aerated water are mentioned from many previous studies. However, without oxygen, the interaction also exists. The anoxic environment cannot maintain for a long time, therefore less attention is on the interaction of NOM and Fe under anoxic condition. The process of interaction can be seen in Figure 2 (Gaffney et al., 2008; Jackson et al., 2012. Jones et al., 2009; Liang et al., 1993; Theis and Singer, 1974; Tufekci et al., 2003; Wolthoorn et al., 2004).

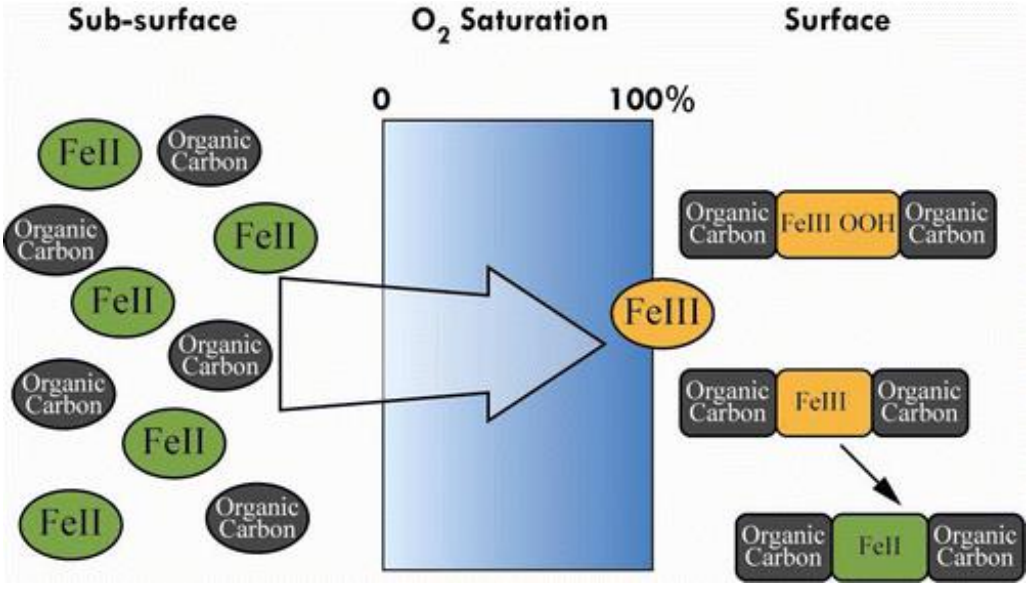

Figure 2 The interaction of NOM and Fe in natural water. Part of Fe(II) reacted with NOM is retained after entering the oxic environment (Jackson et al., 2012).

Specifically, NOM compounds can form dissolved complexes with cations such as Fe(II) and Fe(III) because of their functional groups (carboxylic and phenolic groups) (Mak and Lo, 2011). Therefore, before Fe(II) expose to fully oxic water (surface water), part of it is likely to interact with NOM and then it causes the generation of Fe-NOM complex (Jackson et al., 2012). This means that the interaction of Fe(II) and NOM occurs prior to oxidation in anoxic water and thus the oxidation rate of Fe(II) to Fe(III) will be controlled and inhibited in aerated water by NOM. More importantly, the formation of soluble Fe-NOM complex will result in the rise of dissolved Fe(II) concentration in natural water increases. For this reason, the amount of Fe(III) (hydroxides), which mainly contributes to the removal and sorption of metal pollutants, will be influenced (Mak and Lo, 2011). Furthermore, NOM can combine with Fe(III) (hydroxides or oxyhydroxides) through specific adsorption by ligand exchange with protonated surface hydroxyl groups and also has the ability to maintain Fe(III) (hydr)oxides as colloidal suspensions in natural waters. It is observed that the association between colloidal Fe particles and organic matter exist in oxic water. (Gaffney et al., 2008; Jackson et al., 2012; Mak and Lo, 2011). Apart from inhibition of Fe(II) oxidation, after combination with Fe, NOM can limit the aggregation and flocculation of colloidal Fe (oxy)hydroxide particles, because the stability of colloidal particles is improved by Fe-NOM (Mak and Lo, 2011).

Overall, numerous studies have analysed and investigated the characteristics of NOM and Fe. However, few studies have revealed the specific situation of interaction between NOM and Fe as well as characteristics of Fe-NOM complex. There is a requirement to extend the range of relevant parameters in NOM such as types and concentration, because the particle size and property of both NOM and Fe will be impacted after interaction. In addition, the mixing order of Fe(II) and oxygen is also a important factor (Gaffney et al., 2008; Jackson et al., 2012; Mak and Lo, 2011). Generally, the bioavailability of Fe and the role of Fe in the water are mainly affected by its solubility and speciation. The Fe-NOM interaction will alter Fe speciation and solubility in natural waters, which will also affect its export from waters. Therefore, it is necessary to understand how important the NOM is in determining the speciation and solubility of Fe in order to obtain more information of Fe chemistry in natural water (Rose and Waite, 2003).

1.4 Arsenic

As one of the most toxic elements, Arsenic (As) exists naturally in the environment (atmosphere, rocks, sediments, soils, natural water and organisms) (Ratnaike, 2003). Various factors such as the type and amounts of sorbents, pH, redox potential (Eh) and microbial activities will impact on the forms of As. Large number of studies have proved that the mobility and

toxicity of As depend on its specific chemical forms and oxidation states in the environment (Smedley and Kinniburgh, 2002; Wang and Mulligan, 2006; Wang and Mulligan, 2009). As can occur in the environment in inorganic and organic forms (As acid, arsenous acid, arsenites, arsenates and so on), but it mainly exists in natural water in inorganic form such as oxyanions of trivalent arsenite [As(III)] or pentavalent arsenate [As(V)]. [As(III)] is most common under anoxic conditions and [As(V)] is most prevalent in oxic conditions. [As(III)] is mentioned to has higher toxicity, solubility and mobility by comparing with [As(V)]. The organic forms of As are not quantitatively important and they are likely to be generated by biological activities, are mostly found in surface water. Normally, the capacity of toxic and mobile in inorganic As is greater than organic As (Smedley and Kinniburgh, 2002; Wang and Mulligan, 2006; Wang and Mulligan, 2009). In addition to trivalent (+III) and pentavalent (+V), As also has two oxidation states (-III, 0), of which As metals rarely occurs and (-III) oxidation state is only found in extremely reduced environments (Hughes, 2002; Wang and Mulligan, 2006).

Figure 3 shows the occurrence and mobilisation path of As in environment. A combination of natural processes including weathering reactions, biological activities and volcanic emissions as well as a series of anthropogenic activities such as mining activity, combustion of fossil fuels, the use of arsenical pesticides and so on result in the enrichment of As in soils,

sediments or rocks, which may generate As sources. Once in environment, both naturally occurring and anthropogenically sourced As are affected by the same biogeochemical processes, causing the mobilisation of As that will change As flux. It means more As entering into nearest natural water or agricultural fields from soils, rocks (mines) or sediments in the forms of arsenate ion [As(V)] and arsenite ion [As(III)]. Therefore, more As can enter to atmosphere through evaporation, attributed to elevated As fluxes in water. Humans are exposed to As by a number of ways such as water, soil and air, and therefore As poses the great risk to human health (Gonzalez et al., 2006; Wang and Mulligan, 2006). Meanwhile, most environmental As problems are caused by mobilisation of As under natural processes, which also involves water sources that are closely related to drinking water. These water sources come from water collection spots and are sources of during water. Among various sources of As, drinking water is the main cause of human As toxicity (Ratnaike, 2003; Smedley and Kinniburgh, 2002; Verma et al., 2014). With the increasing awareness of As toxicity and improvement of As quantitative technology, the maximum concentration limit of As in drinking water is set at 10 µg/L (it was 50 µg/L before 2004) by Worth Health Organisation and once the content of As exceeds the limit, the public health will be impacted seriously, leading to an increase in human disease and mortality (WHO, 2011). Elevated concentrations of As will pose hazards to human health and environment on a global scale and therefore there is a requirement to

understand the distribution and cycling of As in the natural environment due to its toxicity. Details will be described in Chapter 5.

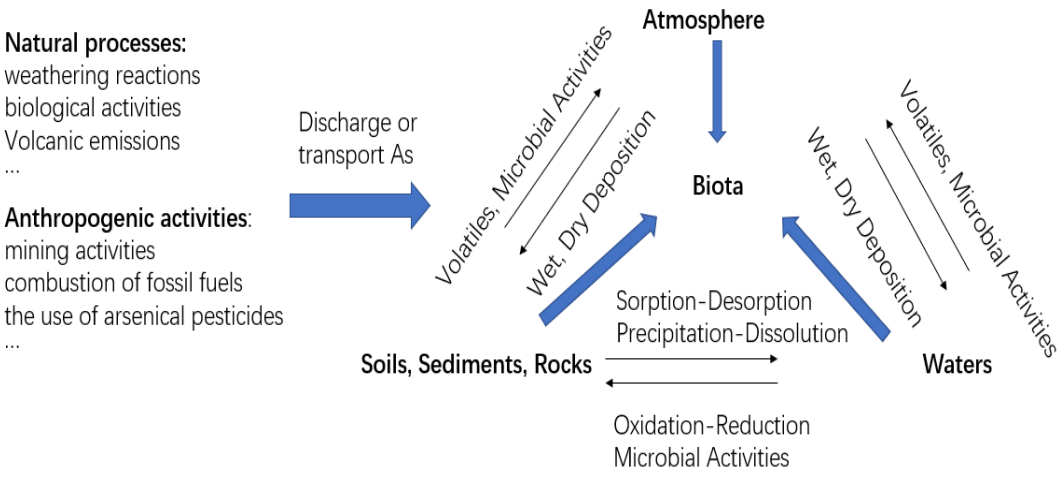

Figure 3 The occurrence and mobilisation path of As during As cycle in environment (Wang and Mulligan, 2006).

1.5 Aim

Human survival requires high-quality water resources and a good aquatic environment, the first requirement of this project was therefore to determine the amount of NOM, Fe and As that will affect the water quality in Peak District. Although measurements were made, hydrological and hydrochemical controls on mobility of NOM, Fe and As will continue to alter their fluxes or characteristics, and the exact causes and effects are yet to be fully understood. Consequently, the aim of this project was to understand the influence of hydrological and hydrochemical controls on mobility of NOM, Fe

and As to manage and predict future changes in water quality in Peak District. The developed long-term sampling procedures including automated sampling to cover non continuous temporalities such as stormflow achieved long-term sampling and the measurement of associated hydrological and hydrochemical conditions measurement in this area, so high-quality and representative datasets were obtained. Each aim of the three chapters in this project were described below.

NOM is a material containing OC and is an essential component of natural water, it not only affects water quality and water treatment, but also aggravates global warming through direct or indirect GHG (C) emissions, resulting in climate change. Among them, indirect emissions are much more than direct emissions and meanwhile more difficult to measure, so more important (Do, 2013). The aim of Chapter 3 is to develop a new monitoring system to study the control of hydrology and hydrochemistry on mobility of NOM by determining OC flux (an indirect emission predictor) in study sites of Peak District during study period and meanwhile make a preliminary prediction of future trends for the impact of ongoing and future climate change on OC flux.

Fe is another important element in natural water. The interaction between Fe and NOM will not only change their size and properties, but also affect the

properties and behaviour of other particles, pollutants or nutrients in water. The aim of Chapter 4 is to develop a new reaction system to investigate the specific circumstances of the interaction between Fe and NOM under different conditions (such as pH, light, temperature and mixing order of Fe, NOM and D.O.) in order to study the effect of NOM on Fe speciation and its mobility. Meanwhile, for maximising the universality of the findings, particular but representative NOM must be selected. NOM selection through size separation rather than chemical composition made it more easily comparable and therefore more generic.

As is a ubiquitous toxic element in upland peat catchment due to atmospheric deposition caused by anthropogenic activities and these uplands are also water collection areas with sources of drinking water, so it will be a potentially serious risk to water quality and mankind within Peak District. Therefore, the aim of chapter 5 is to predict how As flux may change with climate change and to gain a better understanding of hydrological and hydrochemical factors that control the mobility of As in general.

The project involves an iterative process of laboratory simulation and field monitoring.

Chapter 2. Methodologies

General reasons for methods. This project includes two parts: laboratory work and field work. Methods were devised in order to achieve aims of project including a) collect samples for developing a method of Fe/NOM analysis and/or experiments; b) Monitor field parameters involving carbon, Fe and As fluxes and validating laboratory model of Fe/NOM interaction. All methods were improved after training and development during the project and are explained in the following subsections.

Study area. Crowden Great Brook catchment has a total area of 7 km^2 and about 70% of surface area is covered by peat. It is located in the Peak District National Park between Manchester and Sheffield, and the range of its elevation is between from 220 m to 550 m above sea level (Figure 4 and Figure 5). As an upland stream of catchment underlain by the Upper Carboniferous Millstone Grit series, Growden Great Brook catchment is an important area for the analysis of organic carbon fluxes, particle size distribution (PSD) and composition of NOM. Because NOM is commonly quantified in the aqueous phase by dissolved organic carbon (DOC) or organic carbon (OC). Different carbon sources (pedogenic carbon originating from peat soils and aquapenic carbon originating from plants) can be presented in Crowden Great Brook catchment. In addition, the runoff from upland peat catchment is important part of indirect greenhouse gases (GHG)

fluxes. Large proportion of soil carbon are contained in peat and most of it will transfer to stream water through erosion, resulting in a high concentration of aquatic carbon in stream water. The constant movement of stream water causes carbon to be exposed to oxic experiment, so carbon dioxide (CO_2) is easier to produce, thereby intensifying the greenhouse effect, leading to global warming and climate change. Therefore, it is necessary to monitor the C fluxes and understand C emissions.

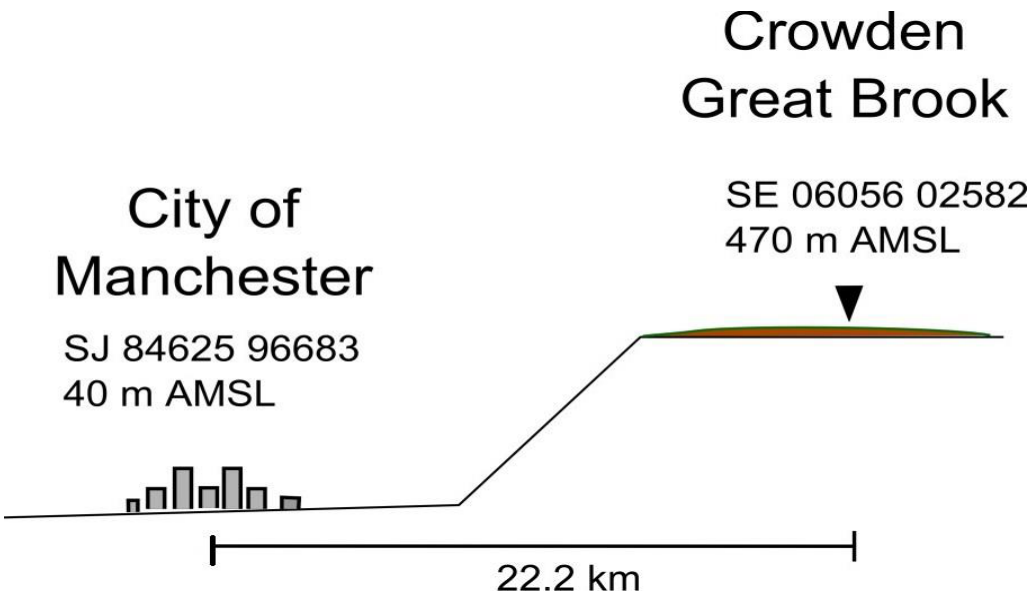

Figure 4 Relative location of the study site (Parra, 2019).

Crowden Great Brook catchment contains two sub-catchments, one is the eroded peat with an area of 0.5 km^2 (site 50, grid reference SE 05650 00943) and the other is uneroded peat with an area of 3 km^2 (site 30, grid reference SE 06172 02965) (Figure 5) (Do, 2013; Gaffney et al., 2008). Site 30 is close to the headwaters of the mainstream and the peat is largely vegetated, but further downstream to the west of the river substantial sections of the peat are in a degraded state (site 50), without vegetation, and subject to erosion of

surface layers (Figure 5) (Hegan, 2012). The condition of ombrotrophic peat is not uniform which allows for determination of the effect of peat condition on the transport of NOM or As. The existence of Crowden Great Brook makes it possible for several variables to be studied while exploring the effects of time and space upon the lability and interactions of carbon with the immediate environment and predicting its future behaviour.

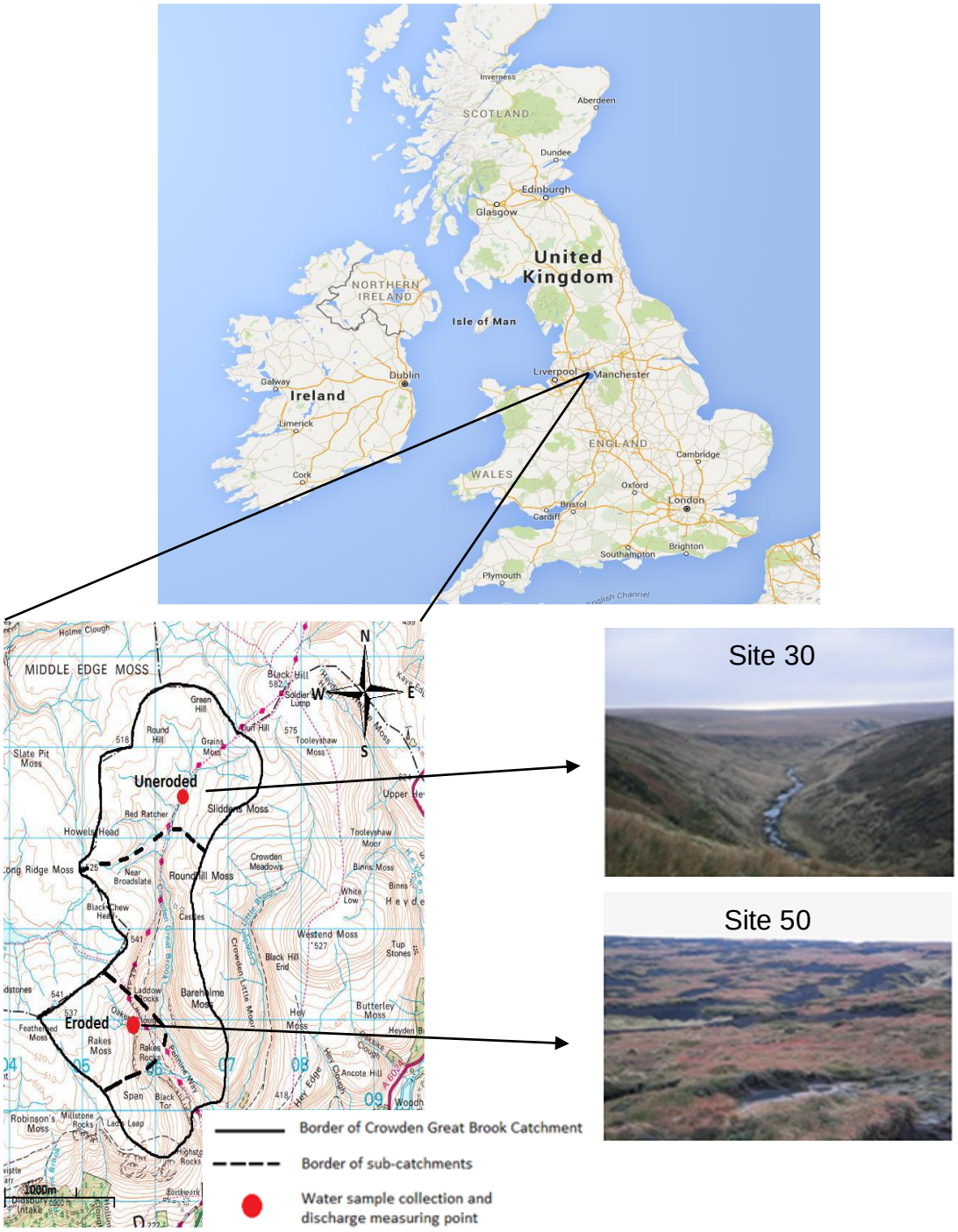

Figure 5 Location of Crowden Great Brook in UK and location of sampling sites in eroded and uneroded sub-catchments at the Crowden Great Brook. Figure adapted from Do (2013), Hegan (2012), Parra (2019) and Todman (2005). It reproduced from Ordnance Survey map date by permission of Ordnance Map, ©Crown copyright.

Furthermore, long-term mining, smelting and other industrial activities have caused environmental and atmospheric pollution in the Peak District and surrounding areas. West Lancashire coal is known to have a high As concentration. The burning of this coal has deposited As across high ground between Manchester and Sheffield (Rothwell et al., 2007; Rothwell et al., 2009). In recent year, the concentration of As has been increasing in surface peat and these As have the opportunity to enter in stream water and move to other places along with the river (Lee and Tallis, 1973; Rothwell et al., 2007). The waters from all branches of runoff in Growden Great Brook catchment will converge and then drain into the mainstream or be collected by stream systems. Finally, these waters flow into Torside Reservoir that is a main place to supply drinking water to Manchester. Therefore, Growden Great Brook catchment is the source place of drinking water for Manchester and the water quality and property in there are closely related to public health (Do, 2013). Therefore, the mobility of As is a potential threat and risk to public health of Manchester which worth our attention.

Flux calculation. Flux calculation depends on the following equation (1):

$$Flux = Q \times [NOM \text{ or } As] \qquad (1)$$

Where Q=Discharge (L/s); [NOM or As]=The concentration of NOM (mg/L) or As (μg/L).

Therefore, in order to calculate flux for NOM or As at different seasons of the year and under different hydrological conditions, Q and concentration must be measured throughout the duration of this project. Best measurement of flux requires high temporal resolution concentration and discharge measurement.

Discharge measurement. It is worth noting that continuous discharge (Q) measurement is impossible because these isolated catchment areas (site 30 and site 50) are located at high altitudes and are inaccessible due to extreme weathers such as rainstorm and heavy snowfall at certain time of the year. In addition, continuous Q measurement needs fixed channel forms and continuous velocity measurement and the installation of the necessary infrastructure in inaccessible locations is prohibitively expensive. Therefore, it is very difficult to measure Q at high frequency. In order to monitor the Q for a year or more years at high resolution, stage (water depth) is used as a surrogate measure of discharge because pressure transducers with datalogging capabilities are available at around £500.

Stage measurement. In order to measure stage at high resolution, a pressure and temperature transducer attached to a sentry logger (intelisys Ltd, Manchester, UK) was instrumented in each catchment area (site 50 and site 30), so the pressure in water can be measured. The location of the transducers is important for minimising the errors during the measurement

process. The best location is the centre of stream bed in upstream. In addition, the changes in atmospheric pressure may affect the pressure measurement of water stage, therefore a barometric pressure transducer was instrumented in research area to measure atmospheric pressure and it will be used as a reference for all sites. The data logging interval of each transducer is set to 15 minutes. Before being placed on field, every equipment will be calibrated by using known standards and Sentry II software (intelisys, UK). The stage calculation relies on the equation (6) below:

$$\text{Stage} = \text{Diver} - \text{Baro} + \text{altitude difference} \quad (1)$$

Where Diver= pressure in water measured by pressure transducer (cm H_2O); Baro= pressure in atmosphere measured by barometric pressure transducer (cm H_2O).

Altitude difference can be made by taking a direct stage measurement at the sites and comparing to the difference from directly subtraction between diver and baro readings. Therefore, the stage of all the sites is continuously monitored all throughout the duration of this project.

Stage-discharge relationship. Stage can be used to calculate discharge by building the relationship between stage and Q. This requires discharge to be measured across the full range of stage. During the entire project period, field work was carried out at least once a month to measure Q so that the

relationship between Q and stage are built. It is worth noting that the hydrological conditions of the catchment areas (site 30 and site 50) are vary greatly and irregularly throughout the year, resulting in unstable Q.

Salt dilution gauging is a common technique to determine the level of Q. NaCl is a conservative tracer in this technique and its dilution is determined by the detection of its value of electrical conductivity (EC) by a four pole EC probe. The measuring range of this probe is between 0-2500 μS/cm and it was connected to a Sentry II data logger (Intelisys, UK) after calibration by a detailed concentration of NaCl standard. After that, this probe was placed in downstream from the sample collection sites and then initial record of EC was started. The data logger was set to record at 2 second intervals. Next, the appointed amount of NaCl (200 mg to 400 mg) was put into the river around 15m upstream from the probe and it will result in the rise of EC reading. The gauging was continued until the EC reading returned to the initial value (Figure 6). It is worth noting that pools should be avoided between NaCl input point and probe to prevent errors of result caused by discharge because it takes longer to flow and even water will get potentially held up in pools. The EC value, mass of NaCl and time interval can contribute to the calculation of Q by the following equation (1) to (5):

$$Q = m / A \quad (1)$$

$$A = A_a - A_b \quad (2)$$

$$A_a = \text{sum}[NaCl] \text{ (from 1 to n) X t} \quad (3)$$

$$A_b = ab \text{ X t X n} \quad (4)$$

$$[NaCl] = (a') \text{ X EC} + (b') \quad (5)$$

Where m=mass of NaCl (g); A=area of peak (g*s/L); A_a=area under curve (g*s/L); A_b=area under baseline (g*s/L); ab=average of baseline value (g/L); t=interval time (s); n= number of data points; [NaCl]=concentration of NaCl (g/L); a', b'=slope and intercept for calibration of EC to [NaCl].

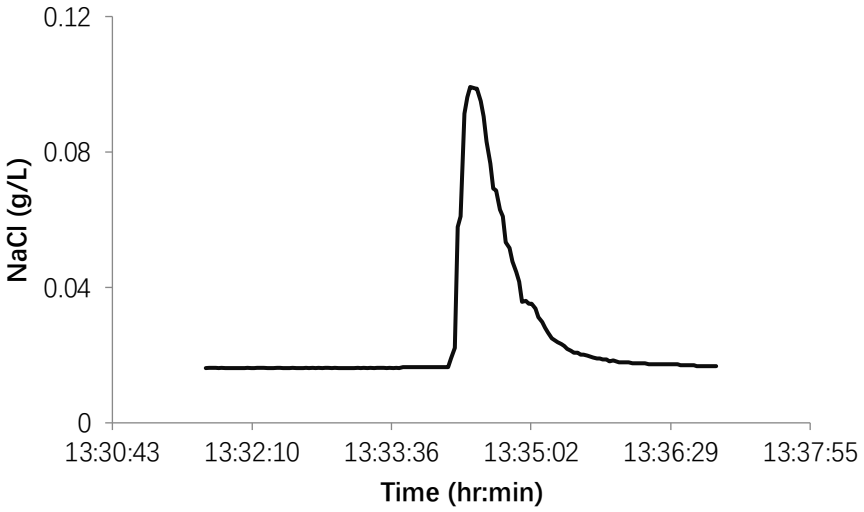

Figure 6 A dilution gauging curve on 16/10/2019.

A series of Q can be measured from multiple discharge measurements by salt dilution gauging and the stage at the same time can also be calculated during the study period or earlier. Therefore, the relationship between stage and Q can be built (Figure 7 A and B). This relationship can be continuously updated as future field work continues.

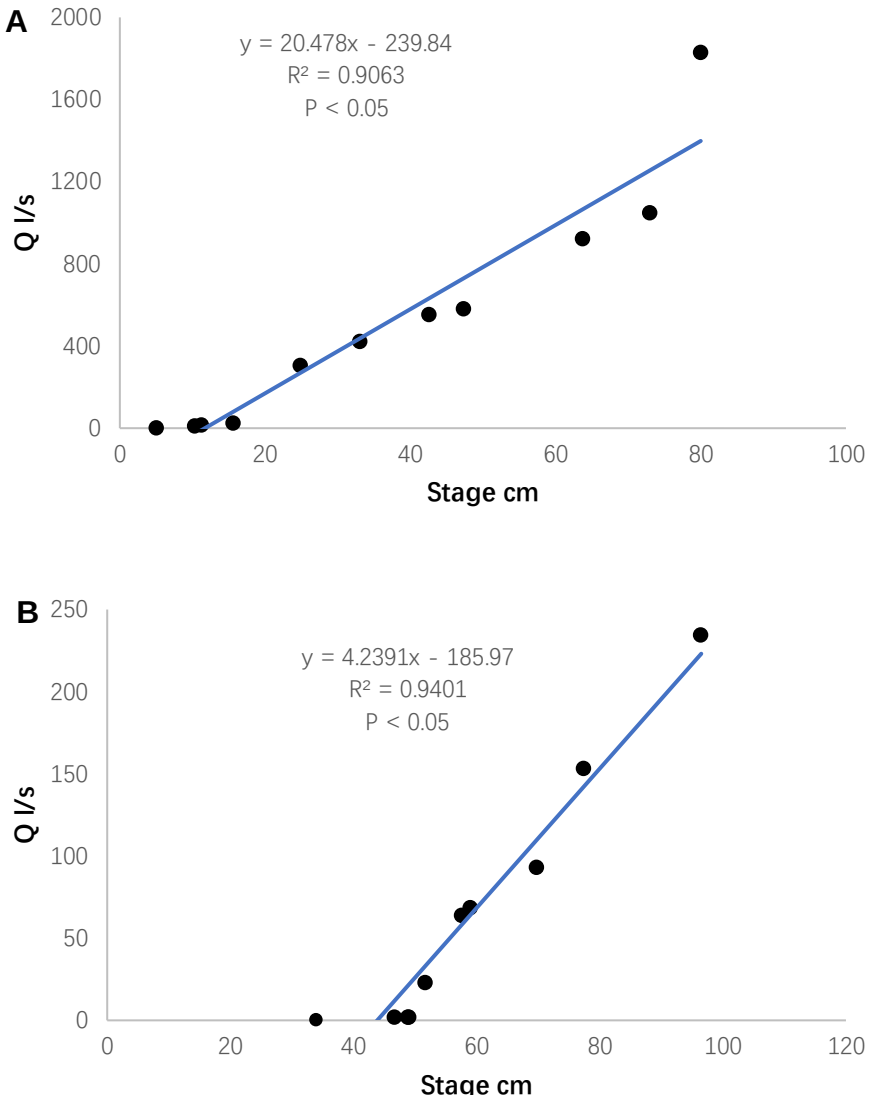

Figure 7 The relationship between stage and Q for (A) uneroded sub-catchment (site 30) and (B) eroded sub-catchment (site 50).

According to stage-discharge relationship, continuous Q (every 15 minutes) including high and low discharge can be calculated. Over the years, Dr. Stephen Boult and his research team have measured the Q of Crowden Great Brook for creating a stage discharge curve and thus a flow duration curve was made (Figure 8). The flow duration curve can be improved by updating discharge measurements. The hydrological behaviour and the proportion of

high discharge events (high intensity rain) in the research sites can be reflected clearly by this curve. It is important to understand that high Q has a great influence on the mobility of NOM. Because a vast majority of water runoff is caused by high discharge events, and it can consume or transfer NOM within peatlands located at high altitudes.

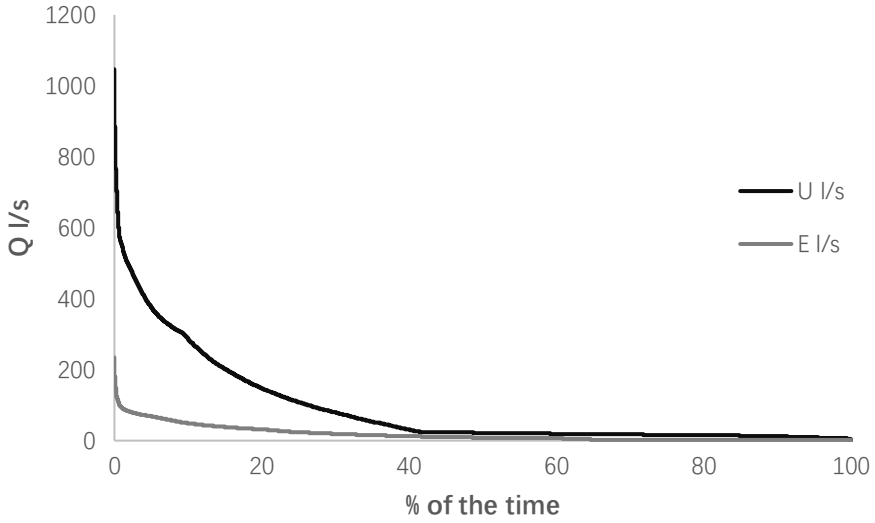

Figure 8 Flow duration curve under 3 years (2017-2019) for uneroded sub-catchment (U) and eroded sub-catchment (E).

Sample collection. In order to measure concentration ([NOM], mg/L; [As], µg/L; [Fe] mg/L) at different stage for flux calculation, auto samplers (Sigma SD900) (Figure 9) were placed at representative study sites (site 30 and site 50) to collect appropriate samples continuously. Each sampler inlet was located above the stream bed and as close as possible to the centre of the flow channel. The stream water in upland peat catchments have significant heterogeneity in hydrochemical characteristics (Rothwell et al., 2007).

Different time periods or different hydrological conditions will affect the NOM content in stream water. Therefore, the study area was visited every month all throughout the duration (3 years) of this project to take water samples under different conditions. In order to find the best representative concentration for accurate assessments of NOM Fe or As in fluvial systems, samples were taken at different resolution including daily sampling (low resolution) for long periods for long-term changes (between discharge events) or hourly sampling (high resolution) for short periods of changing discharge (during discharge events) and each sample was collected into acid washed (10% HNO_3, Analar grade, Fisher chemiclas, UK) 500 ml polypropylene bottle labelled with order and site of sampling. For sampling during high discharge event, each sampler has a float switch that acts an on/off for the samplers. When the water stage is high enough to a certain point, the float switch can detect this situation and activate the sampling process. In addition to sampling through the auto samplers, river water samples were also continuously taken by acid washed (10% HNO_3) high-capacity polypropylene bottles (5 L, 10 L or 20 L) during site visits for subsequent PSD analysis at a higher resolution. All collected samples were taken to the lab directly after each field work for sample analysis.

Figure 9 Sigma SD900 auto sampler with collected samples.

Sample analysis. All water samples were analysed in laboratory after collection by auto samplers and high-capacity polypropylene bottles. The sample analysis includes two parts: physical processing (filtration or size separation and concentration measurement) and chemical analysis (composition analysis). Carbon (C) accumulates in peat as NOM. NOM is of widely varying composition and it is necessary to place it in classes in order to study it. Classification by presence/amount of chemical functional groups is possible but may not be useful as the relationship between functional groups and provenance or behaviour of NOM is not well constrained. In this study we classify by particle size which is unambiguously measured and has direct links to behaviour. For flux calculation, the samples containing NOM generally need filtration at a low resolution by using 5 μm, 1 μm and 0.2 μm cellulose nitrate membrane filters (Whatman, UK) successively, while the samples

containing NOM used for PSD analysis require high resolution size separation techniques. The basic analysis done on samples throughout this project will be explained in the following subsections.

Filtration. As the most common technique for size separation, filtration is widely used in laboratory. In order to achieve size separation for PSD analysis, all of water samples need to be filtered first. Filtration can force fluid through the membrane by a variety of techniques (gravity, pressure and vacuum). However, it is easy for fluid to cause membrane fouling in the process of being forced to pass through the membrane, resulting in reduced filtration efficiency. This filtration problem due to the accumulation of materials is closely related to the amount of carbon in the fluid (such as microbial fouling in porous media, causing by higher amounts) and higher molecular weight molecules in NOM (Chen et al., 2007; Hand et al., 2008). Particles larger than the membrane size will coagulate on the membrane surface when they are forced through the filter and therefore causing the blockage of the membrane by large number of particles and changing the pore size of filter. During this process, this is not a full separation in the true sense and more likely to be caused by artificial force.

In order to solve this problem, as a filtration technique that does not apply pressure to the fluid, tangential flow ultrafiltration (TFU) is introduced in

sample separation. Without pressure, the samples will flow through the membrane during separation process instead of being forced through. In this filtration mode, a portion of sample with smaller size (filtrate) is allowed to pass through to the membrane surface, while the rest of them (retentate) is returned to sample reservoir and recirculated (Figure 10). Therefore, it is possible to carry out large-scale filtration of water samples by TFU (Schwartz and Seeley 2002).

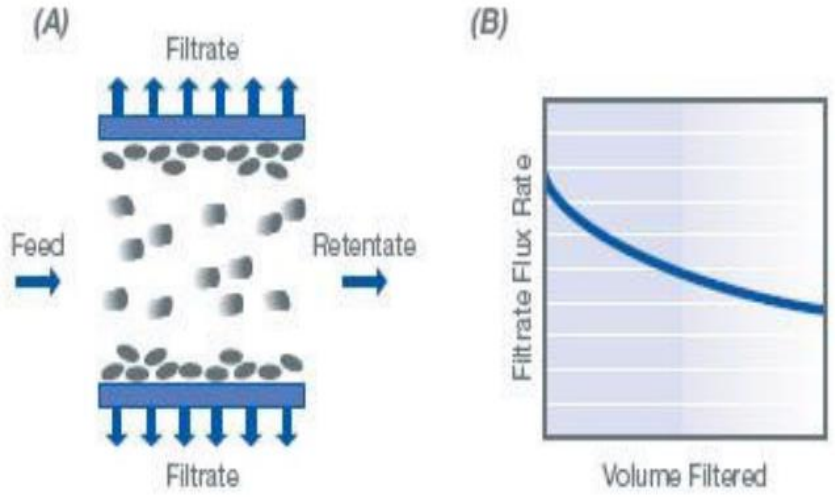

Figure 10 The mechanism and process of TFU (Schwartz and Seeley, 2002).

Stream water samples must be converted into non-settling fractions (colloidal and dissolved) by pressure filtration through 5 µm and 1 µm cellulose nitrate membrane filters before TFU. Filtration through a 5 µm membrane filter in advance is to remove large particles or impurities, thereby preventing clogging of the 1 µm filter. Sub 1 µm sample was separated by TFU into 5 size classes: <1>0.2 µm, <0.2 µm >100 KD, <100>10 KD, <10>3 KD and >3 KD using

polyethersulfone membrane plates (Vivaflow50, Sartorius, UK). The membrane plates were flushed with Deionised water (DIW) prior to use and this was done until no NOM (OC) was detectable in filtrate or retentate. It is worth noting that the specific surface area (SSA) of the sample increases as its size decreases, which is significant for the subsequent processing and application.

TFU was used instead of direct flow ultrafiltration as the direct pressure in the latter can lead to larger particles blocking or being pushed through the membrane. The tangential flow in TFU avoids this problem as fluid passes across the filter plate and material is separated by osmosis. However, whilst pressure filtration has a clear endpoint – when the sample volume has passed wholly into filtrate - TFU does not and separation may be incomplete. Validation is, therefore, necessary but rarely reported. In this work validation of separation was achieved by monitoring the mass of NOM (OC) in the filtrate and separation was deemed complete when the mass became constant (Figure 11). It is important to noted that the mass of NOM (OC) is obtained by multiplying its concentration and volume. As a widely utilized method for the quantitative determination of NOM in analytical chemistry, ultraviolet-visible spectroscopy (UV-Vis) is introduced to monitoring the concentration of NOM in real time by measuring its UV absorbance at 254 nm, this absorbance has a sufficient linear correlation with NOM concentration, so

it is most suitable for the analysis of NOM concentration (Matilainen et al., 2011).

To achieve constant mass the process had to take place for so long that the retentate volume had to be replenished. The stream water was of low electrical conductivity (EC), circa 40µS, so rather than attempt to maintain a constant EC, DIW was used which did result in EC dilution from 40 to 5µS during the process. After use, the membrane plates were flushed circularly with a 300 ml cleaning solution consisting of DIW, 0.5M sodium hydroxide (NaOH) and sodium hypochlorite (NaOCl) for 30 minutes and then rinsed with DIW until the pH is adjusted between 6 and 7.

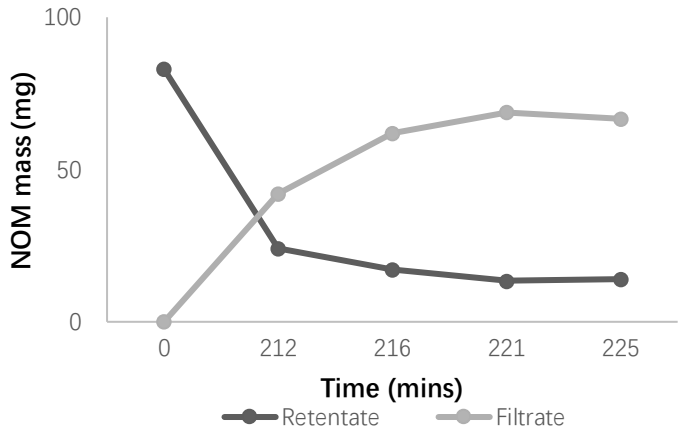

Figure 11 Mass balance of NOM (OC) during TFU process, TFU is completed when mass of retentate and filtrate is constant.

[NOM] measurement. Total organic carbon analyser is commonly used for quantifying the amount of NOM by measuring concentration of total organic carbon (TOC). TOC in liquids includes total amount of particulate and dissolved organic carbon (DOC), where DOC is used to quantify the amount of NOM in water samples. DOC needs further quantitative analysis, and the particulate can be removed by a range of filters. Generally, oxidation is a common method for quantification of DOC and it contains various steps such as burning, radiation and oxidising agents to form CO_2. Infrared (IR) spectroscopy is a main method at present to quantify the amount of resulting CO_2 (Matilainen et al., 2011).

A Shimadzu TOC-5050A analyser (Shimadzu TOC-V CPH, Japan) with the detection limit of 4 parts per billion (ppb) was used in TOC analysis during entire project period. This analyser first measures the amount of CO_2 generated by the combustion of the sample through an infrared detector to determine total carbon (TC), and then measures the amount of CO_2 produced by the decomposition of the sample through an infrared detector again to determine total inorganic carbon (TIC). TOC is calculated by subtraction from TC to TIC. Triplicate measurements were made for each sample measurement and the average value was taken as the final concentration. A calibration curve was generated by different concentration of (1 mg/L, 5 mg/L, 20 mg/L) TC and (0.5 mg/L, 1 mg/L, 5 mg/L) TIC standard solutions to

quantify the amount of TC and TIC in the samples. Since TC and TIC standard solutions are required for each TOC analysis, TC and TIC stock solutions were prepared in advance to facilitate the use of standard solutions, where TC stock solution is made by using 2.125 g potassium hydrogen phthalate (Shimadzu, Japan) in 1 L DIW and TIC stock solution is prepared by using 3.5 g sodium hydrogen carbonate (Shimadzu, Japan) in 1 L DIW. Drift correction calculations by calculating the slope and offset between each pair of standards and linearly extrapolating over time are applied to each sample analysis to ensure that the errors caused by instrument drift are minimised.

[Fe] and [As] measurements. The Inductively Coupled Plasma-Atomic Emission Spectrometry (ICP-AES) (Optima 5300, Perkin-Elmer, United Kingdom) is used for [Fe] measurement and Inductively Coupled Plasma Mass Spectrometry (ICP-MS) (8900 Triple Quadrupole, Agilent, United States of American) is used for [As] measurement. The former is based on the measurement of excited atoms and ions on the wavelength characteristics of specific elements and the latter is the measurement of atomic mass by mass spectrometry (MS). The choice of these two ICP is based on their lower detection limit. The lower detection for ICP-AES is parts per billion (ppb), but for ICP-MS can extend to parts per trillion (ppt) (van de Wiel, 2003). The concentration range of [As] in the samples collected from study area is below

or near the lower detection limit of ICP-AES. Therefore, ICP-MS is the first-choice instrument for [As] measurement.

Both of two instruments are calibrated by using standard solutions with different concentration gradients (0.001 ppm, 0.01 ppm, 0.05 ppm, 0.1 ppm, 0.5 ppm and 1 ppm for ICP-AES; 1 ppb, 5 ppb, 10 ppb, 50 ppb and 100 ppb for ICP-MS) and a bland solution prior to sample analysis. After measuring about 20 samples each time, the instruments need to be recalibrated and rinsed in order to minimise errors and ensure the normal working. It should be noted that samples were submitted in solution preferably (at least < 1 μm) which could ensure that the nebulizer, narrow tube or other site of instrument were not blocked. Therefore, each sample needs to be filtered through 5 μm and 1 μm cellulose nitrate membrane filters (Whatman, UK) to remove particulate matters, and then acidified to 2% with nitric acid before ICP analysis, because acidification can provide a low pH condition to prevent metal precipitation and keep the metals in solution during transportation and storage.

Continuous [NOM] and [As] measurements. [NOM] and [As] of stream samples collected from the study area were measured by specific instruments mentioned above. However, due to the reasons of weather and location explained in subsection ‘‘Discharge measurement’’, the study sites are not

available for being accessed frequently and the capacity of autosampler for collecting and storing samples was limit. Therefore, it is difficult to perform continuous measurement of concentration by high frequency sampling. In order to overcome this problem, two methods including both interpolation and extrapolation were utilised in continuous concentration measurement. The extrapolation was based on the modelling of the rating relationship curve between concentration and Q. Detail information will be explained in the individual chapters (Chapter 3 and Chapter 5).

Although interpolation and extrapolation are prediction methods by estimating hypothetical values based on other observations, the application scenarios should be understood due to the differences in their principles. Interpolation is used to estimate the unknown values that exist within the data sets and extrapolation is used to estimate the unknown values outside the data sets by linear regression models. In this project, the accuracy and reliability of results from both of methods rely on the amount and quality of sampling measurements. Generally, interpolation is more reliable and accurate than extrapolation, but it will be affected by the limited data when predicting unknown values in a longer period, resulting in errors. The random dispersion of rating relationship curve may also lead to non-linear relationship, resulting in errors in the calculation of continuous [NOM] or [As]. Therefore, the reliability of results needs to be verified according to comparison from both of

methods. Detail information will be explained in the individual chapters (Chapter 3 and Chapter 5).

Pyrolysis gas chromatography mass spectroscopy (Py GC/MS). Pyrolysis gas chromatography mass spectroscopy (Py GC/MS) can provide useful information at the molecular level of NOM so that it is a fast, useful and convenience technique for improving knowledge about structure in natural macromolecules (Templier et al., 2005). Under heated and anoxic condition, large complex molecules of NOM are broken into more analytically available fragments in pyrolysis and these fragments will be detected by MS after sweeping into the analytical column of the GC.

The NOM was prepared for Py GC/MS analysis by freeze drying. Approximately 150 ml of NOM sample was placed in 1 L freeze resistant glass vials and then immersed in a 5 L dewar filled with 4 L liquid nitrogen. During the entire freezing process, it is necessary to keep turning the vials to produce a large freezing surface area in a shorter time. The NOM sample was freeze dried subsequently by using an Edwards, K4 Modulyo Freeze Dryer. The dried sample was stored in a 20 ml vials after freeze drying.

Approximately 1 mg of dried NOM sample was weighed into a quartz sample tube and pyrolyzed using a Chemical Data Systems 5200 series Pyroprobe by

heating at 700°C for 20 seconds. Liberated fragments were analysed using an Agilent 7890A Gas Chromatograph interfaced with an Agilent 5975A MSD Mass Spectrometer operated in electron ionization (EI) mode (scanning a range of m/z 104 50 - 600 at 2.7 scans s^{-1}, ionization energy 70 eV and a solvent delay of 1 min.). The gas chromatograph was equipped with a Zebron ZB-5MS column (length 30 m, I.D. 0.25 mm, film thickness 0.25 µm). The pyrolysis transfer line and injection temperature were set at 350°C, the heated interface at 230 °C and the MS quadrupole at 150°C. Helium was used as the carrier gas and the samples were introduced in split mode (split ratio 5:1, constant flow of 5 ml/min). The oven was programmed from 40°C (for 5 mins) to 320°C at 4°C min^{-1} and held at this temperature for 10 mins.

Compounds were identified from chromatographs by comparison of relative retention times and spectra to those reported in the NIST library. Peak areas were calculated for each compound to allow semi-quantitative attribution of their relative proportions. Whilst the characterisation was primarily to allow comparison to other samples; to assemble a “fingerprint” for distinguishing different materials, the compounds detected were grouped by degree of oxidation to also give some functional relevance. Overall, Py GC/MS is definitely a powerful tool for structural analysis about the molecular building blocks of NOM.

Chapter 3. Quantity of OC flux from an upland peat catchment

3.1 Introduction

Climate change is the result of an increase in concentration of greenhouse gases (GHG) and carbon dioxide (CO_2) is the dominant GHG. CO_2 in atmosphere captures some of the heat energy that should otherwise be radiated to space, leading to global warming. Meanwhile, increasing temperature affects the normal atmospheric circulation, resulting to occurrence of extreme weather. These are the drives of large-scale global climate change (Harley et al., 2006).

The concentration of CO_2 in the atmosphere is closely related to the widespread C in nature and the soil carbon (C) is the main contributor due to its higher C content. The mass of carbon (C) in the atmosphere is only half that in the soil C reservoir (Biasi et al., 2014). Therefore, it is critical to quantify current and predict future C fluxes between the soil reservoir and the atmosphere. Soil C is mainly represented by organic carbon (OC) and peat soil is the largest reserve of terrestrial OC (more than one-third of the world's total soil C pool) (Adeolu et al 2018; Dinsmore et al., 2010). Peat soils consist of large number of preserved plant debris is also a long-term storage place for OC, because the impermeable layer of material clogging drainage will be generated when these plant debris decay, producing the anoxic conditions suitable for OC accumulation (Parry, 2014). Therefore, the role of peatlands is

essential in regulating global atmospheric C storage. In recent years, human activities such as deforestation, farmland development and other landscape changes caused by land use increased C release from peat soil to atmosphere or peat soil to water, which have significantly affected CO_2 concentration in the atmosphere and intensified the process of climate change (Roulet, 2000). The main consequences of climate change involving increased temperature and altered precipitation patterns will continue the change the C transport in the peat system. Therefore, many peatlands have been converted to large CO_2 sources (Dinsmore et al., 2010; Gunther et al., 2018). Furthermore, many water collection areas are often correlated with peat soils, so climate change can significantly impact on water quality and treatment (Liski, J et al., 1999; Schiesinger, 1984).

Although many studies have evaluated the C storage in UK peatlands (Chapman, 2009; Dawson et al., 2002; Pawson et al., 2007; Pawson et al., 2008; Worral et al., 2011), C has dynamic behaviours due to the high sensitivity of peatland to environmental changes. Therefore, it is expected that C flux will change in the long-term period due to the different environmental caused by climate change. Because of this potential change, it is necessary to measure change in OC mass balance of upland catchments. The total change will be the sum of changes in direct and indirect emissions. This means that the present and future C can be continuously release to atmosphere directly

(direct flux) from in-situ intact primary peat or indirectly (indirect flux) from transported and dispersed peat (Figure 12). In recent years, many technologies developed for quantifying direct C flux by measuring GHG emissions such as surface chambers, eddy covariance techniques or airborne measurements have been well-studied extensively and played an important role in upland peat catchment (Krauss et al., 2016; Lorke et al., 2015). Meanwhile, since the roots of many plants can extend to the peat soil at a considerable depth, a large number of root litter enters directly into deep layer of peat soil, resulting in higher C content there (more than 60% of C). However, there is an extreme lack of oxygen in the deep peat soil and oxygen outside the soil penetrates slowly because of drying. Therefore, low amount of C is directly oxidised to CO_2 and released into atmosphere from the intact peat at a very slow rate (Ekschmitt et al., 2008). Therefore, direct C emissions from peat soil is less important to study.

Indirect C emissions from peat soil are largely inferred by aquatic OC flux and they mainly come from spatially or temporally dislocated peat deposits caused by stream transportation (Figure 12). Therefore, there is a requirement to quantify OC flux in stream in order to infer the indirect GHG emissions. OC from peat soil is promoted to be released into stream in the form of dissolved OC or particulate OC (DOC or POC) due to the erosion of water and mobilised through multiple sources involving stream system and its

consequent deposition mechanisms, both DOC and POC are significant components of stream. This OC will change more quickly (e.g. participate in reaction to produce more CO_2), because it has a higher SSA and be under wholly oxic conditions whilst in transit. In addition, this long-term continuous output of OC from soil can occur at different points of the entire peatland area, and OC will be constantly dispersed in the system along with the stream. All of these make indirect C flux more complicated and therefore increase the difficulty of quantification. Moreover, OC within transit of stream can be continuously released to the environment in all different forms (particulate, dissolved, gaseous), so the indirect C flux is generally larger and more significant than direct C flux. Therefore, in contrast with direct C flux, indirect C flux is more important. The stream systems are one of the most important globally CO_2 atmospheric emissions and OC flux is a predictor of indirect GHG flux. The determination of OC flux including long-term trend is essential for the assessment of peatland stability (Clark et al., 2007; DelSontro, 2018; Dinsmore et al., 2010; Worrall et al., 2007; Worral et al., 2011).

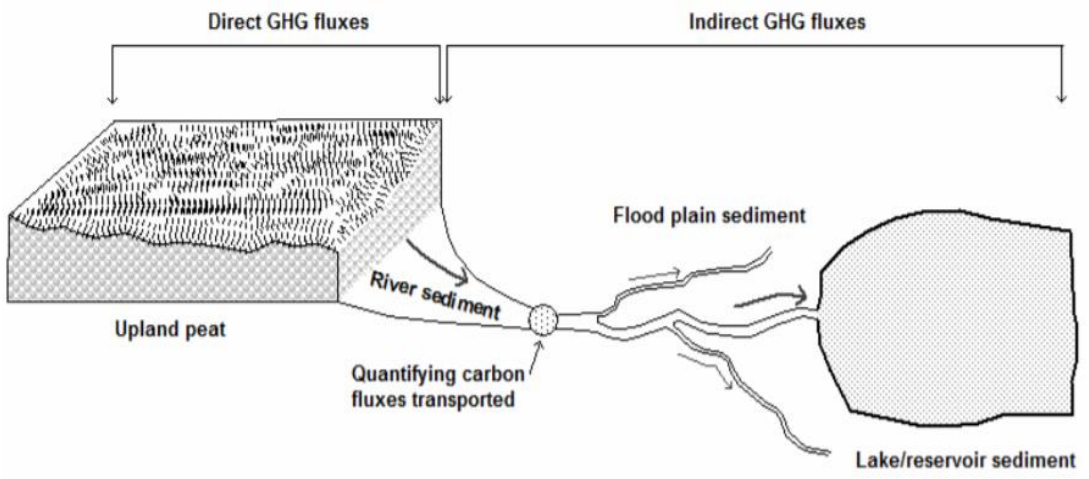

Figure 12 The occurrence and pathways of direct carbon flux and indirect carbon flux from upland peat catchment (Do, 2013; Tranvik et al., 2009).

Although there have been many analysis reports on OC flux in recent years that promote improvements in our understanding of OC emission rates and factors (e.g. hydrology, pH, temperature or land-use management) influencing them (Do, 2013; Pawson et al., 2008), it is still not enough to predict the mobilisation of OC in stream. OC transported in runoff is dispersed and produced via a series of processes each of which is variable under the influence of vary hydrology conditions (Q), leading to different end points of OC transmission (Worrall and Burt, 2005). Therefore, the impact of Q on OC transmission cannot be ignored. Previous studies have shown that discharge event with high Q cause an increase of both DOC and POC in stream, because large number of sediments with OC-rich in peat soil will be significantly released to stream and transported with high Q during high intensity low frequency discharge, resulting in a significant proportion of the

total OC flux that occurs within this period. However, due to inaccessibility of site under heavy rainfall events, it is difficult to estimate the degree of change in C flux during discharge event (Hinton et al., 1997; Pawson et al., 2008). All of this makes indirect flux difficult to measure and has large errors. Therefore, further study is required, which includes understanding factors affecting indirect flux and updating measurement methods to obtain long-term and high-quality datasets. Furthermore, the prediction of future C flux become more difficult because of the intensification of climate change. The peatland is desiccated and cracked with weakened vegetation because of summer drought, leading to physical disintegration of the peat mass through extensive gully erosion, making it more susceptible to increased winter erosive forces. Therefore, the erosion of peatland will be accelerated by enhanced summer temperatures and winter storminess, leading to physical degradation that impacts on C storage in peatland (Evans et al., 2006). The changes in the OC flux are important because the upland peat catchments are not only C stores but water collection areas. OC accumulates in peat as NOM and therefore aquatic OC provide an indication of NOM content in stream. NOM is responsible for water taste, odour and colour, so NOM in stream can be the origin of various problems in quality of drinking water. Meanwhile, NOM also impacts on water treatment through the formation of disinfectants by-products (DBPs) such as trihalomethanes or haloacetic acids after reacting with chlorine-containing disinfectants within water treatment. These DBPs are

harmful to human health (Volk et al., 2002). Overall, given the importance of C storage and water quality, the measure or predict the results of ongoing and future changes in upland peat catchments on aquatic OC fluxes. This is the main aim of this project which is a prerequisite for controlling OC flux to reduce its impact on the global C cycle.

Indirect GHG flux will not be solely a consequence of OC flux but also the lability of the OC. The lability of OC in soil has increased its sensitivity to environmental changes caused by land management. The storage of soil OC is easily influenced by land use and agricultural practices. For example, rapid decomposition caused by the disruption of soil structure will promote loss of OC (Benbi et al., 2015; McLauchlan and Hobbie, 2004). The lability of OC will be affected according to its size and generally the lability and resulting mobility increases in a smaller size, because it is more reactive (higher SSA). Therefore, OC will be separated into two size fractions in this project: mixing of POC and DOC (UF: unfiltered) and DOC (<0.2 µm).

Future prediction and monitoring of representative OC flux are two major challenges in achieving the aim. The Southern Pennies (UK) Peak District National Park with high level of OC content provides a suitable place to monitor and compare OC flux under different environmental conditions, because it has upland peat catchments and is known to have the highest of

erosion rates in peat soil in the world due to land-use management (mismanagement) (Evans et al., 2006). Peatlands in UK are constantly facing natural erosion from environment such as wind, gravity, rainfall and flowing water as well as pressures from anthropogenic activities such as atmospheric pollution, agricultural activities, solid waste pollution and climate change. Therefore, erosion is the likely future situation of upland peat so the eroded site (site 50) with degraded peat and lack of vegetation can be a model of future conditions and used to prediction of future OC mobilisation under higher erosion of warming climate. Meanwhile, there is also an uneroded site in Peak District National Park (site 30), because the revegetation of plant species such as sphagnum moss has been done there, which has restored the natural runoff system and promoted the renewal of peat deposits. Meanwhile, successful environmental improvement strategies (such as using physical barriers to block drainage) have effectively reduced the impact of erosion, water level drops and other adverse conditions (Evans and Warburton, 2011). The existence of these two contrasting sub-catchments (site 50 and site 30) is benefit for predicting the future C flux. This is also the essential requirement for site selection and project development. In addition, the stream water in upland peat catchments have significant heterogeneity in hydrochemical characteristics, resulting in difficult of representative sampling (Rothwell et al., 2007), because different time periods or different hydrological conditions will affect the OC contents in stream. As a water collection area,

Peak District National Park allows long-term sampling and associated hydrological conditions measurement to obtain high quality data sets, which is a solution to solve the problem. The long-term sampling programme was described in subsections ‘‘Sample collection’’ of Chapter 2. This is the important prerequisite for making representative measurement of flux by interpolation and rating relationship (described in subsections ‘‘Continuous [NOM] and [As] measurements’’).

Overall, in order to complete the main aim of this project, it is necessary to monitor the changes in OC flux in Southern Pennies (UK) Peak District National Park for further predict and manage OC mobilisation. The following objectives were set out to achieve the aim:

- Collect samples at different intervals from upland peat catchment of Southern Pennines (UK) Peak District during baseflow and stormflow conditions (discharge events).

- Determine continuous [NOM] and Q by using interpolation and calculate NOM flux for each site.

- Compare the variability in NOM flux between sites and periods and determine the reliability of flux by comparing with another method of

calculating flux.

- Make comparisons to previous estimates made in this catchment to determine whether the change taken place over the years of study?

- Determine how OC change with Q under discharge event and identify the hydrology conditions of controlling OC mobilisation.

3.2 Materials and methods

Sampling and sample analysis. Stream samples containing NOM were taken by using of sampling systems (Sigma SD900) at both study sites (site 50, grid reference SE 05650 00943 and site 30, grid reference SE 06172 02965) of Crowden Great Brook in Peak District National Park. A combination of daily sampling and hourly sampling during baseflow and stormflow conditions (discharge events) from auto sampler was conducted in stream water at all study sites. The mechanisms of sampling were described in detail in the subsection “Sample collection”. From 2017 to 2019, more than 150 and 170 samples were collected respectively from site 30 and site 50, and these include sampling of two discharge event during April 2017 and April 2019. For the purpose of this project, all samples were filtered with 5 µm, 1 µm and 0.2 µm cellulose nitrate membrane filters (Whatman, UK) successively in order to obtain OC concentrations. Subsequent TOC measurement of each size

fraction with TOC analyser procedure outlined in the subsection “[NOM] Measurement” of Chapter 2.

Continuous [OC] measurement and calculation of OC flux. In order to monitor the OC flux for long period during the entire project, a high frequency measurement of [OC] is required. Due to the reasons outlined in the subsection ‘‘Continuous [NOM] and [As] measurement’’ of Chapter 2, it is difficult to perform continuous measurement of [OC] through high frequency sampling. In order to solve this problem, two methods of concentration estimate were conducted in this project. Each method requires calculation of continuous Q by the pattern described in the subsection ‘‘Stage-discharge relationship’’ of Chapter 2.

The first is to use simple interpolation to estimate [OC] between sampling points. [OC] of each daily sample at a specific time was assumed to represent [OC] of a whole day (24hrs) in river, so the instantaneous OC flux per 15 minutes can be calculated by multiplying interpolated [OC] and corresponding Q. The sum of these instantaneous OC flux during sampling period were multiplied by the inter-sample period to give a total mass, and then divided successively by the specific number of days within sampling period and site area to calculate the average daily OC flux. Therefore, the estimated value of OC flux for a whole year or more time can be obtained by multiplying the

average daily OC flux during the sampling period by the specific number of days in a year or more years. The limited number of samples will lead to errors in this method, so it is necessary to introduce another method for comparison to verify the reliability of results. The second method is to try to model flux by rating relationship ([OC] vs Q).

The relationship between Q and [OC] need to be established. [OC] of all samples and corresponding Q at the same time were integrated together to make a linear regression model. The continuous [OC] can be calculated by Q at 15-minute intervals for subsequent OC flux estimation. The sum of each OC mass obtained by multiplying Q and [OC] was divided successively by the conversion factor (the ratio between the number of days in the Q monitoring period and the number of days in a year) and site area to estimate the flux over a long period (one year). However, the random dispersion in rating relationship may lead to errors in the calculation of continuous [OC], thereby affecting the results of OC flux. The reliability of results needs to be verified according to compare OC flux during sampling period or longer period from both of methods.

3.3 Results and Discussion

Quantification of OC flux by using interpolation. In order to ensure the availability of representative and high-quality data set and reduce temporal variations, samples were collected in different months of project period (Figure 13). OC flux for each site was estimated by interpolation and reported in Table 2. Although both of DOC and POC play a key role in most stream ecosystems and have a significant impact on the environment, it is DOC that generally dominates the flux of OC. Therefore, DOC is a major source of C to aquatic ecosystems and has higher mobility than POC (Panton et al., 2020; Sobczak and Findlay, 2002). This can be clearly seen in Table 2. The DOC flux of the site 30 and site 50 were 9.78 t/year/km^2 and 17.1 t/year/km^2 respectively and occupied 95.9% and 88.57% of mixing flux (POC and DOC). Therefore, DOC flux of stream is an important characteristic in aquatic ecosystems. It has a significant impact on the global carbon balance and many chemical reactions such as complexation and mobilisation of metals in stream (Aitkenhead et al., 1999; Mulholland, 2003).

In addition, both DOC and mixing fluxes at site 50 were almost twice higher than those at site 30 (17.1 t/year/km^2 vs 9.78 t/year/km^2 and 19.31 t/year/km^2 vs 10.2 t/year/km^2). This indicates that the erosion of site 50 is a threat to its OC storage of soil, because land degradation and destruction of peat will be caused by erosion, leading to reduction of OC sink. The peat soil at site 50

may be converted to a net source of OC, which undoubtedly increases the amount of OC input, leading to higher PCO and DOC fluxes. Meanwhile, the increase in OC flux will aggravate output of GHG, thereby accelerating the process of greenhouse effect, leading to the rise of temperature. Rising temperature will continue to increase soil erosion (explained in the subsection "Introduction" of Chapter 3), resulting in increased terrestrial runoff and significantly affecting sediments release. This vicious circle can lead to continuously intensifying indirect C flux from peat soil and it has thus become a key global environmental problem (Gomes et al., 2019; Ma et al., 2021; Worrall et al., 2011). Unlike site 50, site 30 with lower erosion and higher vegetation coverage has a much lower OC flux in stream, suggesting that the original peatlands are more likely to act as C sinks rather than net sources (Gorham, 1991; Gorham and Rochefort, 2003).

Table 2 Estimation of OC flux in different forms by interpolation for each site.

Study sites	Mixing flux of POC and DOC (t/year/km^2)	DOC flux (t/year/km^2)	% of DOC flux in total mixing flux
Site 30 (Uneroded catchment)	10.2	9.78	95.9
Site 50 (Eroded catchment)	19.31	17.1	88.57

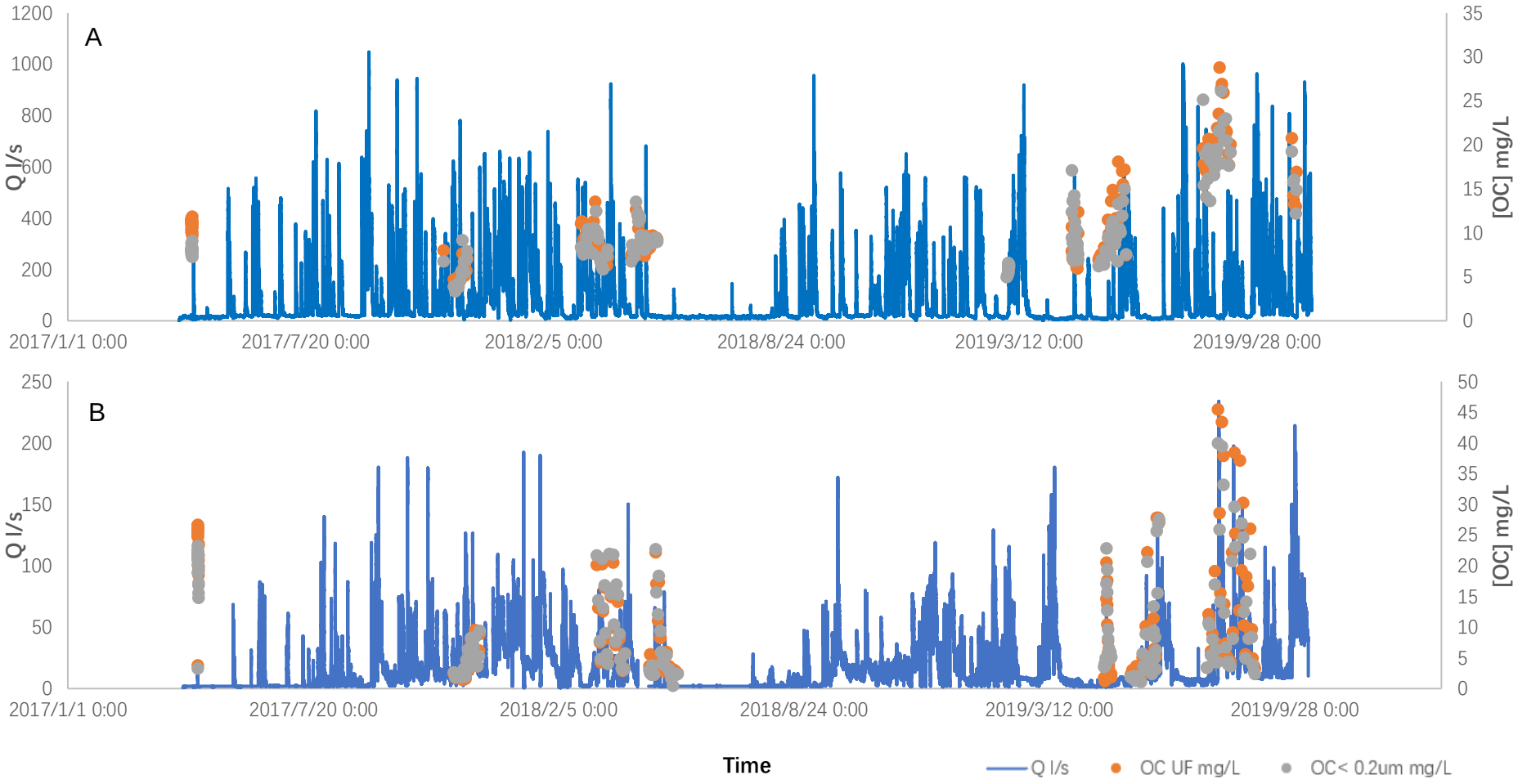

Figure 13 OC sampling and discharge (Q) monitoring for A) site 30 and B) site 50 during study period.

However, the estimation of flux by using interpolation extremely relies on the Q values and OC concentrations that are easily affected by climate or various hydrological conditions during sampling period. Therefore, variations in flux are inherent due to different and limited samples, even for each sampling period (Figure 14) (Walling and Webb, 1985). OC flux is not determined by a single factor, and higher OC concentration or larger Q can contribute to more flux. Although more than 150 and 170 sample results are used respectively for interpolation and the frequency of these samples is as high as daily, it will ignore the large changes in conditions that occur during non-sampling period (Figure 13) and it is not even possible to effectively capture the impact of rapid DOC transport on the flux caused by a heavy rainfall event on a certain day during sampling period, leading to over or under estimation of flux (Panton et al., 2020). Due to the limitations of interpolation by using the low temporal resolution dataset, OC flux was evaluated through modelling of rating relationship ([OC] vs Q) for verifying the reliability of the OC flux.

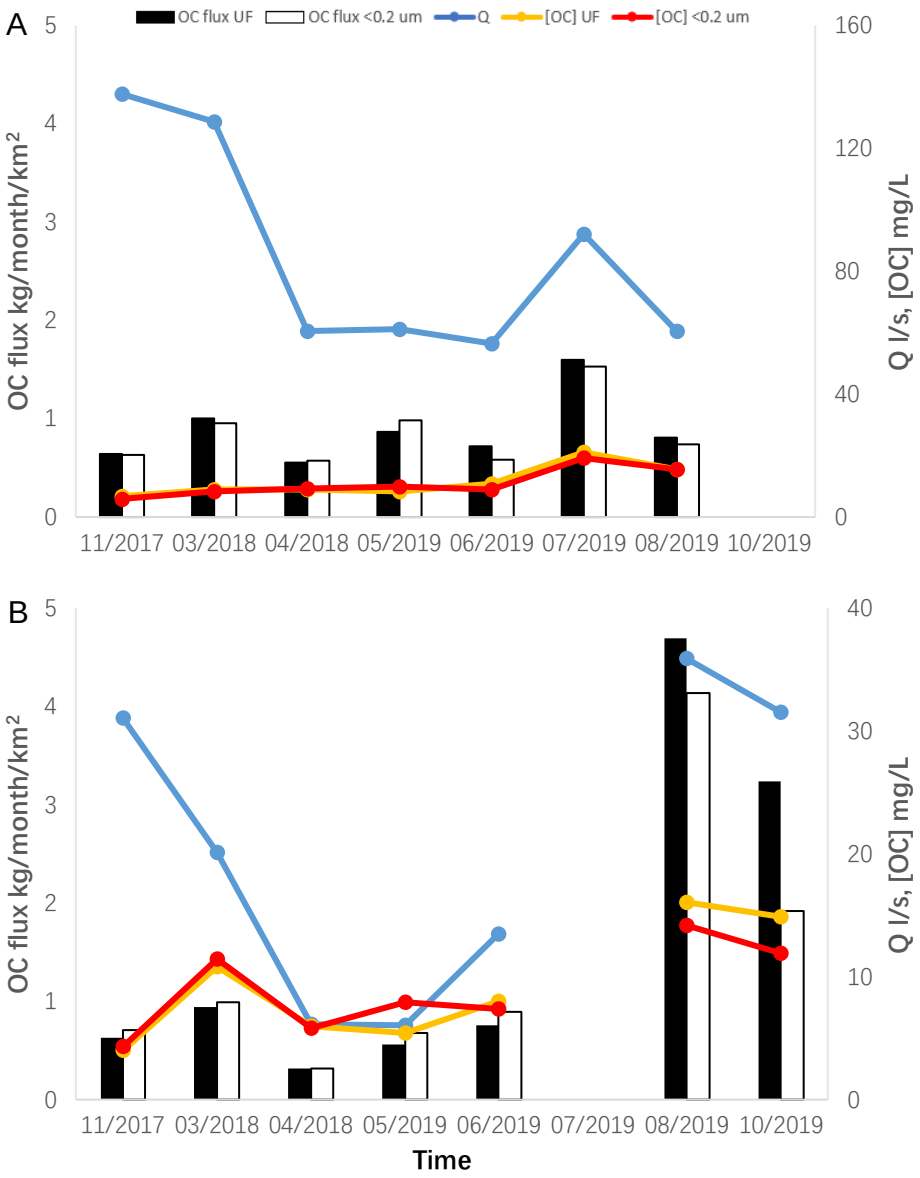

Figure 14 Estimation of OC flux at site 30 (A) and site 50 (B) by interpolation for each daily sampling period.

Comparison of fluxes by interpolation and rating relationships. Due to the limitation in interpolation, another flux estimation method was introduced for each site to verify the reliability of the results by comparing with interpolation. According to Table 3, OC fluxes estimated by rating relationship between [OC] and Q for were slightly higher than those estimated by

interpolation except for the mixing flux of site 30 (10.33 t/year/km^2 vs 10.2 t/year/km^2). Therefore, it is still be proved that DOC is obviously the dominant OC flux in stream and higher OC flux can be caused by erosion. Although the reliability of rating relationship curve requires further analysis, the similar of the estimated values from the two methods at least improves confidence in the accuracy and reliability of the OC flux values. Overall, the global C cycle will be strongly influenced by erosion and this situation must be considered while assessing the indirect C flux. It is necessary to reduce erosion and C release through adopting land protection measures, which is benefit for slowing the climate change (Lal, 2003).

Table 3 Estimation of OC flux in different forms by rating relationship for each site and compare with the values estimated through the interpolation *(Italic values in brackets).*

Study sites	Mixing flux of POC and DOC (t/year/km^2)	DOC flux (t/year/km^2)	% of DOC flux in total mixing flux
Site 30 (uneroded catchment)	10.33 *(10.2)*	9.55 *(9.78)*	92.48% *(95.9%)*
Site 50 (Eroded catchment)	18.35 *(19.31)*	16.5 *(17.1)*	89.91 *(88.57%)*

Comparison of OC flux with previous estimation. Do, P. D. have estimated the POC-containing OC flux in this study area in 2013 (6.74 t/year/km^2 for site 30 and 8.86 t/year/km^2 for site 50). The fluxes measured this time for both sites have increased by comparing to previous estimation, especially at site 50 (more than twice). Erosion is the dominant factor leading to the significant increase in OC flux at site 50 and OC flux will continue to change over long time. The role of stream systems in the export of OC from peatlands has been increasingly recognized in this situation. Therefore, the factors that contribute

to the increasing export of OC have been a significant research focus (Pawson et al., 2012).

Relationship between [OC] and Q. In order to predict and manage of OC transport in stream, it is paramount to determine the association between OC concentration and hydrological factor (Q). Neither POC-containing OC nor DOC (both R^2 were 0.0011) concentration almost had no correlation at site 30 (Figure 15). The dataset is mainly composed of daily samples under baseflow (low Q). Generally, DOC concentration is relatively low during baseflow and will not show a seasonal pattern (Buffam et al., 2001). Therefore, significantly different Q still produces many similar OC concentrations, and different OC concentrations can be shown under similar Q characteristics. Unlike site 30, there is a weak positive but significant correlation between OC and Q at site 50 in Figure 16 (R^2 0.16 for POC-containing OC concentration and R^2 0.11 for DOC concentration, both $P < 0.05$). This indicates that OC is more likely to be affected by Q, because erosion will cause serious depletion of the soil C pool on eroded compared with uneroded or slightly eroded soils, leading to the export of C from peat soil to stream along with Q easily (Lal, 2003). The relationship between [OC] and Q is still not high enough, mainly because daily samples account for majority in the dataset.

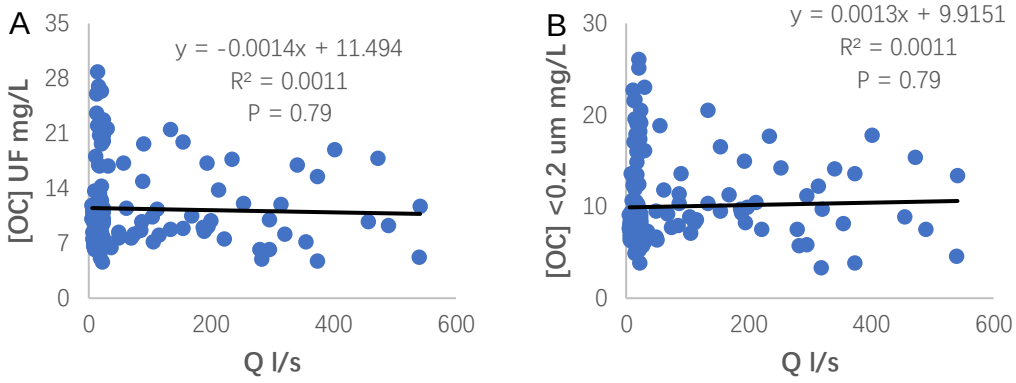

Figure 15 Relationship between [OC] and Q for A) UF and B) <0.2 µm at site 30. Each point represents a Q and [OC] measurement caught at the same time.

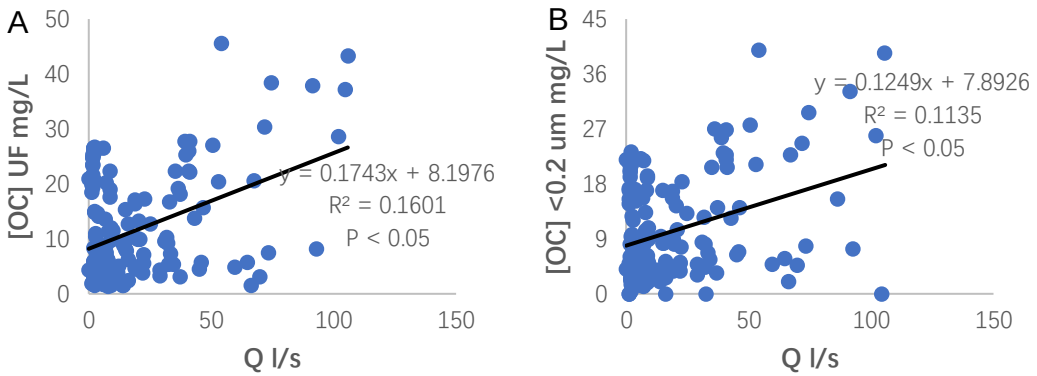

Figure 16 Relationship between [OC] and Q for A) UF and B) <0.2 µm at site 50. Each point represents a Q and [OC] measurement caught at the same time.

Figures 17 and 18 are plotted with Log (concentration) v Log (Q) to verify whether the dilution is the dominant factor affecting OC concentration. However, correlation between Log ([OC]) and Log (Q) did not improve, and it

became even worse at both sites (Figure 17 and Figure 18). Therefore, dilution is not dominant. Overall, the correlation between [OC] and Q based on daily samples from the two sites is relatively low. However, recent studies have reported that the concentration of DOC rises significantly in stream during stormflow (discharge event). Most of OC export from soils to streams during high Q following intense rainfall events. Although the intense rainfall events are short duration that occupy 4 – 24% of time a year, there are large proportion of the annual DOC export (36% to >50%) during this period (Buffam et al., 2001; Clark et al., 2007; Hook and Yeakley, 2005; Panton et al., 2020; Willey et al., 2000). Therefore, it is very important to accurately evaluate the change of DOC concentration during discharge event for the calculation of OC flux and the prediction of future long-term trend. Since the changes of Q within stream is rapid during discharge event, it is difficult to capture the influence of Q on the OC concentration by low temporal resolution sampling (daily sample). Higher DOC concentrations in discharge event are often missed during daily sampling (Clark et al., 2007; Vaughan et al., 2019). In order to quantify the influence of Q on the OC concentration during discharge event, high temporal resolution sampling is necessary (hourly sample).

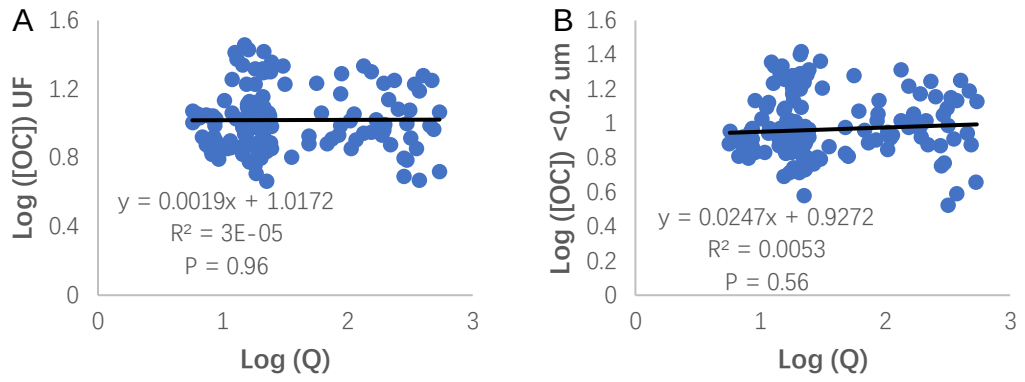

Figure 17 Relationship between Log ([OC]) and Log (Q) for A) UF and B) <0.2 µm at site 30.

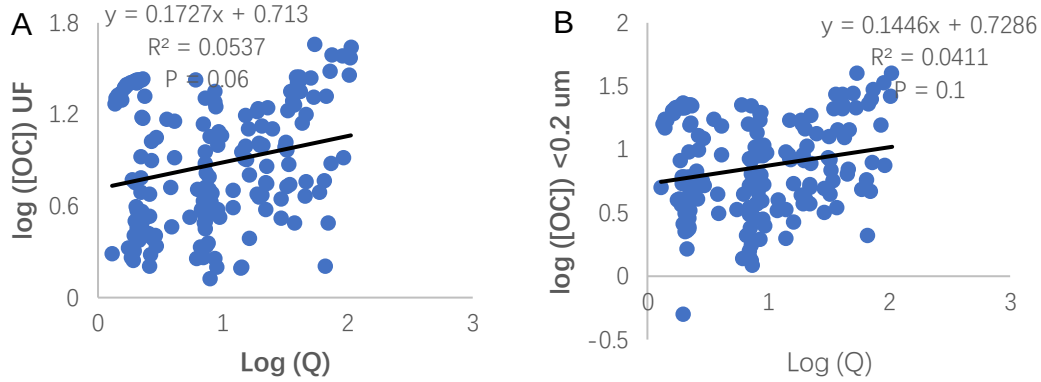

Figure 18 Relationship between Log ([OC]) and Log (Q) for A) UF and B) <0.2 µm at site 50.

Mobilisation of OC within a discharge event. It has been proved that the direct evidence of the impact of variability Q on OC cannot be found in the low temporal resolution sampling results in this study. Therefore, the assessment of high temporal resolution results on 04/2019 was carried out for determining the effect of Q during discharge event. Generally, DOC concentrations in

stream have been taken as indicative of OC concentrations and DOC flux is the dominant OC flux (Sobczak and Findlay, 2002). Meanwhile, DOC concentration of each sample is similar to POC-containing OC concentration, so this subsection mainly analyses the change of DOC concentration with Q. Figure 19 shows changes in Q and [DOC] throughout the discharge event. The DOC concentrations at both sites rose as Q increased and decreased after peak flow (558.4 l/s at site 30 and 89.93 l/s at site 50). This positive and significant correlation between DOC concentration and stream Q was also reflected in Figure 20 (R^2 0.63 for site 30 and R^2 0.39 for site 50, both $P < 0.05$). Multiple previous studies have shown that this correlation is one of the most consistent observations about DOC dynamics (Clark et al., 2007). One of the important drivers of stream Q is precipitation, so vary precipitation patterns will affect stream Q in riverine ecosystems (Frauendorf et al., 2019). The flushing of superficial soils on peat soil during discharge event is a common phenomenon in OC-rich peatland systems. The flushed terrestrial OC is rapidly transported to the stream and mobilised downstream by the increased Q. Meanwhile, DOC concentration in stream can also be contributed by atmospheric deposition that will increase during discharge event (Panton et al., 2020). Therefore, DOC concentrations and Q typically will rise within discharge event, leading to the larger OC yield (Fellman et al., 2009). The instantaneous peak fluxes of DOC at site 30 and site 50 were 215.82 kg/day/km^2 and 354.62 kg/day/km^2). In addition, the high-resolution

time series of [OC] v Q during discharge event for both sites is shown next to [OC] – Q relationship curves. Clockwise trajectory was shown at site 30 (Figure 20 A) and this occurs when concentrations increase more rapidly than the observed Q (Figure 19 A). This is named ‘Proteresis’ and it means a ‘flush’ response. However, the trajectory of site 50 was anticlockwise (Figure 20 B), indicating hysteresis (Figure 19 B) (Boyer et al., 1997).

Since DOC export during discharge event is an important role for the environmental carbon cycle, it is critical to understand the impact of different land types (such as eroded site and uneroded site) on the OC concentrations in order to predict and manage OC mobilisation in the stream (Fellman et al., 2009). According to Figure 19, even if the Q including the peak flow at site 30 was much greater than site 50 for most of discharge event period, the mean DOC concentration at site 50 was close to that at site 30 (7.9 mg/L vs 8.98 mg/L), the peak value of DOC was even higher than that of site 30 (22.82 mg/L vs 14.22 mg/L). This suggest that erosion has aggravated the export of OC from peatland. Erosion is a destructive process, especially under the impact of human activities. It depletes the soil fertility and destroys the soil structure, resulting in loss of OC in peat soil (Lal, 2003). Meanwhile, since transport of surface runoff and sediment can carry the soil C during erosion, water erosion has the greatest impact on OC storage (Ma et al., 2014). Therefore, erosion is important factor for controlling export of OC and it can

influence OC concentrations in stream through hydrological process (e.g. process of runoff and sediment transportation) and land-surface characteristics, resulting in OC to be more significantly influenced by Q. The duration and intensity of rainfall are two principal factors affecting erosion, because the soil aggregates will be broken into individual components by the kinetic energy of raindrops and then removed easily by runoff (Fellman et al., 2009; Ma et al; 2014). In view of the adverse effects of erosion on the global C cycle by accelerating the indirect C flux and meanwhile erosion is likely to be the situation of peatlands in the future, its impacts on release of GHG (CO_2) and global C cycle must pay more attention. The export, transfer and redistribution of soil OC caused by discharge event (high Q) and erosion is obvious. Therefore, due to the acceleration of the greenhouse effect and the risks of climate change caused by erosion, it is important and necessary to project and restore the soil resources by sustainable management of soil, which is increasingly recognized by the international community (Lal, 2003).

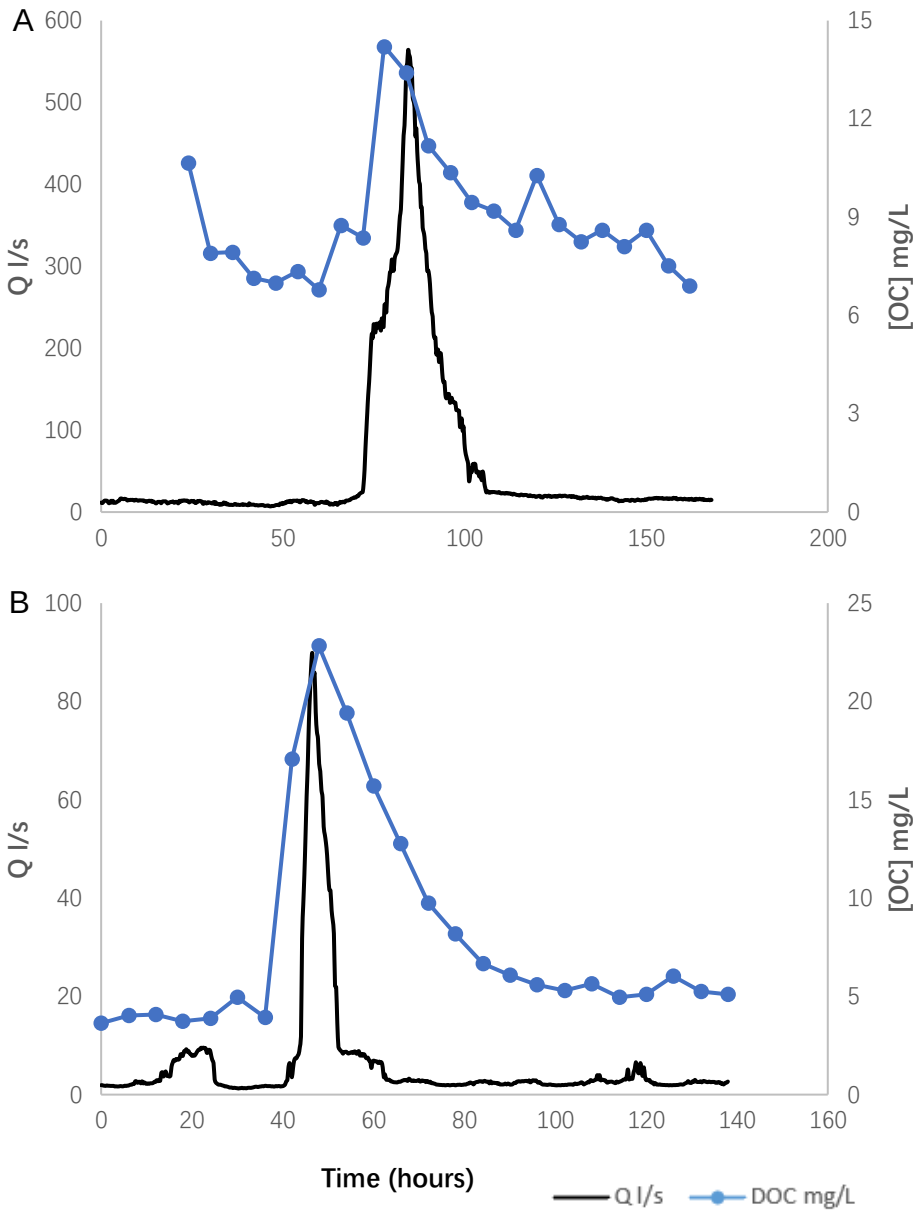

Figure 19 DOC concentration and discharge (Q) for A) site 30 and B) site 50 during discharge event.

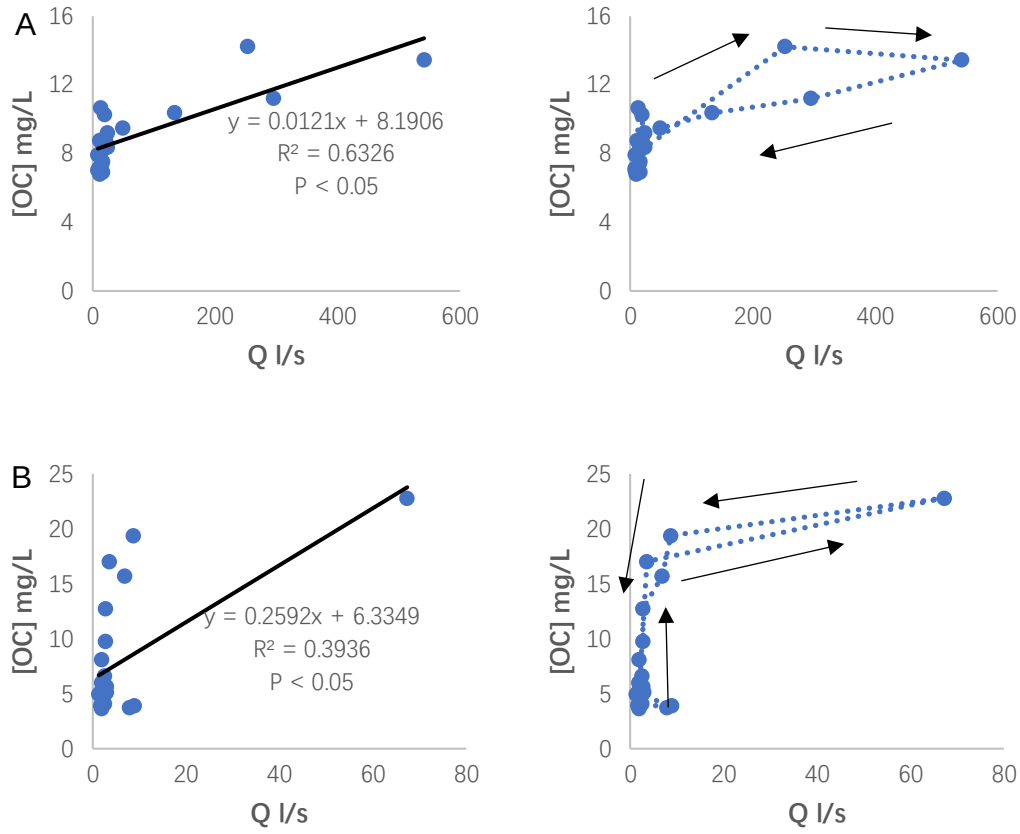

Figure 20 Relationship between [OC] and Q and the high-resolution time series of [OC] v Q during discharge event for A) site 30 and B) site 50. The time series direction is shown by arrows.

3.4 Conclusions

This study evaluated in detail the OC fluxes within eroded (site 50) and uneroded sites (site 30) in Peak District National Park through interpolation and rating relationship. The OC fluxes estimated from two methods are close and it is benefit for improving the accuracy of the results. The determination of OC flux will be the key to predicting the indirect C flux in peatlands and resulting GHG (CO_2). The estimated OC fluxes for both sites significantly

exceed values previously reported in 2013. This suggests that the OC flux will change continuously over a long period of time. DOC fluxes reported from both sites are very high, so it is the dominant in OC flux. In addition, both POC-containing OC and DOC fluxes at eroded site are much higher than those of uneroded site, indicating that larger OC release from peat soil is driven by erosion. Overall, site 50 is an example of a serious eroding peatland where loses large amount of C through land degradation and hydrological process caused by erosion, leading to the significant impact on environmental C balance. Site 30 and site 50 are potentially C sink and C source respectively. The prediction and management of future C fluxes can be improved through comparison of OC fluxes between two sites. For example, a reasonable land management strategy (e.g. increasing vegetation coverage) will reduce erosion in peat soil and protect OC storage.

The analysis of the low temporal resolution sampling results identifies that the correlation between OC concentration and Q is weak at both sites because the OC concentrations under baseflow are generally low and there is no seasonal pattern. In addition, OC – Q correlations at site 50 is slightly higher than that at site 30 and it means that erosion makes release of C more susceptible to Q, leading to mobilisation of OC. The results from high temporal resolution sampling within discharge event demonstrate the important role of Q as a control on the transport of OC from peat soil to

stream. OC concentrations at both sites is susceptible to be influenced by high Q and therefore obviously increased as Q rose. The results confirm previous studies highlighting the significant positive correlation between OC concentration and Q during discharge event. In addition, in the case of a large difference in mean Q between the two sites (site 30 >> site 50), the mean OC concentration is close. This indicates that the erosion is a significant factor that aggravating the mobilisation of OC and attendant emission of GHG. These results can help us to better understand the impact of erosion and climate change on the dynamics of OC in streams.

Overall, when OC is eroded and redistributed via aquatic systems, indirect C flux from peat soil is larger and less well-constrained than direct C flux. As a result, erosion has caused more GHG emissions and aggravated the process of climate change such as changed rainfall pattern and increased temperature. Meanwhile, climate change will continue to intensify erosion in peat soil (e.g. higher temperature causes the drier peat soil), resulting in more C loss. This vicious circle has severely disrupted the global C balance. Therefore, it is critical to quantify current and predict future C fluxes in upland peat catchment and this will be completed and improved by longer-term monitoring and analysing data.

Chapter 4. Effect of NOM on speciation and size of Fe change with flow path, pH, temperature and daylight in natural waters

4.1 Introduction

Fe in natural waters. In water Fe is soluble in the absence of dissolved oxygen (D.O.) as predominantly FeII, whilst particulate in oxic environments as suspended insoluble FeIII(hydr)oxides which may coagulate and be deposited. In natural waters the range of pH and Eh is such that the state of Fe can vary across this full range of valency, solubility and size. The ubiquity of Fe means predicting this variability is, therefore, often critical to managing the aquatic environment because it can change the availability both of metabolites to drive geomicrobial transformations and the ratio of surface area to fluid volume (specific surface area; SSA) (Baalousha, 2019; Viollier et al., 2000).

Fe can be oxidized or reduced within natural waters and each process can be harnessed in microbial metabolism with consequent changes in mobility of Fe and metabolites such as sulfate, nitrate and heavy metals. To predict the location of such transformations can be critical for managing water quality and is dependent on predicting the location of FeII and FeIII (Baalousha et al., 2006; Vignati, 2003; Weber et al., 2006).

The mobility of many contaminants and nutrients in most natural waters is largely controlled by sorption rather than precipitation and consequently the SSA is a critical control on their distribution in the aquatic environment. FeII is the precursor of, and FeIII(hydr)oxide often forms a large proportion of, the SSA in natural waters. Prediction of contaminant and nutrient fluxes within and from the aquatic environment is dependent on predicting the presence and specific surface area of FeIII(hydr)oxide (Weber et al., 2006).

Fe NOM interaction. The relationship of pH to rates of oxidation of soluble FeII and production of particulate FeIII(hydr)oxide has been well understood for many years (Davison and Seed, 1983). However, defining the role of components other than H+ and D.O. in precipitation and the subsequent controls on particle size distribution and are an ongoing requirement of research. Of these other components NOM has often been shown to exert dominant control on Fe speciation and size - via precipitation and agglomeration of FeIII(hydr)oxide. Fe behavior is controlled by both direct interaction with NOM and via inorganic and organic species produced from NOM, typically by photochemical processes (Catrouillet et al., 2014; Chen and Thompson, 2018; Riedel et al., 2003).

Fe complexation with NOM has been shown to slow FeII oxidation, precipitation of FeIII(hydr)oxide particulate and subsequent agglomeration

(Emmenegger et al., 1998; Gaffney et al., 2008; Liang et al., 1993; Jackson et al., 2012). However, in order to improve reliability in prediction of the behavior of Fe in natural waters that contain NOM requires expansion of the range and combinations of variables used in laboratory simulations so as to match an extended range of environmental conditions.

Importance of anoxic interaction of Fe and NOM. In this work the primary extension of conditions is to consider anoxic interaction of FeII and NOM and, therefore, also compare sequential with instantaneous mixing of Fe(II), NOM and D.O. (Figure 21).

Most previous work has focused on the role of NOM in controlling oxidation of FeII and therefore laboratory model systems have mixed FeII, NOM and D.O. at the same time (Chen and Thompson, 2018; Miller et al., 2009; Theis and Singer, 1974; Von Der Heydenm et al., 2014). A central finding of these studies has been the binding of FeII to NOM and its preservation in oxic waters. This observation of binding of FeII by NOM under oxic conditions suggests it could also be bound before being exposed to D.O.. If this were the case it would change Fe behavior in the anoxic subsurface but also make whether the mixing of FeII with NOM and D.O. is coincident or sequential, a variable in controlling the eventual speciation and particle size of Fe in oxic waters.

The coincident mixing (Type A interaction) that has mostly been studied simulates a natural environment limited to the oxycline; a boundary zone between anoxic and oxic waters (Emmenegger et al., 1998; Liang et al., 1993). Sequential mixing (Type B interaction) is likely to be more environmentally relevant as it simulates interaction of Fe and NOM in the subsurface, a zone of much greater extent and in which residence times are longer, prior to exposure of Fe(II) to D.O..

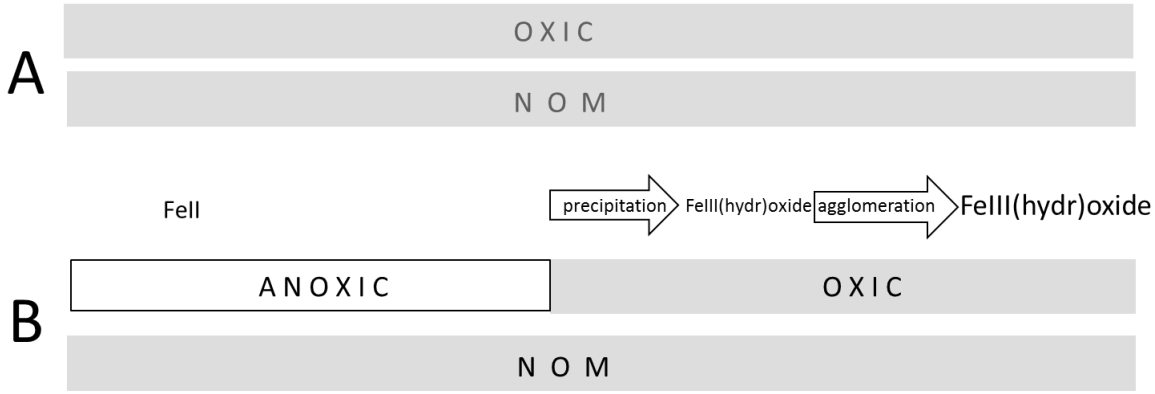

Figure 21 Schematic of A) typical simulation conditions under which transformations of FeII to FeIII(hydr)oxides are studied; coincident mixing [(FeII+NOM+D.O.)] and B) conditions which simulate more generally applicable conditions; sequential mixing [(FeII+NOM) + D.O.].

Limitations of previous work on anoxic binding of FeII. In response to this rationale Jackson investigated Fe(III) (hydr)oxide production after Fe(II) first interacted with NOM in the absence of D.O. and on its subsequent exposure to D.O. saturated waters. Jackson found, using ferrozine assay, that only 7%

of FeII was bound to NOM anoxically, compared to the 78% in an oxic mixture and concluded that anoxic binding would not be a dominant influence on eventual Fe SSA production (Jackson et al., 2012). However, the results may only be relevant to the pH of the study, which at 6.2 is below that of most natural waters. Daugherty found that between 5% and 20% Fe bound to NOM anoxically but neither the subsequent effect on particle size nor comparison to the fate of Fe, when D.O. and NOM exposure were coincident, was made (Daugherty et al., 2017). FeII binding to NOM in natural waters was also observed by Liu but its controls were not investigated, and as in the other studies the NOM was not characterised and selected so as to be as representative of relevant NOM as possible (Liu et al., 2017).

The requirement remains therefore, to determine whether and under what conditions, NOM can control not only FeII mobility in the subsurface but also subsequent speciation and size of Fe in oxic surface waters.

Daylight exposure and temperature. The oxygen status of natural waters is strongly correlated with exposure to daylight and temperature. Anoxic waters are almost inevitably dark and oxic light, consequently, inclusion of daylight exposure as a variable will make simulations more environmentally relevant. Similarly, whilst it is not the case that one is always warmer than the other, for most of the year there is a difference in temperature of ground and surface

waters, which should also be included as a variable. Consequently, environmental relevance requires that simulation of mixing order should also test the impact of daylight exposure and temperature. FeII oxidation is caused by O_2, O_2^- (superoxide) and H_2O_2 (Santana-Casiano et al., 2005) and the concentration of the latter in natural waters is produced by the action of UV light on NOM (Cooper et al., 2005). Furthermore, photolysis of NOM also generates species that oxidise FeII although this process is limited because the organic oxidants which are produced by photolysis in daylight, are only stable in darkness and, furthermore, they promote oxidation only under acid conditions (Garg et al., 2013; Garg et al., 2013). The net result of the presence of FeII, NOM and UV is, therefore, complicated and requires further investigation because, as previously stated, NOM is also known to slow the oxidation of FeII as a result of complexation (Jackson et al., 2012; Theis and Singer, 1974; Miller et al., 2009).

Selection of NOM. Due to the wide compositional heterogeneity of NOM (Jaouadi et al., 2012; Penru et al., 2013), the balance of efficient design of simulations and their general applicability to natural waters can only be achieved by classifying NOM into a small number of types and/or selecting a type of NOM that is representative of many natural waters. Classification by size was chosen because it is directly related to reactivity and mobility, and material can be definitively separated into size classes for use in experiments

(Taujale et al., 2016). Classification by chemical composition is comparatively less effective, as it requires selection of characteristics by which to classify and the relationship of the characteristics to provenance or fate is less clear and consistent than is the case for size (Daugherty et al., 2017).

Waters draining deep peat have been selected as the source of NOM because this largely humic material dominates many natural waters, is present in almost all natural waters and mature NOM shows greater interaction with Fe – humic acid (HA) interacted more than landfill leachate or aquagenic NOM (Cheng and Allen, 2006; Jackson et al., 2012). Large particles of NOM (>1 µm) were removed from samples as they were unlikely to be present or mobile in both groundwater and runoff. In order to reduce site-specificity of this NOM it was standardised by selecting a single class for use. To maximise the relevance of a single size fraction it should be the one likely to have the most pervasive effects; it should form the largest proportion of the TOC surface area, a function of both size and concentration. As concentrations of NOM in each size class are liable to vary seasonally and with discharge a programme of monitoring both NOM and discharge in the stream draining the deep peat was used to allow colloidal particle size distribution of NOM to be recognised and long-term (3 years) mass fluxes of each size class to be calculated.

Whilst provenance and size are used to select the NOM in this study, in order that results can be related to other (future or previous) work in which NOM has been chemically characterised, the selected NOM has also been analysed by gas chromatography mass spectrometry (GC-MS).

Aim and objectives. This work will use laboratory systems to simulate anoxic mixing of Fe and NOM and compare the effects of coincident and sequential mixing order to understand hydrochemical controls on the mobility of Fe. The Crowden Great Brook (Derbyshire, Peak District, UK) is chosen for the river system that allows for production of NOM stocks and easily measurable Fe concentrations. The generality of the findings will be maximised by making the comparison across a range of environmentally relevant pH, temperature and daylight exposures and by selecting the NOM used to be as representative as possible. This also can contribute to prediction of the character and distribution of SSA in natural waters. Fe speciation will be resolved into free Fe(II), bound Fe(II), bound Fe(III) and FeIII(hydr)oxides whilst particle size, as a proxy for SSA, of starting materials and end-products will be assessed by molecular weight cutoffs at 10 and 3 KD. In order to achieve the aim of this work the following objectives are:

- To determine if the Fe-NOM interaction takes place under anoxic and oxic conditions.

- To develop the Fe-NOM experiments by addition of different conditions (Fe:NOM ratios, pH, light, temperature and mixing order of Fe, NOM and D.O.).

- To monitor the rate of Fe-NOM interaction under different experimental conditions and analyze their effect on interaction and products.

- To analyse PSD of Fe or NOM after interaction and determine if there is a change.

4.2 Materials and methods

Collection of NOM. Samples of runoff were collected from an instrumented stream draining an upland peat catchment, Crowden Great Brook, in the Southern Pennines of the UK (UK grid reference SE068001). Whilst pollution and land management practices have damaged extensive areas of upland peat in the Southern Pennines, causing vegetation degradation and erosion, the catchment upstream of the sampling point used in this study had a complete vegetation cover.

Size separation of NOM. NOM was standardised to the non-settling fractions only (colloidal and dissolved) by pressure filtration through 1 µm membrane

filters (Whatman, UK). Prior filtration through 5 µm membrane filter was necessary to prevent clogging of the 1µm filter.

Sub 1µm NOM was separated by TFU into 5 size classes: <1>0.2 µm, <0.2 µm >100 KD, <100>10 KD, <10>3 KD and >3 KD using polyether sulfone membrane plates (Vivaflow50, Sartorius, UK). The membrane plates were flushed with DIW prior to use this was done until no OC was detectable in filtrate or retentate.

TFU was used instead of direct flow ultrafiltration as the direct pressure in the latter can lead to larger particles blocking or being pushed through the membrane. The tangential flow in TFU avoids this problem as fluid passes across the filter plate and material is separated by osmosis. However, whilst pressure filtration has a clear endpoint – when the sample volume has passed wholly into filtrate – TFU does not and separation may be incomplete. Validation is, therefore, necessary but rarely reported. In this work validation of separation was achieved by monitoring the mass balance of the OC. The mass of OC in the filtrate was calculated by multiplying its volume by the TOC concentration and separation was deemed complete when the mass became constant.

To achieve constant mass the process had to take place for so long that the retentate volume had to be replenished. The stream water was of low electrical conductivity (EC), circa 40µS, so rather than attempt to maintain a constant EC, DIW was used which did result in EC dilution from 40 to 5µS during the process.

Selection of appropriate size class of NOM. 20 samples were taken from the monitoring point on Crowden Great Brook across a range of discharge conditions over 3 years. Discharge was monitored at 15 minutes resolution and a flow duration curve was constructed for the monitored period. TFU of each sample produced NOM concentrations for each size fraction, these were then assumed to apply across a range of discharge centred on the discharge measured at the time of sampling. The volume of water discharged within each range was calculated from the flow duration curve and multiplied by the NOM concentration in each size class; this gave the mass of NOM of each size discharged within each discharge class. The masses in each discharge class were summed to give the total mass flux for each size class during the monitored period (Figure 22).

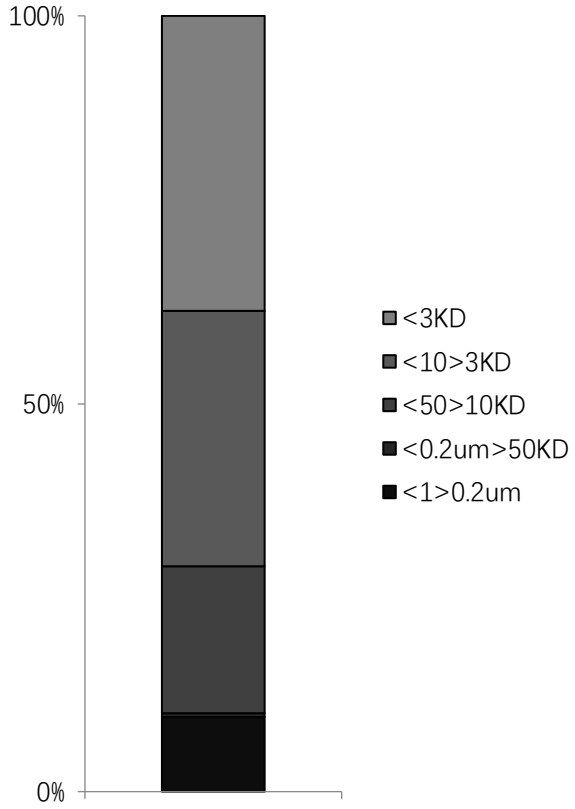

Figure 22 Proportions of total mass of OC within particular size classes in runoff from Crowden Great Brook. Calculated from measurements of concentration and discharge made over 3 years.

30% of the long-term mass flux of NOM was <3 KD, although this fraction was smallest in size and the largest component of flux it could not be used in the experiments as it could not be concentrated because it was the filtrate from the lowest available molecular weight cutoff. The <10>3 KD fraction was the dominant size class of the remaining NOM and was selected for use in the experiments; this was 26% of the NOM flux and small enough to remain mobile in natural waters particularly within the porous materials of the sub-surface. Previous work has shown humic substances to be <14 KD therefore

this study is comparable to those using fulvic substances (10-14 KD) (Yan et al., 2012), also in surveys of natural waters metal binding to NOM the largest proportion of metals including Fe are typically bound by <10 KD NOM (Luan et al., 2015).

Chemical characterisation of selected NOM. The NOM was prepared for analysis by freeze drying. Approximately 1 mg of dry material was analysed by pyrolysis gas chromatography mass spectrometry (Py GC-MS). It was weighed into a quartz sample tube and pyrolysed using a Chemical Data Systems 5200 series Pyroprobe by heating at 700°C for 20 seconds. Liberated fragments were analysed using a Agilent 7890A Gas Chromatograph interfaced with an Agilent 5975A MSD Mass Spectrometer operated in electron ionization (EI) mode (scanning a range of m/z 104 50 - 600 at 2.7 scans s^{-1}, ionization energy 70 eV and a solvent delay of 1 min.). The gas chromatograph was equipped with a Zebron ZB-5MS column (length 30 m, I.D. 0.25 mm, film thickness 0.25 µm). The pyrolysis transfer line and injection temperature were set at 350°C, the heated interface at 230 °C and the MS quadrupole at 150°C. Helium was used as the carrier gas and the samples were introduced in split mode (split ratio 5:1, constant flow of 5 ml/min). The oven was programmed from 40°C (for 5 mins) to 320°C at 4°C min^{-1} and held at this temperature for 10 mins.

Compounds were identified from chromatographs by comparison of relative retention times and spectra to those reported in the NIST library. Peak areas were calculated for each compound to allow semi-quantitative attribution of their relative proportions. Whilst the characterisation was primarily to allow comparison to other samples; to assemble a “fingerprint”, the compounds detected were grouped by degree of oxidation to also give some functional relevance.

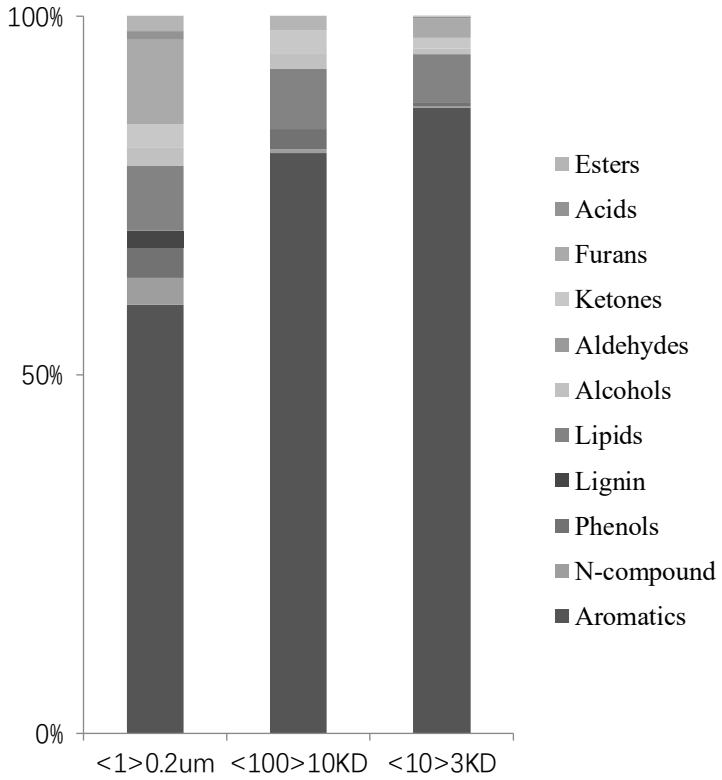

Figure 23 Relative abundance of compounds in terms of degree of oxidation in different size classes of NOM collected from Crowden Great Brook (only size classes in which enough solid could be isolated were analysed).

As size decreased the proportion of aromatic moieties detected by Py GC-MS increased, reaching a maximum in the <10>3 KD fraction used in the experiments (Figure 23). This distribution of moieties suggests the NOM in the <10>3 KD fraction was more mature than that of the larger fractions and should, therefore, be most likely to interact with Fe (Jackson et al., 2012).

Preparation of FeII stock solution. 400 ml DIW, in a custom fabricated gastight container with magnetic stirrer and several sealable ports, a D.O. and pH electrode, was deoxygenated by purging with Ar whilst stirring. Once anoxic solid $FeCl_2$ (Sigma, UK) was added to make a stock of 500 mg/L FeII and then sealed. D.O. and pH were monitored and no changes were recorded during the 48 hour periods between making fresh stock.

Fe speciation, total Fe and total OC. Fe II concentration was determined by ferrozine assay (Stookey, 1970); chelation and subsequent spectrophotometry to measure colour development. Free and bound Fe(II) were resolved by measuring colour development at different times.

Free FeII was measured by taking 0.5 ml sub-samples and mixing with 0.5 ml ferrozine in an open 1.6 ml cuvette (semi-micro cuvette, Fisher Scientific, UK) then measuring colour development after 30 seconds. Each analysis was repeated 3 times.

Bound FeII was measured by monitoring colour development and recording its maximum. This required colour development of a sub-sample to be monitored at hourly and then daily intervals and was only undertaken on the sub-sample taken at the end of the experiment – oxic equilibrium. Given the length of the period in which colour development was monitored it was necessary to preserve the sub-sample from oxidation and evaporation. This was achieved by taking the sub-sample in a syringe and mixing it with ferrozine by connecting a syringe containing de-gassed ferrozine and repeatedly transferring the combined fluid between syringes. Because each time colour was monitored required the sample to be decanted into a cuvette, sub-samples had to be used sacrificially. Therefore, a set of 18 were extracted at oxic equilibrium and for each measurement of colour 3 replicate syringes containing sub-sample and ferrozine were used. Monitoring continued until absorbance was no longer increasing and the maximum value was used to calculate bound FeII concentration from a calibration line.

FeIII(hydr)oxide production during oxidation was calculated from the coincident production of acidity as done previously (Gaffney et al., 2008; Jackson et al., 2012). This was recorded as the cumulative addition of base by the auto-titrator (Titroline 7000, SI Analytics, UK) in order to maintain the pH at the set value. As a control, a solution of FeII in DIW was monitored on exposure to air, with the pH maintained at 6.5. Under these conditions all Fe

should have precipitated as amorphous $Fe(OH)_3$, and when free FeII was no longer detected and base additions had ceased the equivalent of 3M of H^+ had been added for each mole of FeII (Figure 24). Therefore, for subsequent experiments the proportion of Fe present as FeIII(hydr)oxide was calculated by dividing the experimental base addition by that of the control.

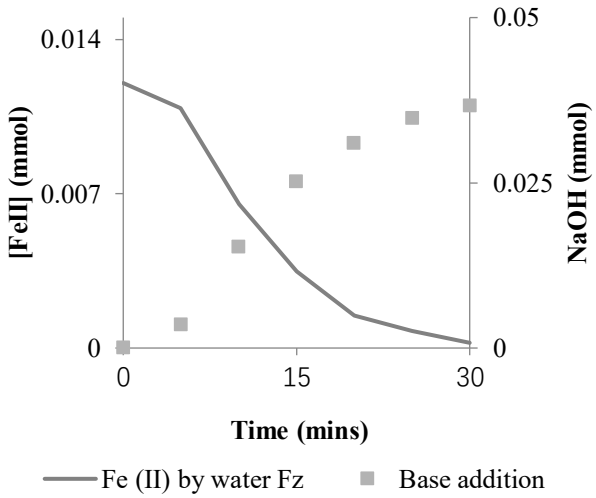

Figure 24 Base addition on oxidation of FeII in DIW in order to maintain pH 6.5, 0.0366 mmol of base for 0.012 mmol of FeII.

Total Fe concentration was analysed by acidifying samples using concentrated HNO_3 to pH < 2 then using inductively coupled plasma atomic emission spectroscopy (ICP-AES) (Optima 5300, Perkin-Elmer, United Kingdom). Total organic carbon (TOC) concentration was determined by furnace and digestion in a total organic carbon analyzer (Shimadzu TOC-V CPN, Japan). In both cases a set of standards were run every five samples with drift assumed to be linear and, therefore, corrected by interpolation. The

pre-drift-corrected error on all standards was below 5%.

Type A interaction. 400 ml with OC concentration of 17.2 mg/L was prepared by addition of the selected <10>3 KD NOM to DIW in a custom fabricated gastight container with magnetic stirrer and several sealable ports a D.O. and pH electrode. Adjustment to the selected pH (6.5 or 7.5) was by auto-titration with 0.01M NaOH (Analar, Sigma, UK). The fluid was stirred in an open vessel with the auto-titrator set to maintain the fluid at the experimental pH, and base addition was monitored continuously during the subsequent oxidation. When pH was stable after the addition of NOM, FeII stock was added by pipette to make the requisite Fe concentration.

0.5 ml sub-samples were extracted periodically to determine free FeII concentration until this fell to zero or remained constant between sub-samples. At this point a set of 18 sub-samples were taken in syringes to determine bound FeII concentration. The remainder of the fluid was passed across a 10 KD plate, as above, to determine whether there had been any change in PSD of Fe or NOM. The endpoint of the filtration was recognised when the mass of OC in the filtrate became constant and the TOC and total Fe concentrations of filtrate and retentate were then determined.

Type B interaction. The fluid containing NOM was prepared as for Type A above. To measure anoxic interaction the fluid was then deoxygenated by purging with Ar whilst stirring. FeII stock was added to make the requisite Fe concentration via a sealable port.

0.5 ml sub-samples were extracted periodically to determine free FeII concentration. When this remained constant between sub-samples the fluid was then either used sacrificially to determine whether there had been any increase in PSD, of Fe or NOM, or the simulation continued with the admission of D.O..

The former was achieved anoxically by connecting the sealed vessel to the TFU system and using gas impermeable tubing including the peristaltic pump tubing (Masterflex C-Flex, Silicone, Cole Parmer), and passing the sample over the 10 KD plate. In the latter case the stirred vessel was opened to air and base addition was monitored continuously during the subsequent oxidation. 0.5 ml sub-samples were extracted periodically to determine free FeII concentration until this fell to zero or remained constant between sub-samples. At this point a set of 18 sub-samples were taken in syringes to determine bound FeII concentration. The remainder of the fluid was passed across a 10 KD plate, as above, to determine whether there had been any increase in PSD of Fe or NOM. The endpoint of the filtration was recognised

when the mass of OC in the filtrate became constant and the TOC and total Fe concentrations of filtrate and retentate were then determined.

Conditions under which Type A and Type B were compared. Type A and B simulations were compared under the conditions listed in Table 4.

Table 4 Listing of variables and their ranges across which anoxic mixing (Exp. 1) and Type A and Type B mixing of Fe, NOM and D.O. were simulated. Cells in bold highlight the parameters being compared.

	Anoxic mixing	Type A and Type B simulations		
	Experiment 1 Fe:NOM	Experiment 2 pH	Experiment 3 Temp	Experiment 4 Light
pH		**6.5**	6.5	6.5
	7.5	**7.5**		
Temp. ^{0}C			**10**	
	25	25	**25**	25
Light	Day	Day	Day	**Day**
				Night
NOM	**1:5**			
	1:10	1:10	1:10	1:10
	1:15			

pH was set at either 6.5 or 7.5 by auto-titrator running as a pH stat and temperature set and maintained at 10 or 25^{0}C by running the experiments within an incubator. The incubator (Gallenkamp Cooled incubator, UK) also allowed daylight to be excluded or standardised; a full spectrum LED light (Sansi, C21GL-DE27, Sansiled.com) with 153 µmol/s/m^2 and 1448 lumens illuminated 0.25 m^2 (5792 Lux). This level of illumination was much greater

than the open laboratory and simulated outdoor daylight conditions between overcast and indirect sunlight.

4.3 Results and Discussion

Fe speciation in the absence of NOM. In the absence of NOM, at pH 6.5 and 7.5, at 25^0C in daylight, Fe introduced as free FeII was shown by ferrozine assay to have remained as such for the monitored period of 300 minutes in the anoxic vessel (Figure 26 and 27) and TFU showed no change in PSD in the Fe solution. On exposure to air free FeII concentration fell to zero and coincident acid production was sufficient that 98% of the FeII had converted to FeIII(hydr)oxide in 35 minutes at pH 6.5 and 17 minutes at pH 7.5. These findings demonstrated that the apparatus was able to maintain the experimental conditions and the monitoring procedures were effective.

Anoxic interaction of FeII and NOM. Under anoxic conditions in the presence of NOM it is apparent (Figure 25) that not all FeII is a free ion; some becomes bound to NOM and this binding also causes some NOM to coagulate and both NOM and Fe to become >10 KD (Figure 25); both processes are discussed below.

Anoxic binding of Fe to NOM. The rate and amount of FeII binding at pH 7.5 increased (46, 80, 100, 100%) as the Fe:NOM decreased (1:5, 1:10, 1:15,

1:30) (Figure 25). FeII binding capacity for each mg of OC in the NOM can be determined from the 1:5 and 1:10 Fe:NOM ratios to be in the range 0.067 - 0.08 mg of Fe. This is based on the assumption, which will be returned to in the section on coagulation, that all OC is identical with respect to its binding capacity. At pH 6.5 and Fe:NOM of 1:10 FeII binding reached a maximum of 18% a binding capacity (mg FeII / mg OC) of 0.018. The lower capacity is a consequence of the higher $[H^+]$ and increased competition for binding sites on the NOM.

The 20% of FeII deduced to be bound at pH 6.5 and 80% at pH 7.5, using ferrozine assay, is much higher than the 7% deduced to be bound by Jackson et al., (2012). However, Jackson experimented at pH 6.2 and Fe:OC of 1:7 mg/L rather than the 1.7:17 mg/L of this study. Jackson's conclusion that the anoxic binding was insignificant, compared to the subsequent binding on oxidation, appears to have been a judgement specific to a pH that is relatively low for most natural waters and to a particular Fe:OC ratio. Previous studies demonstrate the capacity of different kinds of OM to bind with Fe in subsurface redox conditions (Daugherty et al., 2017; Liao et al., 2017; von der Heyden et al., 2014).

Binding of otherwise free FeII and therefore its fate in the sub-surface can be strongly controlled by NOM concentration but the importance of this influence

decreases with pH. In the sections below on the effect of mixing order, the impact of this sub-surface influence on Fe speciation and size when waters are subsequently exposed to D.O. is determined by comparison to Fe evolution when FeII, NOM and D.O. are mixed simultaneously.

Anoxic coagulation of NOM by Fe. Anoxic binding with FeII has caused some of the <10 KD NOM to coagulate as 40 - 90% of FeII became > 10 KD at pH 6.5 and pH 7.5 (Figure 25). This phenomenon will reduce mobility of Fe and NOM particularly in porous material and is likely to be pervasive in the subsurface where very small NOM, as used in the simulations (<10 KD), will dominate. The impact on mobility will be a function of the size increase, however, in the experiments this could only be defined by a lower limit (10 KD), as the suspension was only passed over a 10 KD plate, and the upper limit may have been greater.

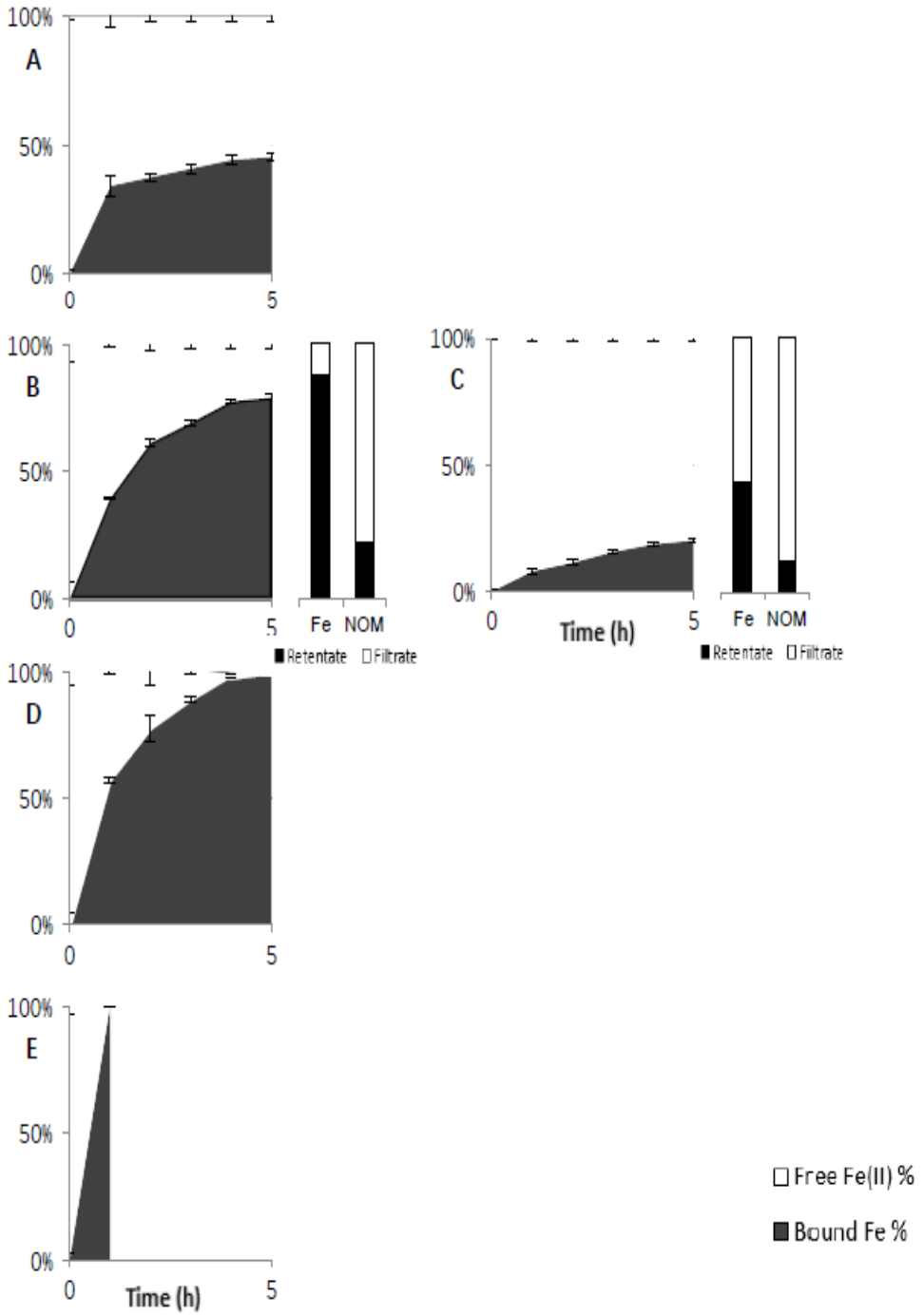

Figure 25 Fe speciation over time under 25 degrees, full daylight and anoxic conditions. (A) Fe:NOM ratio is 1:5 at pH 7.5; (B) Fe:NOM ratio is 1:10 at pH 7.5 and PSD of Fe and NOM at the end point are shown beside; (C) Fe:NOM ratio is 1:10 at pH 6.5 and PSD of Fe and NOM at the end point are shown beside; (D) Fe:NOM ratio is 1:15 at pH 7.5; (E) Fe:NOM ratio is 1:30 at pH 7.5.

Table 5 Speciation and size of FeII and NOM in mass and % of total in an anoxic suspension of 1.7 mg/L Fe and 17 mg/L OC.

		Bound FeII	FeII >10 KD	OC > 10 KD
pH 6.5	%	18	42	12
pH 7.5	%	80	90	20
pH 6.5	mg	0.31	0.71	2.04
pH 7.5	mg	1.36	1.53	3.40

TFU was carried out anoxically at only one Fe:NOM ratio (1:10) but at both pH 7.5 and 6.5, the changes in particle size observed allow further information to be inferred about the NOM involved in, and the strength of anoxic FeII NOM binding:

At pH 7.5, 1.53 of the 1.7 mg of Fe has become >10 KD but only 3.4 mg of OC has become >10 KD, therefore, the binding capacity of OC for FeII is 0.45 mg (Table 5). This is much higher than the FeII binding capacity derived above on the assumption that all NOM is equal with respect to its binding capacity. Therefore, even after NOM has been constrained to a narrow size class (<10>3 KD), it remains heterogeneous with only 20% having a suitable composition for it to interact with FeII.

At pH 7.5 the amount of FeII that has been bound is almost the same as the amount that becomes > 10 KD by coagulating the NOM to which it is bound.

The amount coagulated is in fact slightly greater and this positive discrepancy is greater at pH 6.5. The discrepancy probably arose because although binding was complete at 5 hours, the TFU process took a further 1-2 hours during which coagulation may have continued. However, if coagulation of all FeII that binds to NOM is immediate and therefore also complete at 5 hours, the discrepancy indicates that FeII is more easily released from the bound coagulated Fe by ferrozine chelation than by the process of TFU.

The effect of mixing order. At pH 6.5, differences in mixing order (Type A or Type B) (Figure 26) result in differences in the rate at which Fe speciation changes and differences in the ultimate proportions of FeIII(hydr)oxides, bound FeII and FeIII at oxic equilibrium.

Under Type B at pH 6.5, 15% of FeII was bound anoxically and after admission of D.O. and equilibration the amount of bound FeII remains similar but total bound Fe increased to 50%. In this study it could be shown, rather than just suggested as by Gaffney (Gaffney et al., 2008), that this increase consists of FeIII that becomes bound before it can hydrolyse. If NOM is assumed to be saturated with FeII during the anoxic period then the subsequently available FeIII must occupy different NOM or different site on the NOM to that occupied by FeII.

The outcome of Type A mixing differs to Type B in that slightly more (62%) Fe becomes bound at oxic equilibrium and, whilst as under Type B this consists of both FeII and FeIII, the 30% of FeII bound was higher than the 15% under Type B. The latter difference is, however, inconsistent as bound FeII concentration was assumed to reach its maximum capacity during the 5 hours anoxic equilibration period of Type B. The inconsistency is likely to arise from the errors on these 2 measurements of bound FeII and, therefore, there are no clear differences in Fe speciation at oxic equilibrium between Type A and Type B. Differences may become clearer, however, as the amount of anoxic binding of FeII increases, as this was only 15% at pH 6.5.

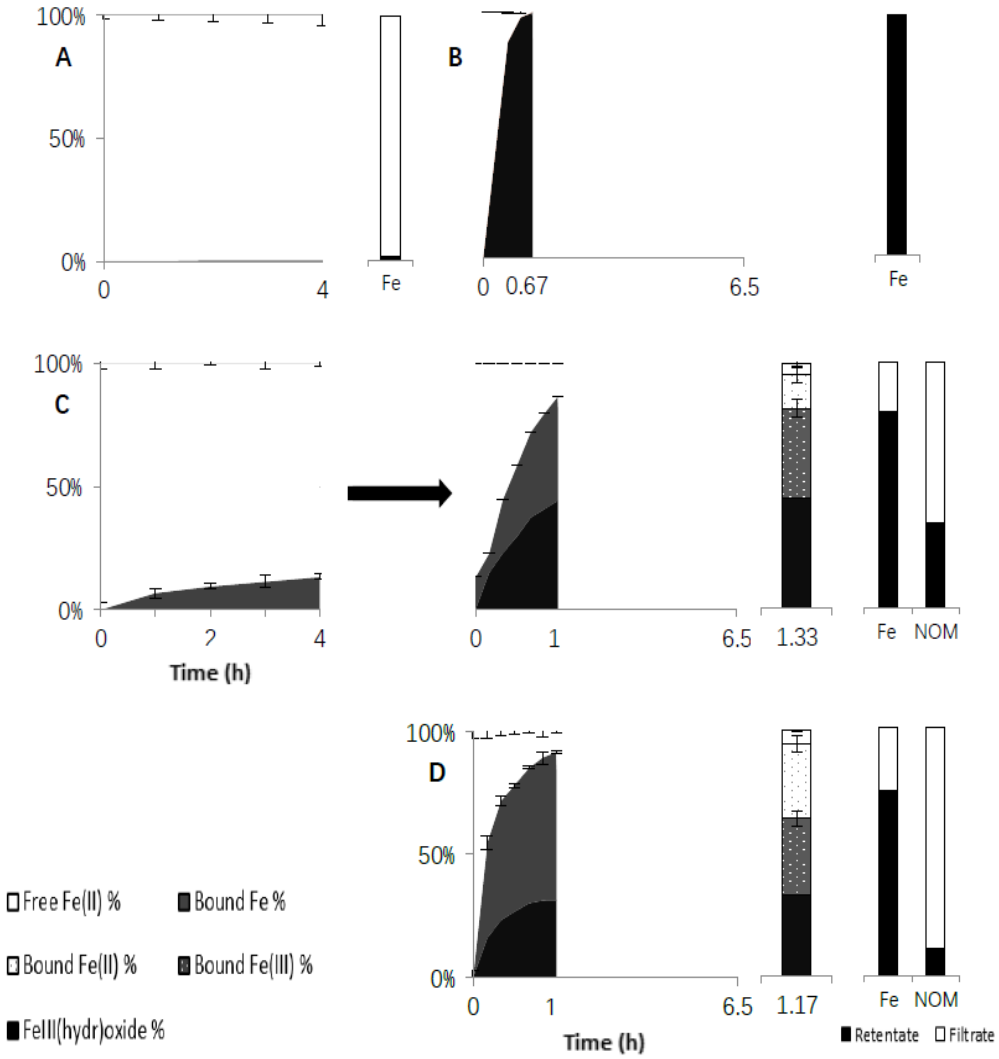

Figure 26 Fe speciation over time under 25 degrees, pH 6.5 and full daylight conditions. PSD of Fe and NOM at the end point are shown beside. (A) Anoxic control and (B) Oxic control; (C) Type B and full Fe speciation at the end point are shown beside; (D) Type A and full Fe speciation at the end point are shown beside.

Effects of increased pH. As noted above, at pH 7.5 80% rather than 20% of FeII is bound anoxically as a consequence of the lower [H+] and reduced competition for binding sites. Subsequently, under Type B mixing (Figure 27), the amount of bound Fe after admission of D.O. remains around 70% rather than increasing as seen at pH 6.5. This difference in speciation between pH 6.5 and 7.5 is probably because the NOM was nearly completely saturated with FeII during the anoxic period. Under Type A only 7% of Fe is bound by NOM at oxic equilibrium because at pH 7.5 in the presence of D.O., hydrolysis of Fe to FeIII(hydr)oxide competes more effectively against its binding to NOM.

Although at pH 7.5, the bound Fe was not resolved into bound FeII and FeIII, it is clear that the divergence in Fe speciation at oxic equilibrium in natural waters caused by difference in mixing order (of FeII, NOM and D.O.) will be greater in more alkaline waters. Anoxic binding of Fe to NOM can be a strong control on the subsequent fate of Fe in the oxic environment. The strength of the control increases with the amount of anoxic binding and the rate of oxic FeIII hydrolysis, both of which are positively related to pH (Catrouillet et al., 2014; Daugherty et al., 2017).

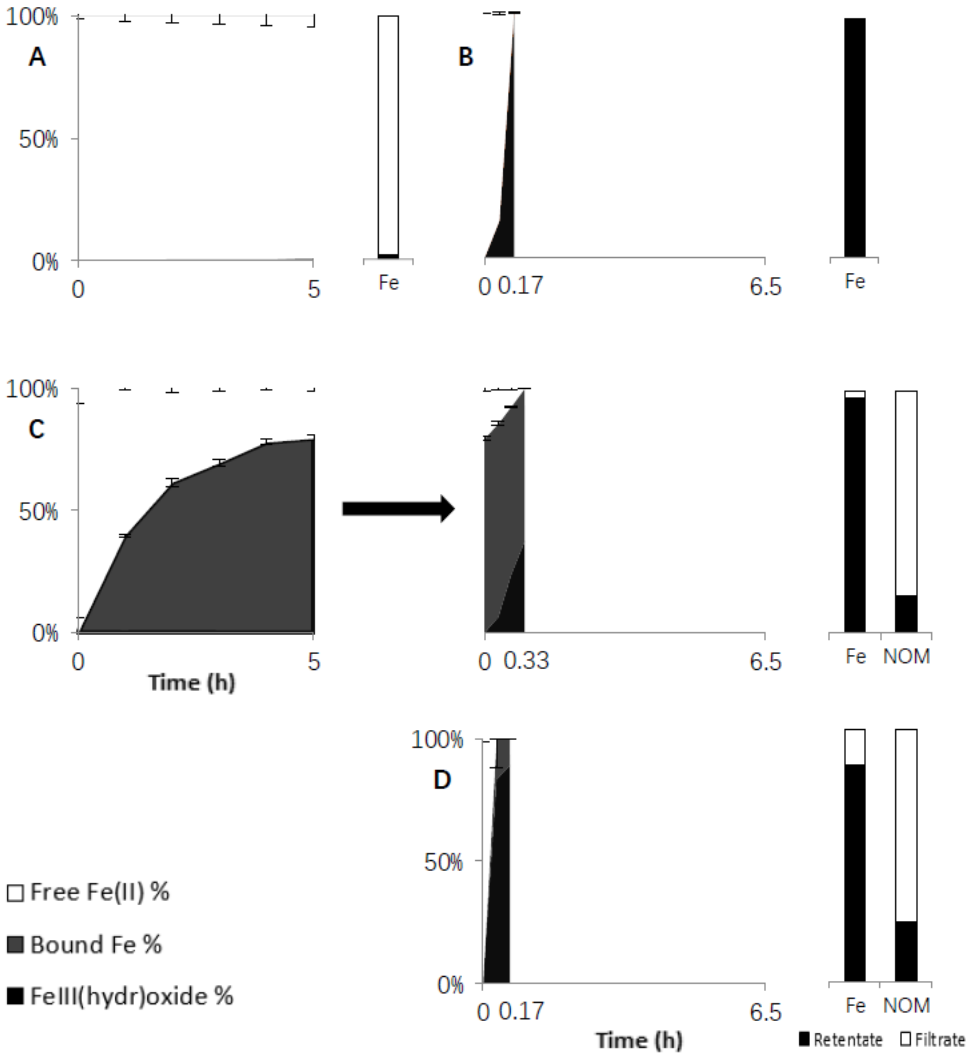

Figure 27 Fe speciation over time under 25 degrees, pH 7.5 and full daylight conditions. PSD of Fe and NOM at the end point are shown beside. (A) Anoxic control and (B) Oxic control; (C) Type B and (D) Type A simulation.

Effects of temperature. At 10^0C the system without NOM, takes 6 times as long to come to equilibrium after the admission of D.O. than at 25^0C; the processes of both FeII oxidation to FeIII and its subsequent hydrolysis to FeIII(hydr)oxide have been slowed (Figure 28). It is apparent that slowing of

these processes has changed the speciation at equilibrium; only 45% of FeII hydrolyses to FeIII(hydr)oxide, compared to the >95% at 25^{0}C. This must be because at 10^{0}C FeII binds to the FeIII(hydr)oxide that is the product of its oxidation. That there is this difference between 25 and 10^{0}C may be because the slowing of FeII binding is relatively less than that of FeIII hydrolysis.

Systems containing NOM also take 6 times as long to come to equilibrium after the admission of D.O., at 10^{0}C compared to 25^{0}C. At 10^{0}C, FeIII(hydr)oxide, the proportion of which increases during oxidation, adds to the constant amount of NOM as a second sorbent of Fe.

However, the amount of bound Fe remains similar at 10^{o}C whether or not NOM is present. Whilst the speciation techniques used do not allow the bound Fe to be resolved into Fe bound to FeIII(hydr)oxide or to NOM, the size distribution of the Fe at 10^{o}C differs in the presence of NOM. Without NOM there is effectively no <10 KD Fe but 8-15% in its presence, this suggests that some Fe binds to NOM rather than just to FeIII(hydr)oxide.

The results of oxidation under Type A and B should be similar as there is very little anoxic FeII binding in the cold. Both mixing orders result in similar speciation including bound FeII, bound FeII and FeIII(hydr)oxide. There is more FeIII(hydr)oxide production under Type B but in this case TFU was

carried out after 20 hours rather than the 7 hours for Type A and this may have allowed further coagulation to occur.

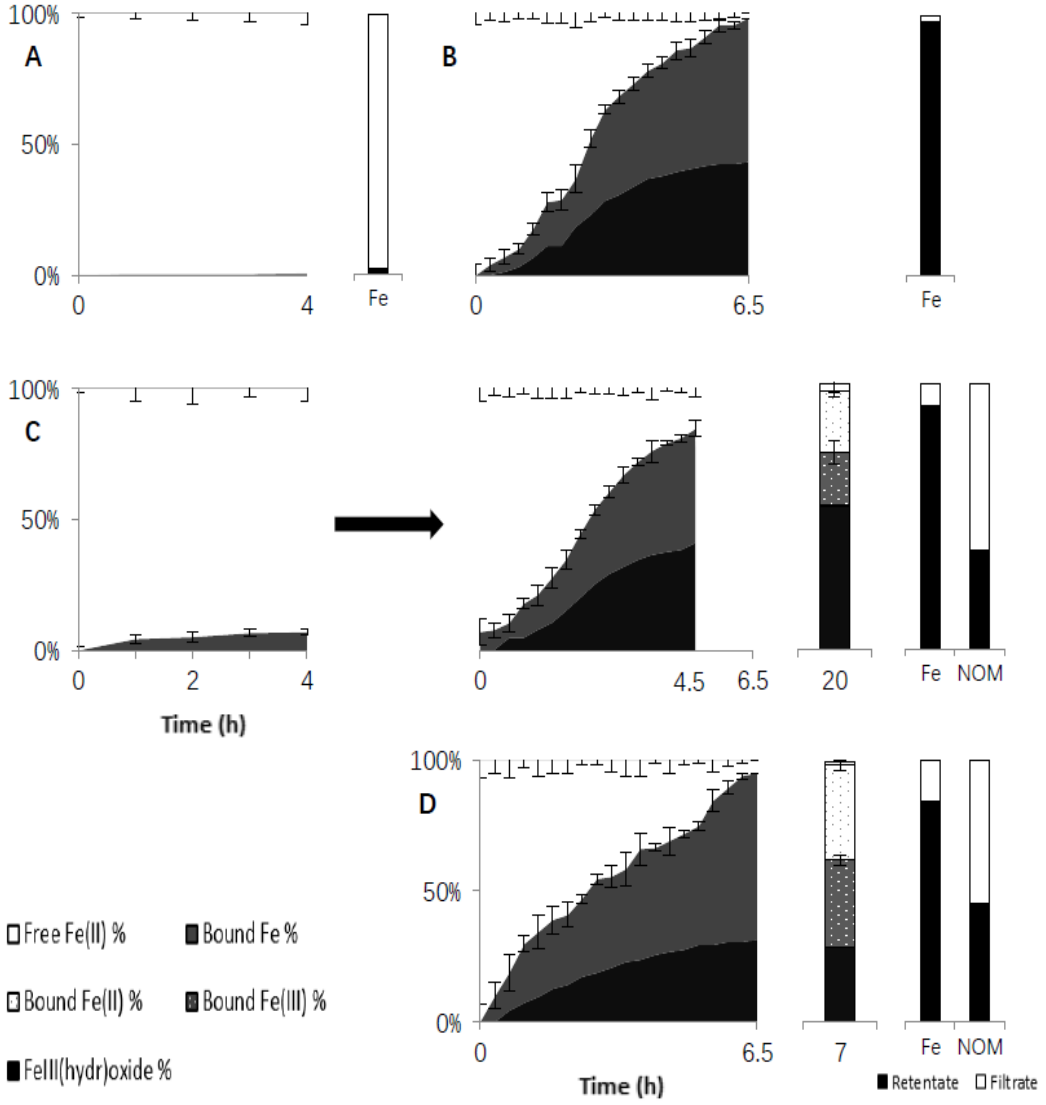

Figure 28 Fe speciation over time under 10 degrees, pH 6.5 and full daylight conditions. PSD of Fe and NOM at the end point are shown beside. (A) Anoxic control and (B) Oxic control; (C) Type B and full Fe speciation at the end point are shown beside; (D) Type A and full Fe speciation at the end point are shown beside.

Effects of darkness. In darkness and in the absence of NOM it is apparent that FeII oxidation to FeIII has been slowed as only 45% of FeII ultimately hydrolyses to FeIII(hydr)oxide, compared to the >95% in daylight (Figure 29). The slow oxidation is likely to result from the limitation on photochemical superoxide production and subsequent H_2O_2 production. Because oxidation is slow FeII has time to bind to the FeIII(hydr)oxide that is the product of its oxidation. The net result at equilibrium is similar to that under cold conditions only 45% of Fe is present as FeIII(hydr)oxides and the remaining 55% of Fe is bound to this.

The experiment conducted in dark conditions (Figure 29) is the most realistic simulation of the period of anoxic Fe/NOM interaction as anoxic conditions are likely to coincide with darkness in natural waters. The 40% of FeII bound to NOM is higher than that at 10 or 25^{o}C, (5 or 15%) when anoxia was coincident with daylight. The higher amount of anoxic Fe binding to NOM in darkness suggests that the impact on Fe mobility, in the subsurface will be greater than suggested by the experiment under daylight. It is not clear why daylight would limit anoxic FeII binding to NOM. Light is widely recognised to degenerate NOM but the rate of bulk decomposition is too slow to have an impact over the 6 hour anoxic periods (Drozdova et al., 2020). The possibility remains that some functional groups are preferentially destroyed by light and these are the particular groups involved in Fe binding. This latter point is

supported by the experiments above in which the proportion of bulk NOM involved in Fe binding was <20%.

Fe speciation that developed on subsequent admission of D.O. cannot be directly compared between dark and daylight as prior to admission of D.O. there was only 10% anoxically bound Fe in daylight but 40% in the dark. However, it is apparent that darkness enhanced Fe binding to NOM; its proportion increased from 40 to 96% compared to 45% bound and 45% FeIII(hydr)oxide at oxic equilibrium under daylight (Figure 29 C and Figure 26 C). Also, the bound Fe has a higher proportion of FeII rather than FeIII in darkness than in daylight. These differences may be a consequence of the role of photolysis of NOM in producing compounds that enhance FeII oxidation and/or light induced reduction of FeIII/NOM complexes (Garg et al., 2013; Garg et al., 2015; Waite and Morel, 1984).

As seen in the simulations under daylight there is little or no impact of mixing order on the ultimate oxic speciation of Fe in darkness. Despite the much greater amount of anoxically bound Fe in darkness (40%) Type A and Type B mixing result in speciation that becomes similar within around 1 hour.

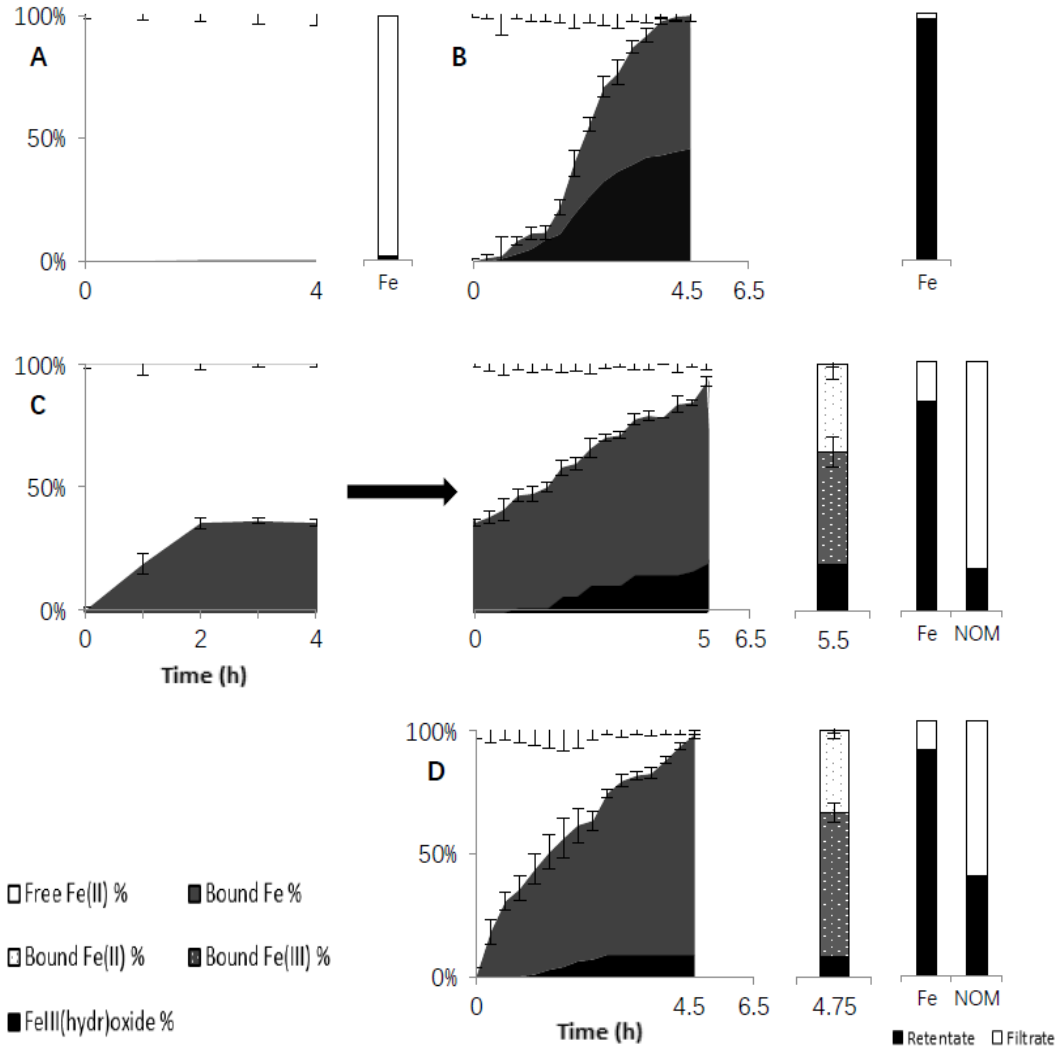

Figure 29 Fe speciation over time under 25 degrees, pH 6.5 and dark conditions. PSD of Fe and NOM at the end point are shown beside. (A) Anoxic control and (B) Oxic control; (C) Type B and full Fe speciation at the end point are shown beside; (D) Type A and full Fe speciation at the end point are shown besides.

4.4 Conclusions

Environmental implications. Whilst the NOM used was inevitably site-specific the hydrological context of sampling and subsequent pre-treatment

gives some generic applicability to the findings, similarly the range of pH covers a large proportion of natural waters. The work has direct implications for mobility of Fe and its utility in microbial metabolism, and indirect implications for mobility of pollutants and nutrients through influencing specific surface area of FeIII(hydr)oxides.

The work shows FeII mobility cannot be assumed to be that of a free aqueous ion as a proportion will become particulate by association with NOM. This particulate Fe will be less mobile in the subsurface and the proportion is a function of NOM concentration and pH (Theis and Singer, 1974; von der Heyden et al., 2014; Chen and Thompson, 2018). This reduction in mobility is strongly dependent on pH, the shift from <10 KD to >10 KD doubling from pH 6.5 to 7.5. Across the range of variables when systems containing NOM are oxidised 8-26% of Fe remains <10 KD. Therefore <10 KD Fe must be produced and present under oxic conditions in a wide range of environmental scenarios. This may be as FeII or FeIII bound to NOM or FeIII(hydr)oxide, with their relative importance determined by the particular scenario. The persistence across a range of conditions of FeII or FeIII in oxic waters suggest there is a ubiquitous but not widely recognised store of potential energy that can be harnessed by microbes.

The anoxic – subsurface – interaction of FeII with NOM, which was from 5 to

as much as 40% the range of environmental variables deployed, was expected to have a persistent effect on subsequent FeII oxidation. However, there was no clear difference between Fe speciation at oxic equilibrium with and without prior anoxic Fe/NOM mixing, and any differences whilst equilibrium was reached were maintained for <1 hour which is likely to only be of limited importance relative to hydrological residence or transit times. There is a possibility that mixing order could change oxic speciation if anoxic binding was greater than 40% and this binding proportion was observed at pH 7.5.

Temperature changes from 10 - 25^{o}C cause large changes in speciation of Fe. At 25^{o}C NOM provides the only binding sites for Fe and therefore the main control of the preservation of Fe in oxic waters, but at 10^{o}C FeII can be preserved even in the absence of NOM, by binding to the product of its own oxidation, Fe(III)hydroxide. If NOM is present Fe will bind to both it and FeIII(hydr)oxide but Fe bound to the former has the potential to be a finer colloid (<10 KD).

Darkness causes a similar slowing of Fe oxidation as cold; with the same result in the absence of NOM that FeII has time to bind to the FeIII(hydr)oxide that is the product of its oxidation. Darkness also enhances the binding of Fe to NOM. In the simulated subsurface anoxic binding in darkness reached 40% of Fe at pH 6.5 and will increase with pH. Above ground, darkness allows

more Fe binding and particularly FeII binding as in daylight the balance of photochemical processes lie on the side of photolysis of NOM into compounds that enhance oxidation and light induced reduction of FeIII/NOM complexes (Garg et al., 2013; Garg et al., 2015; Waite and Morel, 1984).

The range of experimental conditions also allow the impacts of NOM on solubility (10 KD cutoff) of Fe to be broadly described. In the absence of NOM all Fe on oxidation becomes >10 KD, both at 25^0C, when all the Fe is FeIII(hydr)oxide, and at 10^0C, when 46% is FeIII(hydr)oxide and the remainder is bound Fe. The presence of NOM prevents 20-26% Fe becoming >10 KD at 25^0C and 8-16% at 10^0C.

Chapter 5. Controls on the mobility of As in natural waters: The role of NOM, Fe and changing hydrological conditions

5.1 Introduction

As one of the most toxic elements, Arsenic (As) exists naturally in the environment (atmosphere, rocks, sediments, soils, natural water and organisms) (Ratnaike, 2003). Various factors such as the type and amounts of sorbents, pH, redox potential (Eh) and microbial activities will impact on the forms of As. Large number of studies have proved that the mobility and toxicity of As depend on its specific chemical forms and oxidation states in the environment (Smedley and Kinniburgh, 2002; Wang and Mulligan, 2006; Wang and Mulligan, 2009). As can occur in the environment in inorganic and organic forms (As acid, arsenous acid, arsenites, arsenates and so on), but it mainly exists in natural water in inorganic form such as oxyanions of trivalent arsenite [As(III)] or pentavalent arsenate [As(V)]. [As(III)] is most common under anoxic conditions and [As(V)] is most prevalent in oxic conditions. [As(III)] is mentioned to has higher toxicity, solubility and mobility by comparing with [As(V)]. The organic forms of As are not quantitatively important and they are likely to be generated by biological activities, are mostly found in surface water. Normally, the capacity of toxic and mobile in inorganic As is greater than organic As (Smedley and Kinniburgh, 2002; Wang and Mulligan, 2006; Wang and Mulligan, 2009). In addition to trivalent (+III) and pentavalent (+V), As also has two oxidation states (-III, 0), of which

As metals rarely occurs and (-III) oxidation state is only found in extremely reduced environments (Hughes, 2002; Wang and Mulligan, 2006).

Figure 30 shows the occurrence and mobilisation path of As in environment. A combination of natural processes including weathering reactions, biological activities and volcanic emissions as well as a series of anthropogenic activities such as mining activity, combustion of fossil fuels, the use of arsenical pesticides and so on result in the enrichment of As in soils, sediments or rocks, which may generate As sources. Once in environment, both naturally occurring and anthropogenically sourced As are affected by the same biogeochemical processes, causing the mobilisation of As that will change As flux. It means more As entering into nearest natural water or agricultural fields from soils, rocks (mines) or sediments in the forms of arsenate ion [As(V)] and arsenite ion [As(III)]. Therefore, more As can enter to atmosphere through evaporation, attributed to elevated As fluxes in water. Humans are exposed to As by a number of ways such as water, soil and air, and therefore As poses the greatest risk to human health (Gonzalez et al., 2006; Wang and Mulligan, 2006). Meanwhile, most environmental As problems are caused by mobilisation of As under natural processes, which also involves water sources that are closely related to drinking water. These water sources come from water collection spots and are sources of during water. Among various sources of As, drinking water is the main cause of

human As toxicity (Ratnaike, 2003; Smedley and Kinniburgh, 2002; Verma et al., 2014). With the increasing awareness of As toxicity and improvement of As quantitative technology, the maximum concentration limit of As in drinking water is set at 10 μg/L (it was 50 μg/L before 2004) by Worth Health Organisation and once the content of As exceeds the limit, the public health will be impacted seriously, leading to an increase in human disease and mortality (WHO, 2011). Elevated concentrations of As will pose hazards to human health and environment on a global scale and therefore there is a requirement to understand the distribution and cycling of As in the natural environment due to its toxicity.

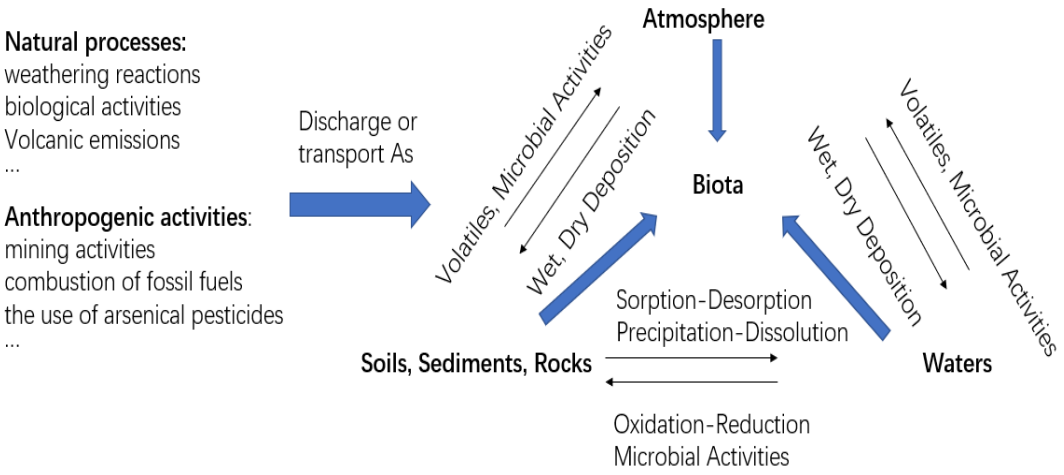

Figure 30 The occurrence and mobilisation path of As during As cycle in environment (Wang and Mulligan, 2006).

Ombrotrophic peat bogs are characteristic of many upland areas in UK and it play a major role in the storage, transformation and mobilisation of As (Langner and Kretzschmar, 2012). The atmosphere is its only source of pollutants input such as As. Large amounts of As are released to atmosphere via long-term and large-scale anthropogenic activities involving fossil fuel combustion, mining and smelting activities, and industrial applications. Therefore, many upland sites of UK have been polluted by atmospheric deposition of As in the past few hundred years. For example, Coal from West Lancashire coalfields is known to have high As content. Substantial coal burning resulted in significant deposition of As across the high ground around towns and cities of northwest England. These organic-rich uplands have been identified as storage sites for past atmospheric deposition of As. The As concentrations in the near-surface layer of upland peat soils often exceed background concentrations because of the long-range transport of metalloids in the atmosphere. Some recent studies have found that upland peat catchments dominated by organic-rich peat soils and peat bogs not only in the storage, but also play a major role in transformation and mobilisation of As. In peat soils, the humidity affected by seasonality of rainfall and temperature, as well as related changes in redox conditions can influence As mobility, resulting to its transfer from soils to peatland streams or pore waters. Therefore, increasing work demonstrates that the As found in the uplands of northern England is associated with historical industrial activities, and its

environmental fate is affected by the metallic minerals (particularly Fe), NOM (including both aqueous and solid phases) and related environmental conditions (Q) (Rothwell et al., 2007; Rothwell et al., 2009; Rothwell et al., 2010; Rothwell et al., 2011).

In addition, these uplands are also water collection areas and known to be undergoing changes due to land management practices and further changes as climate warms (described in Chapter 3). Therefore, there has been concern about the mobilisation and transport of previously deposited As from peat soils to receiving surface waters or subsurface waters and the possible damage of these As pollutants on the aquatic ecosystem, which will affect the quality of drinking water. The mobility of As will be affected by discharge rate (Q) in stream water. As the inherent 'flow through' systems, stream water relies on Q to mobilise substances stored in the system and the interaction between substances depends on the time available affected by Q within the system. The dependence of mobilisation of different substances stored in the system on the time available may also impact the resulting associations, leading to a hysteresis effect. Furthermore, Q will vary due to seasonal variations, resulting in differences in dilution effect of stream water. Overall, discharge of a system will impact on the movement of water through the ground and it is a complex process that should be of concern (Morel et al., 2009; Semdley and Kinniburgh, 2001; Worrall et al., 2002). However, there is

a lack of data on As concentration in streams draining heavily polluted peatland environments, even though As leaching from atmospherically contaminated peatland catchments has been highlighted as a potential environmental hazard. For the potential contribution of peatlands to the As mobilisation and consequences on water quality through runoff, there is a requirement to understand how As is transported within organic-rich stream environments.

The Southern Pennies (UK) Peak District National Park with high level of NOM content provides a suitable place to monitor and compare As flux under different environmental conditions, because it has upland peat catchments and is known to have the potential to accumulate high concentrations of As due to anthropogenic activities. This is also the essential requirement for site selection and project development. The stream water in upland peat catchments have significant heterogeneity in hydrochemical characteristics, resulting in difficult of representative sampling (Rothwell et al., 2007), because different time periods or different hydrological conditions will affect the NOM, Fe and As contents in stream water. As a water collection area, Peak District National Park allows long-term sampling and associated hydrological conditions measurement to obtain high quality data sets, which is a solution to solve the problem. The long-term sampling programme was described in subsection ‘‘Sample collection’’ of Chapter 2. This is the important

prerequisite for making representative measurement of flux by interpolation and rating relationship (described in subsection ‘‘Continuous [NOM] and [As] measurments’’). Furthermore, it has two contrasting sub-catchments of eroded peat (site 50) and uneroded peat (site 30) to help with the problem of predicting the future. These two sub-catchments have different availability of Fe and NOM and Fe may be more available in site 30. Meanwhile, it can simulate the catchment with higher erosion that is expected under a warming climate as upland peat begins to dry. Peatlands in UK are constantly facing natural erosion from environment such as wind, gravity, rainfall and flowing water as well as pressures from anthropogenic activities such as atmospheric pollution, agricultural activities, solid waste pollution and climate change. Therefore, erosion is the likely future situation of upland peat so eroded site (site 50) can be potentially use as a model of future conditions and used to prediction of future As mobilisation. Site 30 can be regarded as an uneroded site, because the revegetation of plant species such as sphagnum moss has been done there, which has restored the natural runoff system and promoted the renewal of peat deposits. Meanwhile, successful environmental improvement strategies (such as using physical barriers to block drainage) have effectively reduced the impact of erosion, water level drops and other adverse conditions. Overall, in order to complete the main aim of this project, it is necessary to monitor the changes in As flux in Southern Pennies (UK) Peak District National Park for further predict and manage As mobilisation.

Although a lot of research has been done on the sources of As, the mobilisation of As is still receiving less attention. The mobilisation of As is known to associate with NOM and/or Fe in aqueous environment. NOM is ubiquitous in the environment and is highly reactive to inorganic and organic pollutants, thus it can play an important role in affecting the speciation, solubility, mobility and bioavailability of contaminants. Previous studies have shown that the underground NOM is the main energy source for the As mobilisation during subsurface water flow process, has the ability to influence the sorption behaviour of As by interacting with the mineral surfaces and/or As itself. Therefore, NOM can play an essential role in releasee of As from soils or sediments to groundwater (Abdelrady et al., 2020; Shama et al., 2011; Wang and Mulligan, 2009). In addition, NOM (mainly dissolved organic matter) can change chemical form of As by changing the redox conditions as well as the complexation reactions with As in aqueous environment, which greatly influence the mobility of As. There is already evidence that the NOM-As colloids/complexes generated by complexation reactions accelerates the mobilisation of As (Chen et al., 2017; Shama et al., 2011; Wang and Mulligan, 2009) These binary and ternary NOM-As colloids/complexes also affect the mobilisation of As by competing with As for sorption sites on mineral surfaces (Aftabtalab et al., 2021).

The processes of precipitation, dissolution, adsorption on and desorption from the surfaces of metal oxides (particularly Fe) are able to strongly control the mobility of As in soil and sediments (Rothwell et al., 2009). The adsorption/coprecipitation on the surface of Fe(oxy)(hydr)oxide significantly affects the enrichment of As and controls the concentration of As in the environment, so the existence of As is closely related to Fe in sediments or aerated soils. As mobility will decrease because of the sorption and coprecipitation of arsenate by Fe(oxy)(hydr)oxides under neutral pH and oxidising conditions, but it will rise by dissolution of Fe(oxy)(hydr)oxides under low pH and reduced redox potential. However, As concentration is controlled under strongly reducing conditions through the formation of sulfide minerals (Aftabtalab et al., 2021; Bauer and Blodau, 2006; Chen et al., 2017). In addition to the direct interaction with As through various ways described above, NOM in water will also interact with As indirectly by the interaction with mineral oxides. For example, by coupling to reduction of As-bearing Fe oxides, oxidation of NOM can cause As (arsenate) absorbed on Fe(III)(oxy)(hydr)oxide mineral coating sediment particles to dissolute and subsequent release under reducing conditions, so it is likely to affect the adsorption of As on the surface of Fe(oxy)(hydr)oxide. The reduced Fe(II) are therefore mobilised along with associated As (arsenite). Due to the redox reaction and reductive dissolution of As from As-containing minerals, the flux (and concentration) of As have changed consequently (Aftabtalab et al., 2021;

Hery et al., 2008; Solaiman et al., 2009). Moreover, organic mineral coprecipitates and adsorption complexes are formed because NOM can often coexist with Fe(III)(oxy)(hydr)oxides in natural environment. The coprecipitation and adsorption of NOM will lead to the changes in the physical and chemical properties of Fe(III)(oxy)(hydr)oxides and eventually affect the microbial-mediated Fe/As mobilisation by impacting on the structure of mineral and slowing down microbial Fe reduction (Cai et al., 2020). Although the importance of NOM to As mobilisation is well know, there are still few studies on the interaction of NOM with As and Fe or Fe(oxy)(hydr)oxides in groundwater, surface water and soil. Much research focuses on the mechanism and types of NOM, or other factors affecting As mobilisation. The specific controls on As mobilisation via NOM or Fe are still not understand in details, and there are limit data on the reliable quantitative As mobilisation with environmentally relevant sources and how As mobilisation affected by NOM or Fe. Therefore, there is a requirement to understand how Fe, NOM and As interact by monitoring Fe and NOM in order to find an effective method to predict and manage As mobility, especially in the aqueous environments (Morel et al., 2009; Semdley and Kinniburgh, 2001; Worrall et al., 2002).

In addition to the influence of Fe and NOM, size of As is critical to predicting its behaviour. Many studies believe that whether As is particulate or dissolved

has different mobility, and therefore rely on the 0.45 µm or 0.2 µm cut-offs to distinguish this but much of the As may be present as <0.2 µm >10 KD colloidal particles or <10 KD truly dissolved forms. Therefore, soluble and particulate As, Fe and NOM must be resolved at the nanometre level (<10>3KD) (Cai et al., 2002; Sarmiento et al., 2012; Wen et al., 1999).

The main aim of this project is to predict how As flux in an important UK water collection area may change with climatic change and to gain a better understanding of factors that control the mobility of As in general. The following objectives were set out to achieve the aim:

- Collect samples at different intervals from upland peat catchment of Southern Pennines (UK) Peak District during baseflow and stormflow conditions (discharge events).

- Determine continuous [As] and Q by using interpolation and calculate As flux for each site.

- Compare the variability in As flux between sites and periods and determine the reliability of flux by comparing with another method of calculating flux.

- Determine how As change with Q, NOM and Fe and identify the main factors of controlling As mobilisation.

- Separate the collected samples by TFU and assess how As differ between size fractions under different NOM and Fe.

5.2 Materials and methods

Sampling and sample analysis. Sampling including both spot sampling and use of automatic sampling systems (Sigma SD900) was carried out throughout the study period at study sites (site 50, grid reference SE 05650 00943 and site 30, grid reference SE 06172 02965). The mechanisms of sampling were described in detail in the subsection ‘‘Sample collection’’ of Chapter 2. A combination of daily sampling and hourly sampling during baseflow and stormflow conditions (discharge events) from auto sampler was conducted in stream water at all study sites. From 2017 to 2019, more than 100 samples were collected at each site and this includes sampling of two discharge events during April 2017 and April 2019.

All samples were analysed according to the analysis procedure outlined in the subsection ‘‘Sample analysis’’ of Chapter 2. Continuous measurement of As is described in the following subsection.

Continuous [As] Measurement and calculation of As flux. [As] of each stream samples collected from study area were measured by ICP-MS. In order to monitor the As flux for long period during the entire project, a high frequency measurement of [As] is required. Due to the reasons outlined in the subsection ‘‘Continuous [NOM] and [As] measurement’’ of Chapter 2, it is difficult to perform continuous measurement of [As] through high frequency sampling. In order to solve this problem, two methods of concentration estimate were conducted in this project. Each method requires calculation of continuous Q by the pattern described in the subsection ‘‘Stage-discharge relationship’’ of Chapter 2.

The first is to use simple interpolation to estimate [As] between sampling points. [As] of each daily sample was assumed to represent [As] of a whole day (24hrs) in river. These interpolated [As] were combined with continuous Q to calculate instantaneous As flux per 15 minutes by multiplying with the corresponding Q. All the results of instantaneous As flux during sampling period were added up and then multiplied by the inter-sample period to determine a total mass. Next, the total mass was divided successively by the specific number of days within sampling period and site area to calculate the average daily As flux. The estimated value of As flux for a whole year or more time was then obtained by multiplying the average daily As flux during the sampling period by the specific number of days in a year or more years.

However, the accuracy and reliability of the results from interpolation are difficult to determine, because it depends on the amount of sampling measurements and the time intervals of Q. Therefore, it needs to be verified by comparing with another method. The second method is to try to model flux by rating relationship ([As] vs Q).

In order to estimate As flux yearly by using a rating relationship curve, the results including [As] of all samples and corresponding Q at the same time were used in linear regression models. The calculation of continuous [As] is based on the continuous Q measurements at 15-minute intervals, which are then used to estimate the As flux. The reliability of results needs to be verified according to compare NOM flux during sampling period or longer period from both of methods and the reason is the same as that in estimation of NOM flux, which is described in the subsection ‘‘Continuous [NOM] and [As] measurement’’ of Chapter 2.

5.3 Results and Discussion

As concentrations of stream waters. Samples were collected in different months of project period, which can ensure the representativeness of flux calculations and reduction of impact from temporal variations (Figure 31). Table 6 summarises the means and ranges for Q and concentrations of dissolved As, Fe and NOM at each study site during project period. The mean

and maximum concentrations of As in Peak District stream water at site 30 are 0.94 µg/L and 4.82 µg/L respectively (the two values at site 50 are 0.44 µg/L and 1.94 µg/L) over the monitoring period. The maximum concentration limit of As in drinking water is set to 10 µg/L by WHO (WHO, 2011). Therefore, the As concentration in Peak District stream waters did not exceed the guideline value.

However, there may be a potential environmental hazard at site 30. Its As concentration was significantly higher than site 50 (0.94 µg/L vs 0.44 µg/L) and the maximum value is closer to 10 (4.82 µg/L vs 1.99 µg/L). More importantly, there is a large variation in its range (0 – 4.82 µg/L). This indicates that As concentration at site 30 is unstable. Previous research results also proved this point. Rothwell et al., determined the As concentration in this area around 2010 and the range was 0.2 µg/L – 7.28 µg/L. Hegan also monitored the As concentration at the same site (site 30) in 2012 and the range was 0 – 15.9 µg/L. This result indicates that stream water in the Peak District National Park was contaminated with dissolved As at that time. Although the situation has improved, further work to determine the factors that impact on the As content is necessary for better predict and manage the As mobility in stream water. This is benefit for avoiding potential risk to public health.

According to Table 6, the mean Fe concentration site 30 is also higher than site 50 (0.98 mg/L vs 0.2 mg/L) as the same as the situation of As and it was as high as 5.98 mg/L for a time. This may be related to the local geology of the site. The peat in site 30 is covered by a marine shale belt containing a relatively high level of Fe (Hegan, 2012). Unlike Fe and As, the NOM concentrations are similar within both study sites (the rate of change was only 20%, while As and Fe were 53% and 80% respectively). In addition, the impact of Q cannot be ignored when comparing the difference in concentrations between the two sites. The previously deposited As and Fe can be leached from blanket peats into the stream system under both baseflow (low Q) and stormflow (high Q) conditions. During sampling period, the Q of site 30 is much higher than site 50 (67.8 l/s vs 13.35 l/s) and its variation is larger, reaching a maximum of 747.62 l/s (149.8 l/s for site 50). The main reason is probably due to larger area or deeper depth of the river channel at site 30. NOM can effectively mobilise and transport As under high Q conditions. Furthermore, geological factors such as the existence of gullies and lack of vegetations are also not conducive to the accumulation of As in pore water or peat under stormflow conditions (Hegan, 2012; Rothwell et al., 2007).

Table 6 Summary of As, Fe, NOM concentrations and discharge over study sites.

Study sites	Research elements	Aqueous concentration	
		Mean	Range
Site 30 (Uneroded catchment) NO. of sample points: 122	As (µg/L)	0.94	0 – 4.82*
	Fe (mg/L)	0.98	0 – 5.98*
	NOM (mg/L)	11.34	6.24 - 26.09
	Q (l/s)	67.8	5.69 – 747.62
Site 50 (Eroded catchment) No. of sample points: 128	As (µg/L)	0.44	0 – 1.99
	Fe (mg/L)	0.2	0 - 0.72
	NOM (mg/L)	9.33	0.5 - 31.88
	Q (l/s)	13.35	1.24 – 149.8

*There is only one sample with Fe concentration of 18 mg/L and As concentration of 10 µg/L. The rest of them are within the range.

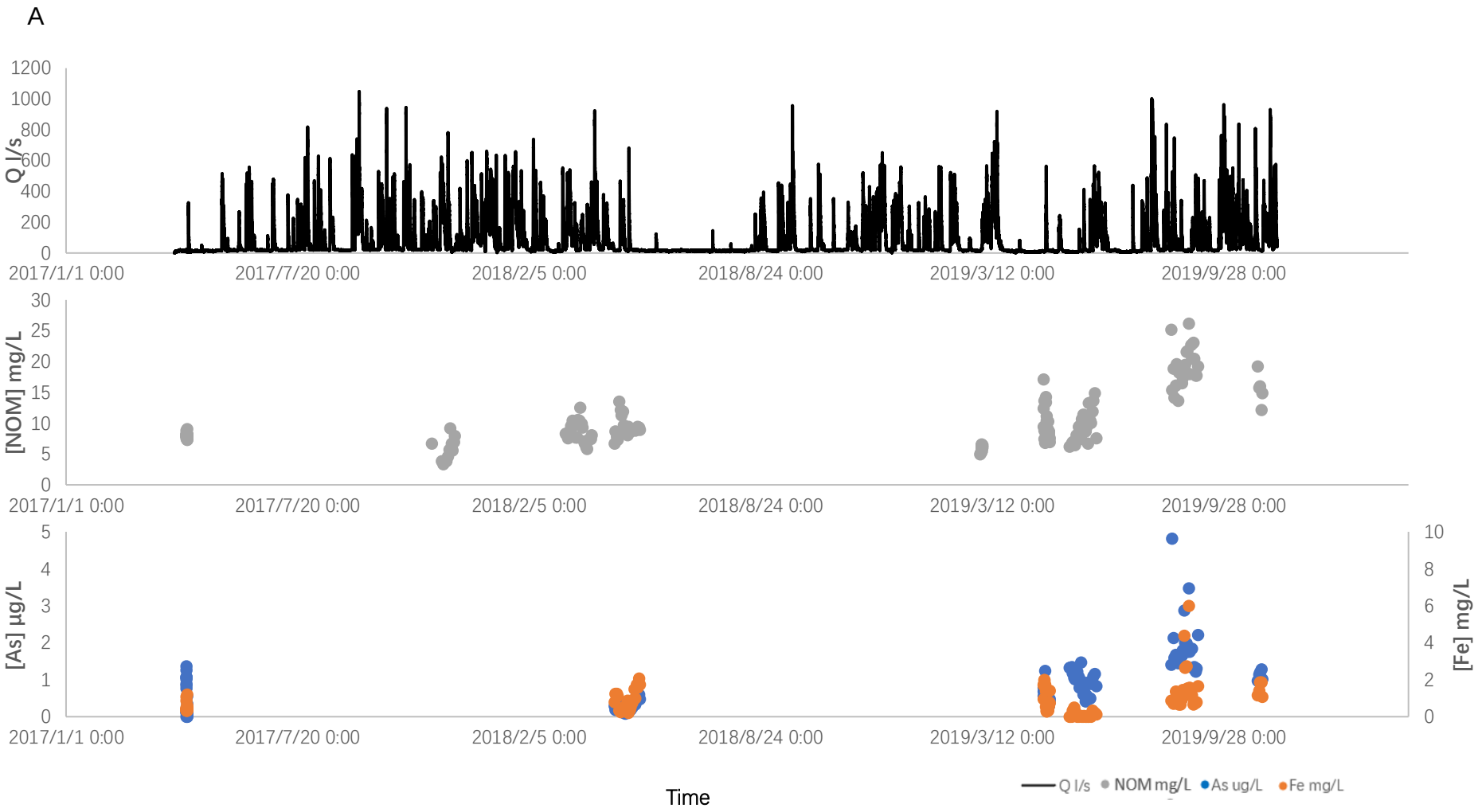
A
Q l/s
1200
1000
800
600
400
200
0
2017/1/1 0:00
2017/7/20 0:00
2018/2/5 0:00
2018/8/24 0:00
2019/3/12 0:00
2019/9/28 0:00
[NOM] mg/L
30
25
20
15
10
5
0
[As] µg/L
5
4
3
2
1
0
[Fe] mg/L
10
8
6
4
2
0
Time
Q l/s
NOM mg/L
As ug/L
Fe mg/L

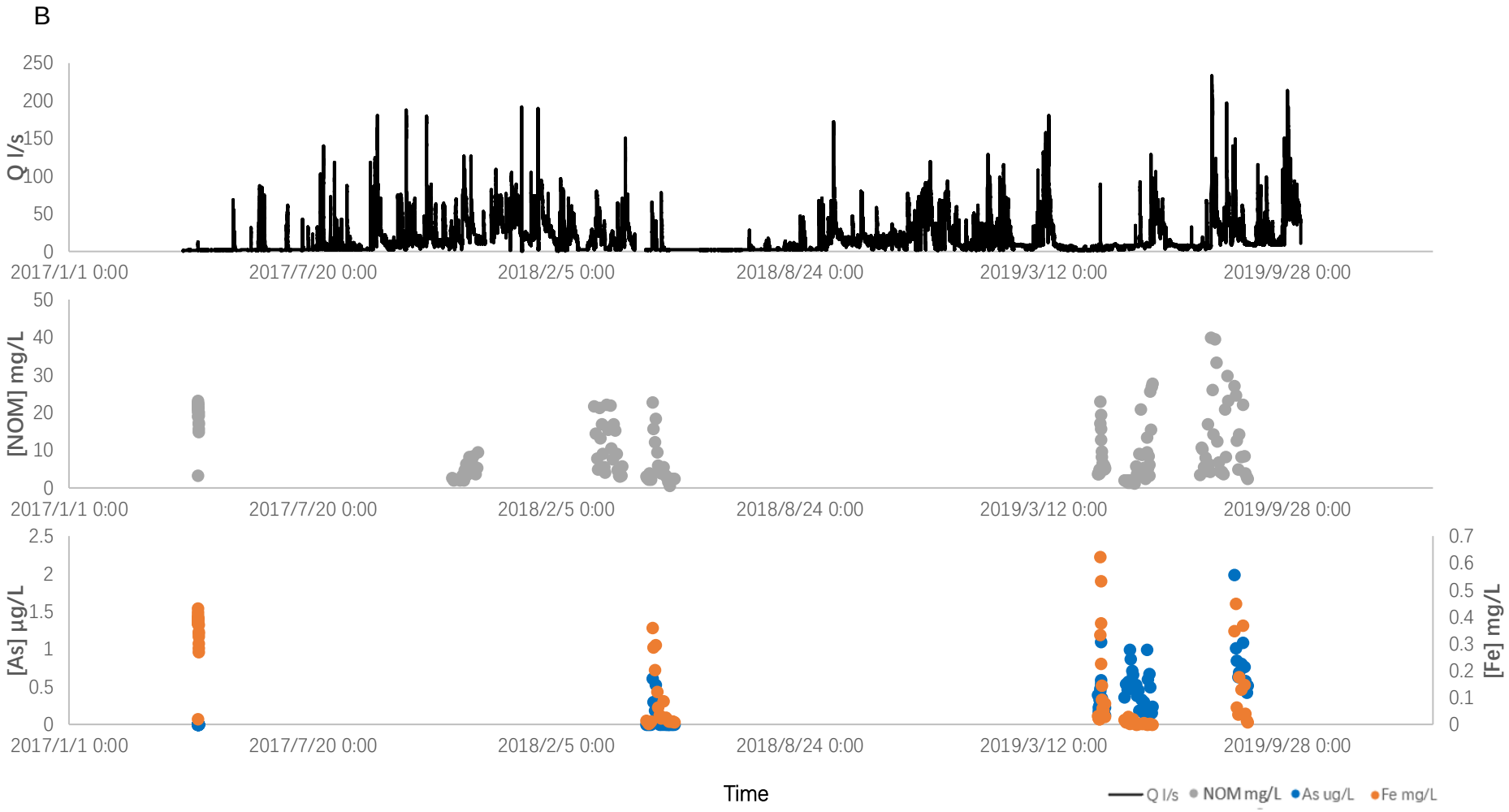

Figure 31 Dissolved NOM, As, Fe concentrations and discharge (Q) for A) site 30 and B) site 50 during study period.

Quantification of As flux by using interpolation. Estimation of As flux for each site are shown in Table 7. Fluvial fluxes for site 30 and site 50 were calculated by interpolation were 0.84 kg/year/km^2 and 0.45 kg/year/km^2 respectively. Multiple factors can contribute to the higher As flux at site 30. The altitude of site 30 (around 470 m) is higher than site 50 (around 320 m), so it is closer to the atmosphere and distance from the As emission source appears as a driver of As fluxes (Leclerc et al., 2021). The larger area also provides a place with stronger As storage capacity (Table 7). In addition, Q will also have a great impact on the flux and it may determine whether the site acts as a source or a channel of As transportation. Flux usually increases as Q rises and therefore higher Q improve the mobility of As (Figure 32) (Hegan, 2012; Leclerc et al., 2021; Rothwell et al., 2011).

Rothwell et al., and Hegan have determined the As flux in this study area in 2011 (6.5 kg/year/km^2 for neighbouring catchment) and 2012 (0.3 kg/year/km^2 for site 30 and 0.35 kg/year/km^2 for site 50) respectively, but the results were different. The fluxes measured this time are low in comparison to Rothwell, but higher than those of Hegan. The flux estimated by interpolation is extremely dependent on the Q values and sample concentrations that are easily affected by climate or various hydrological conditions during sampling period. Therefore, variations in flux are inherent due to different and limited samples, even for each sampling period (Figure 32) (Walling and Webb,

1985). Although more than 80 sample results are used for interpolation and the frequency of these samples is as high as daily, it will ignore the large changes in conditions that occur during non-sampling period (Figure 31). Due to the limitations of interpolation by using the low temporal resolution dataset, As flux was evaluated through modelling of rating relationship ([As] vs Q).

Table 7 Estimation of As flux by interpolation for each site.

Study sites	Research elements	Aqueous flux estimated by interpolation
Site 30 (Uneroded catchment)	Area (km^2)	3
	As ($kg/year/km^2$)	0.84
Site 50 (Eroded catchment)	Area (km^2)	0.5
	As ($kg/year/km^2$)	0.45

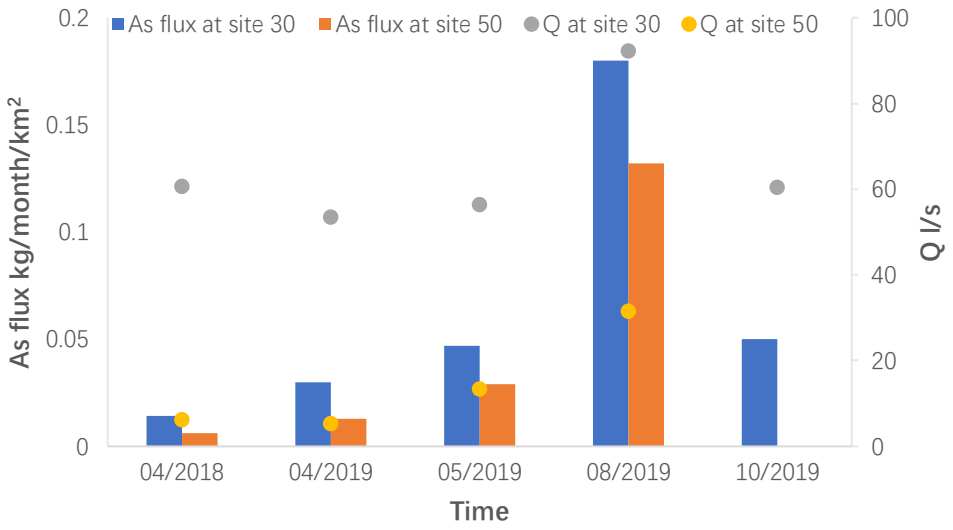

Figure 32 Estimation of As flux by interpolation for each daily sampling period.

Comparison of fluxes by interpolation and rating relationships. In view of the limitation in interpolation, another flux estimation method was used for each site in order to verify the reliability of the results. From Table 8, it can be seen that the As fluxes estimated by rating relationship between [As] and continuous Q for both sites were higher than those estimated by interpolation (1.1 kg/year/km^2 vs 0.84 kg/year/km^2 for site 30 and 0.88 kg/year/km^2 vs 0.45 kg/year/km^2 for site 50). It can still be reflected that As moves significantly as Q increases, because the mean Q at site 30 obtained through continuous measurement of Q during entire project is much greater than that at site 50 (88.47 l/s vs 17.87 l/s). Although the reliability of rating relationship curve requires further analysis, the higher values at least shows that the continuous dataset including [As] and Q increase the flux calculation. Continuous (or high temporal resolution) sampling and monitoring are necessary for avoiding overestimation or underestimation of flux. The increasing concentration measurements can significantly improve the reliability of results.

Table 8 Comparison of As Flux (kg/year/km^2) between interpolation and rating relationship for each study site.

Study sites	As flux estimated by interpolation	As flux estimated by rating relationship
Site 30 (Uneroded catchment)	0.84	1.1
Site 50 (Eroded catchment)	0.45	0.88

Relationship between [As] and Q, [Fe] or [NOM]. In order to predict and manage of As mobilisation, it is paramount to determine the association between As and different elements in the stream. Various types of factors including hydrological (e.g. dilution and flow path), chemical (e.g. sorption and complexation) and physical (e.g. coprecipitation) will influence on the mobilisation of As by changing concentration and then flux (Rothwell et al., 2011). Different roles from Q, [Fe] and [NOM] on As and the correlation coefficient were shown in Figure 33, Figure 35 and Figure 36 respectively. There is almost no correlation between As and Q at site 30 (R^2 0.0087). Regardless of the significant differences in Q, many similar As concentrations were still generated and meanwhile different As concentrations were also shown under similar Q characteristics. Those situations also occurred at site 50, but with less frequency. Therefore, although greater than that of site 30 (R^2 0.28 vs R^2 0.0087), the correlation between As and Q at site 50 was still

not high (but significant due to P < 0.05) (Figure 33). Erosion at site 50 affects mobilisation of As through changing the soil porosity and land-surface characteristics (e.g. leading to lack of vegetation), making the As more likely to be affected by Q. For example, discharge event with high Q will introduce As into stream from peat (Hegan, 2012; Zhang et al., 2020). Overall, the relationship between [As] and Q from the two sites indicate that the main factor affecting the concentration of As in stream may not be dilution effect and changes in the flow path that are influenced by vary Q.

Figure 34 with Log (concentration) v Log (Q) is drawn to test whether the dilution is the dominate factor. However, correlation between Log([As]) and Log (Q) in Figure 34 did not improve and it became even worse at site 50 (R^2 0.011 for site 30, R^2 0.22 for site 50). Therefore, dilution is not dominant and it is necessary to determine the impact of other factors on controlling the seasonal supply, storage and transport of As in stream water (Jansson, 1996; Rothwell et al., 2011).

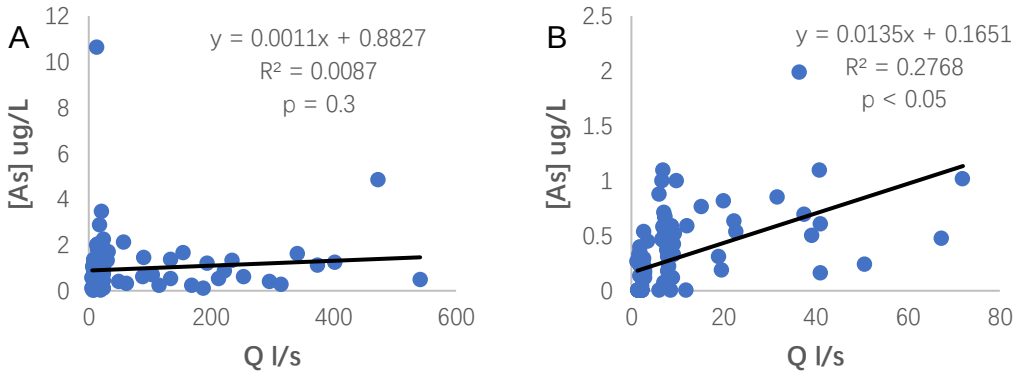

Figure 33 Relationship between [As] and Q for A) site 30 and B) site 50.

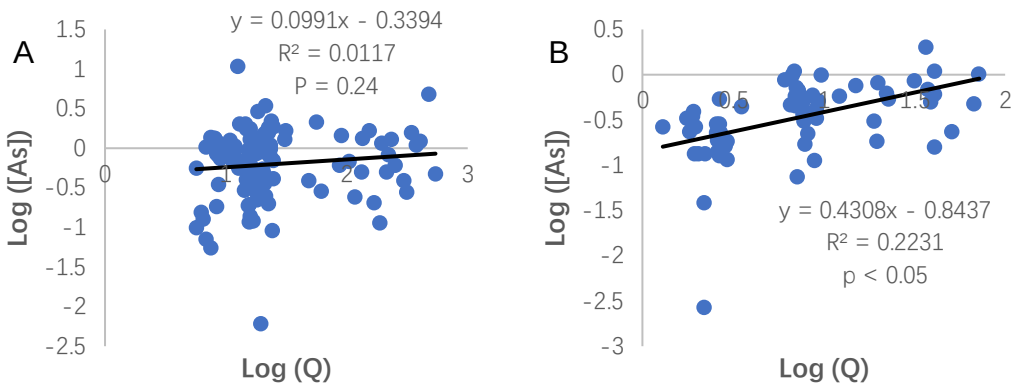

Figure 34 Relationship between Log ([As]) and Log (Q) for A) site 30 and B) site 50.

According to Figure 35, [As] was strongly correlated with [Fe] at site 30 (R^2 0.68), while the relationship between As concentration and Fe concentration is weaker (but still significant) at site 50 (R^2 0.23). Geological differences between site 30 and site 50 is the primary reason for different correlation. The marine shale band underlying the peat at site 30 produces more source of Fe and the consequent higher aqueous concentrations. This means an increase in Fe(III) oxide deposits formed through the oxidation of Fe(II), and as the As carriers and specific elements associated preferentially with As, more amount of the Fe(III) oxides can promote the interaction with As, resulting in a stronger correlation. Fe(III) oxides are able to concentrate As by sorption from the surrounding sediment or water, resulting in higher As content (Meharg et al., 2006; Mueller and Hug, 2018). In addition, the accumulated As bound with Fe phases will also release by the reductive dissolution of Fe(III) oxides to

stream. The cycle of this whole process promotes the positive relationship between [As] and [Fe] (Kim et al., 2018; Schreiber et al., 2003).

In addition to being associated with Fe, As also has a strong correlation with NOM. Stronger and significant positive correlation between As concentration and NOM concentration with both the site 30 (R^2 0.31, $P < 0.05$) and site 50 (R^2 0.6, $P < 0.05$) were shown from Figure 36. Many studies have proved that NOM plays a great role in the aquatic environment and can strongly affect the distribution and mobility of As by redox reactions, competitive adsorption, desorption, complexation reactions and co-deposition. For example, the sorption behaviour of mineral surface (Fe(III) oxides) on As will be changed by the dissolved organic matter (DOM), resulting in the mobilisation of As in the sediment. The NOM-As complexes generated by the complexation reactions and co-deposition of NOM and As can also drive As to be released from sediments. The existence of NOM-As complexes indicates that NOM can be a source of As, because As mobilisation may be improved through an adsorption/desorption mechanism between NOM and humic substances in reducing conditions. In addition, due to the strong adsorption affinities within NOM and Fe oxides, NOM can often coexist with Fe(III) oxides, which can not only be the adsorption phase for As, but also compete with As for adsorption sites on the oxides surface, leading to the release of As from minerals (Anawar et al., 2013; Bauer et al., 2008; Harvey et al., 2002; Kim et al., 2018;

Meharg et al., 2006). Overall, it is precisely because NOM can significantly affect As from various ways in stream, therefore the occurrence of correlations for NOM and As is expected. One of the samples at site 30 had high concentration of As and Fe resulting in an outlier (Figure 33 A and 35 A).

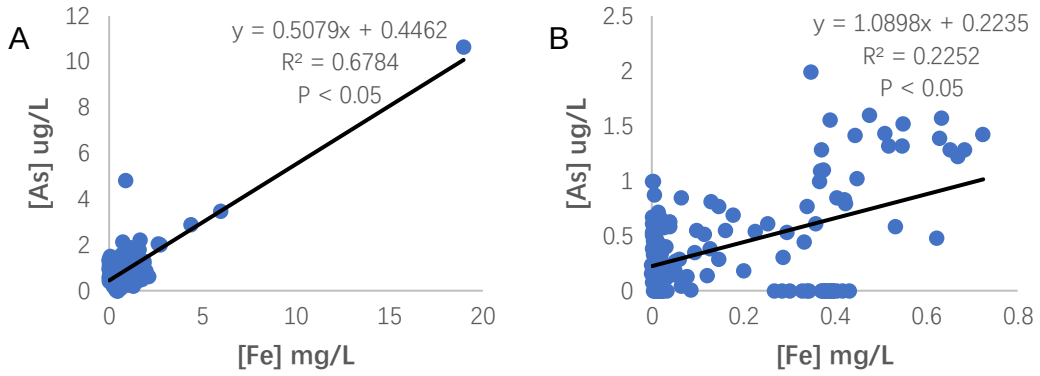

Figure 35 Relationship between [As] and [Fe] for A) site 30 and B) site 50.

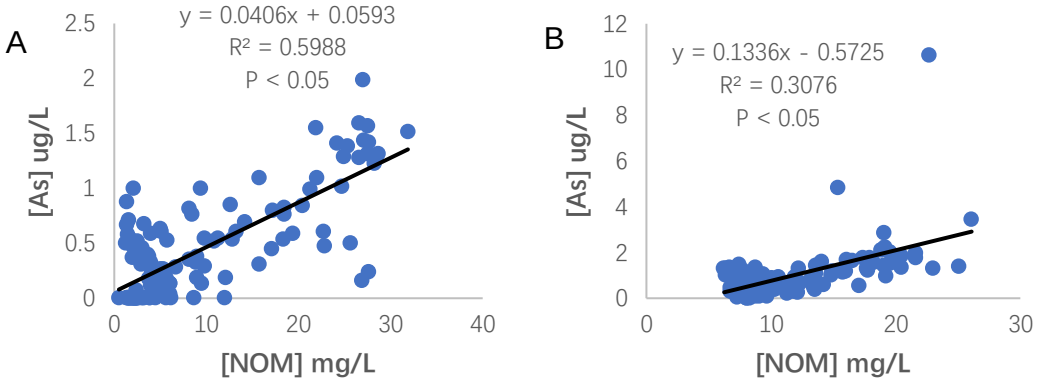

Figure 36 Relationship between [As] and [NOM] for A) site 30 and B) site 50.

These correlations for both Fe and NOM with As show that their role in As mobilisation is important. Fe is the dominant element that control the mobilisation of As at site 30 (R^2 0.68 vs R^2 0.23), while at site 50 it is NOM (R^2

0.6 vs R^2 0.31). In general, the average of Q, [Fe] and [NOM] at site 30 are greater than those of site 50, so it is reasonable to cause larger amount of As flux. However, it is unable to determine the variability of As dataset as a whole by Q. The hysteresis effect generated by Q can hide the true impact from a rising Q or high Q event (discharge event) on As. This may be an explanation for the lack of correlation between [As] and Q. Overall, the reasonable of this explanation need to be verified and this process can be considered by examining a time series of data at high resolution during a discharge event.

Mobilisation of As within a discharge event. The importance of Q in the mobilisation of As is well known from the As flux calculation. Therefore, the understanding in the specific impact of Q on the transmission of As under a temporal change is an important condition for controlling the mobilisation of As in stream. Since no direct evidence can be found from low temporal resolution sampling results, in order to determine the effect of the variability in Q, assessment of the high temporal resolution sampling results on 04/2019 was carried out. Figure 37 shows changes in Q, [NOM], [Fe] and [As] throughout the discharge event. The NOM concentrations at both sites were positively correlated with Q and they rose as Q increased but decreased after peak flow (558.4 l/s at site 30 and 89.83 l/s at site 50). The peak value of NOM at site 50 is bigger than that of site 30 (22.82 mg/L vs 14.22 mg/L). In rivers drainage catchments with NOM rich soils, most of NOM will release

from soils to streams during discharge events. Therefore, the increase in NOM concentration is a common trend observed within discharge event (Morel et al., 2009; Rothwell et al., 2007).

The same as NOM, [Fe] at site 50 had positive correlation with Q and the clear peak profile (the peak value is 0.623 mg/L) was shown in Figure 37 F. Although [As] also had a clear peak profile, the peak value (1.1 µg/L) was only seen after the maximum Q. Unlike site 50, the Fe concentration was at a high value (2 mg/L) before Q rose (Figure 37 E) due to geological factor mentioned before and then decreased as the Q increased. This may be because the dilution at high Q. In addition, [As] reached the highest value (1.25 µg/L) before the peak of Q due to the impact of Fe (Figure 37 E) but the main reason for subsequent decline is uncertain. The As concentration at both site 30 and site 50 are likely to be affected by the NOM and Fe during rainstorm and this requires further analysis for correlation.

The erosion is important in the transport of NOM and Fe from peat to stream, because it will affect the change pattern or level of NOM and Fe concentrations in stream by altering hydrological process (e.g. process of runoff and sediment transportation) and land-surface characteristics, resulting in [NOM] and [Fe] to be more significantly influenced by Q of a high degree of variability. The reduction of both vegetation coverage and the surface litter

created by erosion at site 50 makes that area unable to store water effectively and reduce soil erosion. In addition, the NOM-rich or Fe-rich peat sediment accumulated on vegetation near surface generally will resuspend in eroded site and it can be mobilised by storm flow in stream. Therefore, large amount of NOM and Fe may not be allowed to accumulate within peat or porewater during discharge event, resulting in the direct or indirect (following the sediments) input of Fe and NOM from soil to water (Haag et al., 2001; Kerr and Cooke, 2017; Zhang et al., 2020). As will be accumulated in sediments by sorption or other interaction with Fe or NOM under relative low Q during the whole process of sediment entering the stream and continuing to move. Next, the As-rich sediments will become the dominate diffuse source in stream under high Q, resulting in the mobilisation of As from sediment to water by dissolution. This means the content of As in stream will increase as well as the mobility (Eggleton and Thomas, 2004; Mayes et al., 2008). This can be reflected in Figure 37, the highest concentration of NOM and Fe is much greater than their usual concentration at site 50 within discharge event (22.82 mg/L vs 9.33 mg/L for NOM, 0.623 mg/L vs 0.2 mg/L for Fe). This subsequently caused the concentration of As to rise more than usual. (1.1 µg/L vs 0.44 µg/L). Due to the erosion is the likely future situation of upland peat, the situation that occurs in eroded site 50 needs to be paid enough attention, because it means that the erosion may cause the release of As and promote the mobility of As, which represents a potential risk to public health.

Optimizing land use and rational land management strategies make it possible to control As mobilisation in stream by reducing soil erosion (Zhang et al., 2020). As for site 30, the extent of increase in NOM is lower due to the less erosion. Meanwhile, lower input causes the Fe to be more affected by the dilution of high Q, leading to reduction of concentration. The contents of NOM and Fe in stream are important factors influencing the As due to the correlation between NOM and Fe with As. The finding of Figure 38 and Figure 39 can serve as important reference for their correlation.

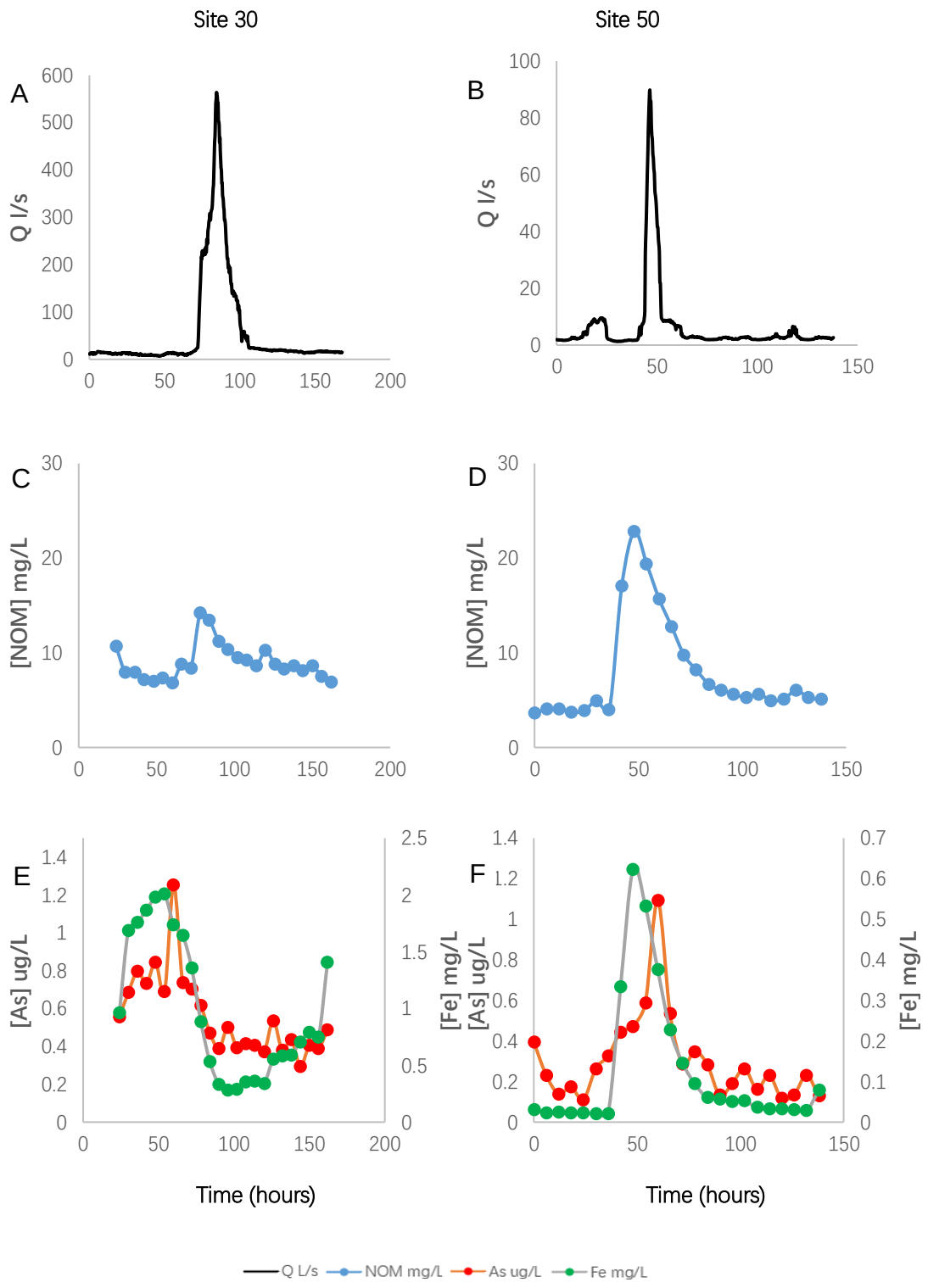

Figure 37 Dissolved NOM (C and D), As, Fe (E and F) concentrations and discharge (Q) (A and B) for site 30 and site 50 during discharge event.

The concentration of As was significant correlated with Fe within both sites (R^2 0.62 at site 30 and R^2 0.49 at site 50, both $P < 0.05$) (Figure 38). The positive relationship supports the role of Fe in mobilising As within stream. A weak negative correlation (R^2 0.11) between NOM and As at site 30 was shown in Figure 39 A and this suggests that Fe is the dominant factor to control the transport of As in that area. Therefore, once the Fe concentration have been diluted by high Q, the concentration of As at site 30 decreased as well (Figure 37 E). In addition, unlike site 30, the As of site 50 was positively correlated with NOM (R^2 0.4841). Therefore, NOM and Fe at site 50 have the same effect on As. Due to the different roles of NOM and Fe on As in different sites or periods, future work should consider the potential effects of ratio between [NOM] and [Fe] in order to determine the specific factors that affecting As mobilisation.

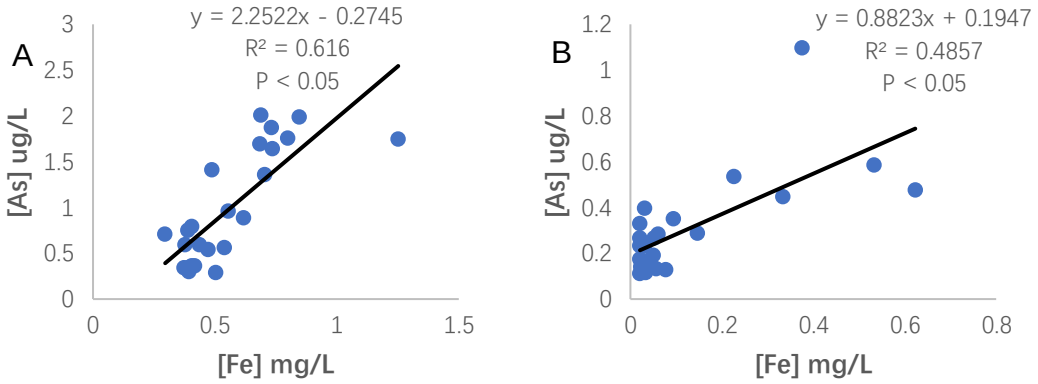

Figure 38 Relationship between [As] and [Fe] for A) site 30 and B) site 50 during discharge event.

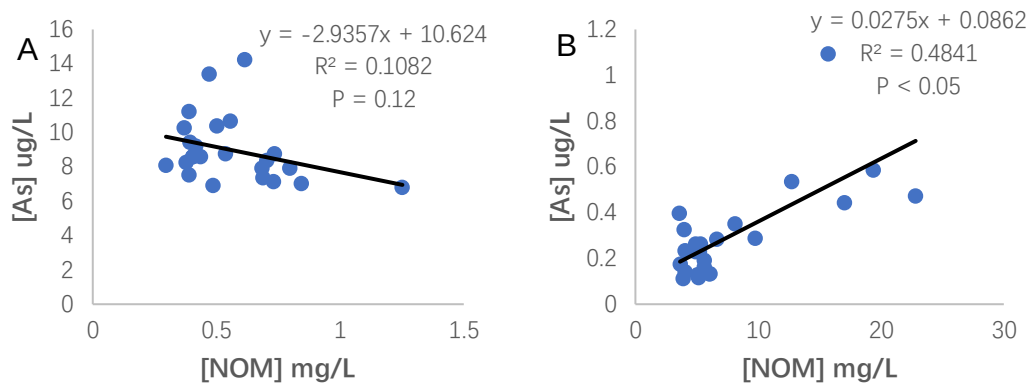

Figure 39 Relationship between [As] and [NOM] for A) site 30 and B) site 50 during discharge event.

Figure 40 demonstrates that the correlations between As concentrations and Q were still low for both of sites (R^2 0.0862 for site 30 and R^2 0.0757 for site 50). The change of [As] that was observed in Figure 37 E and F during discharge event of rising Q may be not directly caused by Q. It has been shown that the concentration of As is strongly influence by amount of NOM and Fe (Meharg et al., 2006; Neubauer et al., 2013). Meanwhile, it is well known that Fe, NOM concentrations are easily affected by Q during discharge event (Figure 37), which in turn impacts on the resulting associations (hysteresis effect). Therefore, Q has the possibility of indirectly impact on As through changing the content of NOM and Fe in stream. Overall, the value of high temporal resolution sampling is demonstrated by this study. The changes of elements within environment are various during discharge event, so it is difficult to capture by low temporal resolution sampling (Vaughan et al., 2019). The complexity of As mobilisation in stream can also be seen in Figure 41

The presence of both rising and falling hydrograph limbs causes the low correlation between As and Q. The trajectory of site 30 was clockwise and this occurs when concentrations increase more rapidly than the observed Q. This is named ‘Proteresis’, which means a ‘flush’ response. However, different trajectory (anticlockwise) was shown at site 50, indicating hysteresis (Boyer et al., 1997).

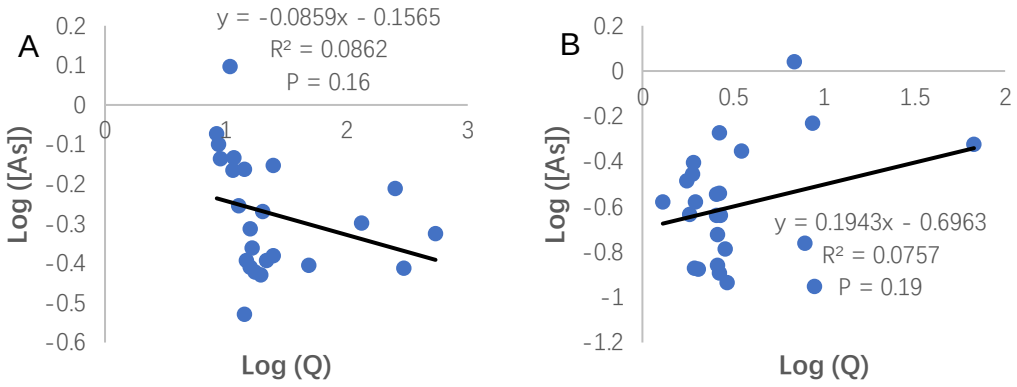

Figure 40 Relationship between Log ([As]) and Log (Q) for A) site 30 and B) site 50 during discharge event. The trajectory of site 30 is clockwise.

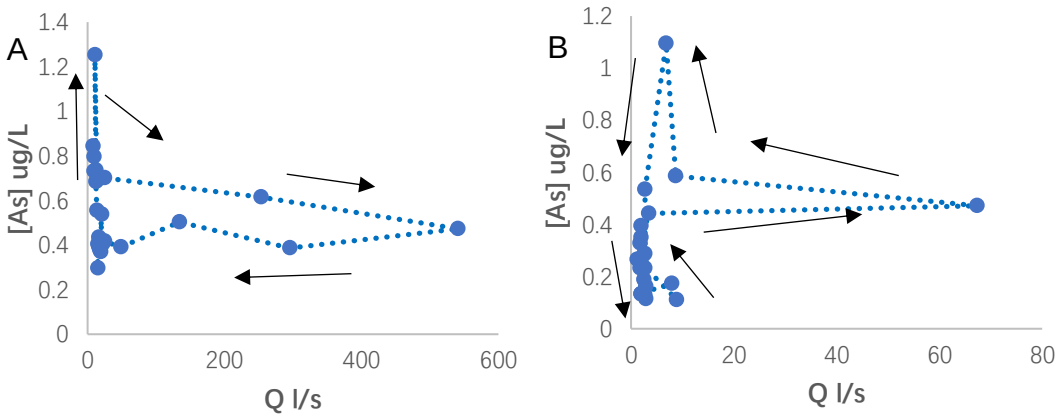

Figure 41High-resolution time series of [As] v Q during discharge event for A) site 30 and B) site 50. The time series direction is shown by arrows.

Changes in PSD of As, Fe and NOM. The determination of the correlation between PSD of As and the PSD of NOM and Fe is benefit for better understanding of the factors that control the mobility of As in stream system. PSD of As, Fe and NOM were shown in Figure 42 The correlation between PSD of Fe and As was the significant at site 30, because within three samples, both Fe and As had similar types of PSD (mainly <1>0.2 μm when Q was 235 l/s, mainly <1>0.2 μm. <10>3 KD and <3 KD when Q was 268 l/s and 333 l/s) and the same change trend of each particle size content (mass). NOM of three samples had all size classes (weak content in <0.2>50 KD) and each size had low change during different Q. The PSD of As appears to be controlled by Fe suggests that the major factor for As transport within site 30. It can be seen in Table 9, the correlation between Fe and As in main particle size is higher than NOM and As. At site 50, the higher Q resulted in the large amount of As, Fe and NOM and this conform to the influence of erosion on the content of As, Fe and NOM described above. There is no clear dominant that controls the transport of As. This indicate that both NOM and Fe are related to the mobilisation of As. According to Table 9, both NOM and Fe have the high correlation with As in particle size <0.2>50 KD, <50>10 KD and <3 KD. The focus of future work can be to explore the reasons that lead to Fe or NON becoming the dominant factor in controlling As transmission (e.g. different Fe/NOM ratios or different mixing order between Fe, As and NOM).

In addition, a significant portion present of both As and NOM was in form of truly dissolved species (<10 KD) and it almost increased as the Q rose (Figure 42). This suggests that most mobilised NOM and As in the stream is present as truly dissolved forms, not colloids or particles. Unlike As and NOM, Fe is mainly particle (<1>0.2 µm). It is very likely that Fe and NOM affect the transport of As in particulate form and dissolved form respectively. The dissolved As in stream exhibits a higher mobility during the periods of rising Q.

Table 9 Correlation coefficients of Fe and NOM with As for each size within both sites.

	Site 30				Site 50			
As	Fe		NOM		Fe		NOM	
size	R^2	P	R^2	P	R^2	P	R^2	P
<1>0.2 µm	0.98	0.08	0.13	0.76	0.4	0.56	0.24	0.67
<0.2>50 KD	0.98	0.08	0.96	0.13	0.92	0.17	0.5	0.5
<50>10 KD	0.05	0.86	0.55	0.47	0.77	0.31	0.83	0.27
<10>3 KD	0.99	0.05	0.1	0.79	0.05	0.84	0.1	0.79
<3 KD	0.88	0.23	0.85	0.25	0.98	0.08	0.98	0.08

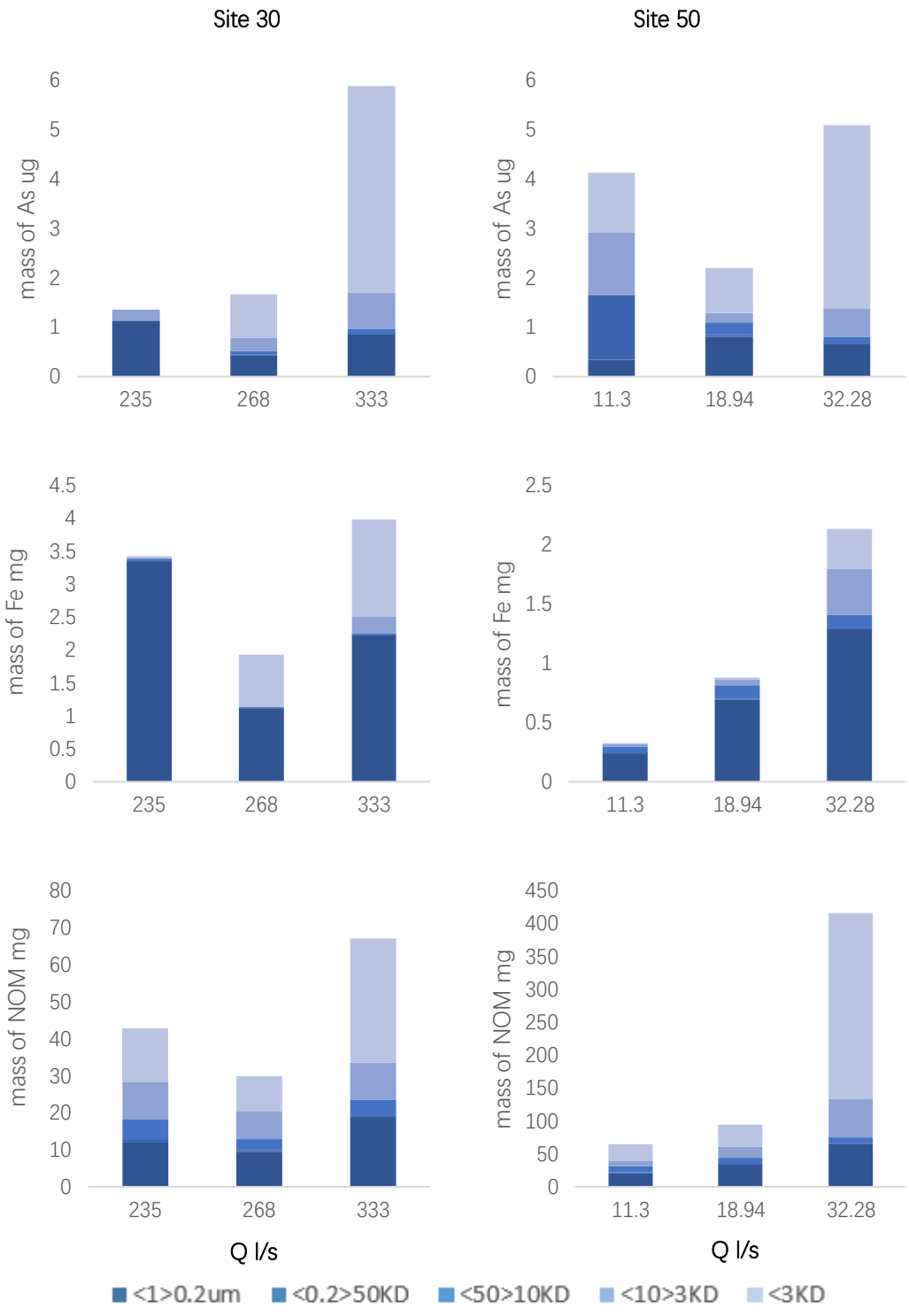

Figure 42 PSD of As, Fe and NOM for each site.

5.4 Conclusions

The detailed study of dissolved As content and its mobilisation under a range of hydrological conditions in different sites of Peak District, UK has shown the dissolved As is variable temporally and spatially. This is reflected in the concentrations monitoring and fluxes estimation. Generally, the average and range of As concentration and Q at site 30 are greater than those of site 50, leading to higher As fluxes estimated by methods based on interpolation or rating relationship. The previously deposited As are leached from the peat to stream system and can continue to move under baseflow and stormflow (discharge event). This is a potential risk to the water resources around Peak District, so it is necessary to determine the factors that affect the mobilisation of As.

Mobilisation processes of As can be identified by measurement of several potential controlling variables (Q, [Fe] and [NOM]). The low correlation between Q and As indicates that dilution effect and changes in the flow path are not the dominant factors that affecting As content. As is correlated with both Fe and NOM to varying degrees dependent to on different quantities or the ratio between the quantities. At site 30, Fe is the dominant factor controlling As mobilisation due to the higher correlation with As, while at site 50 it is NOM. Since the different dominant observed in the two sites, future work can try to understand the reasons that cause Fe or NOM to become the

dominant factor controlling the transport of As in stream by determining mixing order and ratio between Fe, NOM or As.

The analysis of the high temporal resolution sampling results identifies that the erosion is important factors influencing the mobilisation of Fe, NOM and As during discharge event. Erosion affects the hydrological processes and land-surface characteristics, resulting in the lack of vegetation and resuspension of sediment. Fe and NOM at site 50 are more susceptible to be influence by high Q and therefore obviously increased, which cause the subsequent release of As. Although the direct correlation of As and Q is low, particular discharge events are responsible indirectly for the transport of As into stream. Fe and NOM exhibit different mobility in two sites during discharge event with high Q. Unlike site 50, less input of Fe and NOM due to less erosion. Fe is still major factor to control the mobilisation of As at site 30 and diluted during discharge event. This is also shown in the correlation of PSD between Fe and NOM with As. Within site 30, the PSD of Fe and As is closely correlated and this is reflected in correlation coefficients for each size fraction, while the PSD of As was correlated with both Fe and NOM at site 50. In addition, the form of NOM and Fe are also important factors on the transport of As. The former mainly participates in the transport of As in a particle form, while the latter is in a truly dissolved form.

Chapter 6. General Discussion

6.1 Quantity of OC flux from an upland peat catchment

In general, the increasing in release of OC exacerbated climatic warming, thus increasing the understanding in OC release has great relevance for environmental research. The ability to estimate OC release over time is essential to understand the processes involved in release and mobilisation of OC. The UK peatlands are rich in OC, therefore estimating OC fluxes from peatlands is an important concern when addressing issues such as climatic warming and water quality. In this study, two methods (interpolation and rating relationships) used allowed comparison of OC fluxes on a system. Although OC fluxes measured by the two methods are similar, the results are still not 100% reliable because there is still a sampling interval during the study period due to uncontrollable factors (equipment malfunctions or extreme weather makes research site inaccessible). Therefore, in order to achieve the accuracy of OC quantification, the sampling intervals should be improved such as sampling at the highest possible resolution to obtain more samples in the further monitoring of OC fluxes.

OC fluxes were increased significantly compared to previous estimations by Do (2013) for the same site, suggesting that OC flux can continually change. Therefore, it is crucial to understand the factors that contribute to the increasing export of OC. In this study, higher OC flux in the eroded site means

that erosion drives the loss and mobility of OC in upland peat catchment, leading to a significant impact on environmental C balance. Considering that the eroded nature of the sub catchment studied can be a model of future situation (reason explained in subsection “Introduction” of Chapter 3), future upland peat catchments are expected to increase more C mobilisation and my therefore aggravate climate change caused by global warming. In addition, OC exports are easily increased by high Q during stormflow, especially in the eroded site. The results can help us to better understand the impact of erosion and climate change on the dynamics of OC in upland peat catchment. Therefore, in order to reduce local C release and its negative environmental impact, the reasonable land management strategy (improvement of vegetation coverage) should be further developed.

6.2 Effect of NOM on speciation and size of Fe change with flow path, pH, temperature and daylight in natural waters

The importance of hydrochemical controls of NOM was highlighted in this study. Although NOM used is site specific, the subsequent size separation provides some generic applicability to the findings. The most abundant (<10>3 KD) size fraction is used in this project. Meanwhile, the range of pH in which the Fe-NOM interaction occurred covers a large proportion of natural waters. Due to the presence of NOM, FeII cannot be assumed to be a free aqueous ion. The mobility of Fe will be reduced through associating with NOM

to become particulate and the proportion is a function of NOM concentration and pH. Large changes in speciation of Fe will be caused between 10 and 25 ^{o}C. At 10^{o}C, FeII can be preserved by binding to both the product of its own oxidation, Fe(III)hydroxide and NOM, but bound to the latter has the potential to be a finer colloid (<10 KD). At 25 ^{o}C, Fe is only bound with NOM, so NOM will be the main control of the preservation of Fe in oxic water. Darkness slows down Fe oxidation as well as 10 ^{o}C, so FeII has time to bind to the FeIII(hydr)oxide without NOM. In addition, darkness also enhances the binding of Fe to NOM. This work found that Fe-NOM interactions have a direct effect on Fe speciation and size, altering solute (Fe) mobility and SSA. Therefore, it has direct implication for Fe utility in microbial metabolism, and indirect implications for mobility of pollutants and nutrients through influencing SSA area of FeIII(hydr)oxides, as the surface of FeIII(hydr)oxides can control pollutants and nutrients by sorption, changes in SSA lead to changes in sorption sites.

6.3 Controls on the mobility of As in natural water: The role of NOM, Fe and changing hydrological conditions

Even a slight rise in the amounts (the maximum concentration limit is 10 µg/L) of toxic element As could pose a threat to the natural environment and public health, it is necessary to measure As concentrations and monitor its fluxes under a range of hydrological and hdyrochemical conditions. The results of As

concentrations and fluxes in this study were variable significantly compared to previous estimations by Hegan (2012) and Rothwell (2011) for the same study site, reflecting that the dissolved As is variable temporally and spatially. Under baseflow and stormflow, Fe and NOM can control the mobility of As in stream. At site 30, the dominant factor is Fe while at site 50 it is NOM. As has different degrees of correlation with Fe and NOM, which may depend on their different quantities or ratios between quantities. In addition, the form of NOM and Fe are also important factors on the mobility of As, the former mainly participates in the transport of As in a particle form, while the latter is in a truly dissolved form. Understanding the factors that affect As release are benefit for As mobility management and control. Future work can try to understand the reasons that cause Fe or NOM to become the dominant factor controlling the mobility of As in stream by determining mixing order and ratio between Fe, NOM or As, this may help to further prediction of the mobility and ultimate fate of As.

Fe and NOM at eroded site are more likely to be affected by high Q during stormflow and rise, indicating that erosion is an important factor influencing the mobilisation of Fe, NOM by changing hydrological process, which cause the subsequent releasee and mobility of As. Less input of Fe and NOM due to less erosion at uneroded site during stormflow. Fe is still dominant factor to control the mobility of As and diluted during high Q, resulting in reduction of As

concentration. Therefore, the previously deposited As will leach and move in upland peat catchment to stream system continuously due to the erosion and climatic change (stormflow) and it means that there is a potential risk to the water resources around Peak District. Therefore, the reasonable land management strategy (improvement of vegetation coverage) should be further developed to reduce the impact of erosion and stormflow period on As release, which is benefit for controlling the harm of As pollution on environment and public health.

Reference

Abdelrady, A., Sharma, S., Sefelnasr, A., & Kennedy, M. (2020). Characterisation of the impact of dissolved organic matter on iron, manganese, and arsenic mobilisation during bank filtration. Journal of environmental management, 258, 110003.

Accardi-Dey, A., & Gschwend, P. M. (2002). Assessing the combined roles of natural organic matter and black carbon as sorbents in sediments. *Environmental Science & Technology*, *36*(1), 21-29.

Adeolu, A. R., Mohammad, T. A., Daud, N. N. N., Sayok, A. K., Rory, P., & Stephanie, E. (2018). Soil carbon and nitrogen dynamics in a tropical peatland. In Soil Management and Climate Change (pp. 73-83). Academic Press.

Aftabtalab, A., Rinklebe, J., Shaheen, S. M., Niazi, N. K., Moreno-Jiménez, E., Schaller, J., & Knorr, K. H. (2021). Review on the interactions of arsenic, iron (oxy)(hydr) oxides, and dissolved organic matter in soils, sediments, and groundwater in a ternary system. Chemosphere, 131790.

Aiken, G. R., Hsu-Kim, H., & Ryan, J. N. (2011). Influence of dissolved organic matter on the environmental fate of metals, nanoparticles, and colloids.

Aiken, G., McKnight, D. M., Thorn, K. A., & Thurman, E. M. (1992). Isolation of hydrophilic organic acids from water using nonionic macroporous resins. *Organic Geochemistry*, *18*(4), 567-573.

Aitkenhead, J. A., Hope, D., & Billett, M. F. (1999). The relationship between dissolved organic carbon in stream water and soil organic carbon pools at different spatial scales. Hydrological Processes, 13(8), 1289-1302.

Baalousha, M., Vd Kammer, F., Motelica-Heino, M., Baborowski, M., Hofmeister, C., & Le Coustumer, P. (2006). Size-based speciation of natural colloidal particles by flow field flow fractionation, inductively coupled plasma-mass spectroscopy, and transmission electron microscopy/X-ray energy dispersive spectroscopy: colloids− trace element interaction. Environmental science & technology, 40(7), 2156-2162.

Baalousha, M., Stoll, S., Motelica-Heino, M., Guigues, N., Braibant, G., Huneau, F., & Le Coustumer, P. (2019). Suspended particulate matter determines physical speciation of Fe, Mn, and trace metals in surface waters of Loire watershed. *Environmental Science and Pollution Research*, *26*(6), 5251-5266.

Baborowski, M., & Tadjiki, S. (2003). Colloidal Particles in Sediment Pore

Waters: Particle Size Distributions and Associated Element Size Distribution in Anoxic and Re‐oxidized Samples, Obtained by FFF‐ICP‐MS Coupling. *CLEAN–Soil, Air, Water*, *31*(4‐5), 400-410.

Barber, L. B., Leenheer, J. A., Noyes, T. I., & Stiles, E. A. (2001). Nature and transformation of dissolved organic matter in treatment wetlands. *Environmental science & technology*, *35*(24), 4805-4816.

Bauer, M., & Blodau, C. (2006). Mobilization of arsenic by dissolved organic matter from iron oxides, soils and sediments. Science of the Total Environment, 354(2-3), 179-190.

Bauer, M., Fulda, B., & Blodau, C. (2008). Groundwater derived arsenic in high carbonate wetland soils: Sources, sinks, and mobility. Science of the Total Environment, 401(1-3), 109-120.

Benbi, D. K., Brar, K., Toor, A. S., & Singh, P. (2015). Total and labile pools of soil organic carbon in cultivated and undisturbed soils in northern India. Geoderma, 237, 149-158.

Biasi, C., Jokinen, S., Marushchak, M. E., Hämäläinen, K., Trubnikova, T., Oinonen, M., & Martikainen, P. J. (2014). Microbial respiration in Arctic upland

and peat soils as a source of atmospheric carbon dioxide. Ecosystems, 17(1), 112-126.

Boyer, E. W., Hornberger, G. M., Bencala, K. E., & McKnight, D. M. (1997). Response characteristics of DOC flushing in an alpine catchment. Hydrological processes, 11(12), 1635-1647.

Cai, X., ThomasArrigo, L. K., Fang, X., Bouchet, S., Cui, Y., & Kretzschmar, R. (2020). Impact of Organic Matter on Microbially-Mediated Reduction and Mobilization of Arsenic and Iron in Arsenic (V)-Bearing Ferrihydrite. Environmental Science & Technology, 55(2), 1319-1328

Cai, Y., Cabrera, J. C., Georgiadis, M., & Jayachandran, K. (2002). Assessment of arsenic mobility in the soils of some golf courses in South Florida. Science of the total environment, 291(1-3), 123-134

Catrouillet, C., Davranche, M., Dia, A., Bouhnik-Le Coz, M., Marsac, R., Pourret, O., & Gruau, G. (2014). Geochemical modeling of Fe (II) binding to humic and fulvic acids. Chemical geology, 372, 109-118.

Chang, C. J., Huang, C. P., Chen, C. Y., & Wang, G. S. (2020). Assessing the potential effect of extreme weather on water quality and disinfection by-

product formation using laboratory simulation. *Water research*, *170*, 115296.

Chapman, S. J., Bell, J., Donnelly, D., & Lilly, A. (2009). Carbon stocks in Scottish peatlands. Soil Use and Management, 25(2), 105-112.

Chen, C., & Thompson, A. (2018). Ferrous iron oxidation under varying pO2 levels: the effect of Fe (III)/Al (III) oxide minerals and organic matter. Environmental science & technology, 52(2), 597-606.

Chen, J., Xiu, Z., Lowry, G. V., & Alvarez, P. J. (2011). Effect of natural organic matter on toxicity and reactivity of nano-scale zero-valent iron. *water research*, *45*(5), 1995-2001.

Cheng, T., & Allen, H. E. (2006). Comparison of zinc complexation properties of dissolved natural organic matter from different surface waters. Journal of environmental management, 80(3), 222-229

Chen, Y., Dong, B. Z., Gao, N. Y. & Fan, J. C. (2007). Effect of coagulation pretreatment on fouling of an ultrafiltration membrane. Desalination, 204(1-3), 181-188.

Choudhary, M., Jetley, U. K., Khan, M. A., Zutshi, S., & Fatma, T. (2007).

Effect of heavy metal stress on proline, malondialdehyde, and superoxide dismutase activity in the cyanobacterium Spirulina platensis-S5. *Ecotoxicology and environmental safety*, *66*(2), 204-209.

Clark, J. M., Lane, S. N., Chapman, P. J., & Adamson, J. K. (2007). Export of dissolved organic carbon from an upland peatland during storm events: Implications for flux estimates. Journal of Hydrology, 347(3-4), 438-447.

Cooper, W. J., Zika, R. G., Petasne, R. G., & Plane, J. M. (1988). Photochemical formation of hydrogen peroxide in natural waters exposed to sunlight. Environmental science & technology, 22(10), 1156-1160.

Croot, P. L., & Heller, M. I. (2012). The importance of kinetics and redox in the biogeochemical cycling of iron in the surface ocean. *Frontiers in microbiology*, *3*.

Daugherty, E. E., Gilbert, B., Nico, P. S., & Borch, T. (2017). Complexation and redox buffering of iron (II) by dissolved organic matter. Environmental science & technology, 51(19), 11096-11104.

Davis, J. A. (1984). Complexation of trace metals by adsorbed natural organic matter. *Geochimica et Cosmochimica Acta*, *48*(4), 679-691.

Davison, W., & Seed, G. (1983). The kinetics of the oxidation of ferrous iron in synthetic and natural waters. Geochimica et Cosmochimica Acta, 47(1), 67-79.

Dawson, J. J. C., Billett, M. F., Neal, C., & Hill, S. (2002). A comparison of particulate, dissolved and gaseous carbon in two contrasting upland streams in the UK. Journal of Hydrology, 257(1-4), 226-246.

DelSontro, T., Beaulieu, J. J., & Downing, J. A. (2018). Greenhouse gas emissions from lakes and impoundments: Upscaling in the face of global change. Limnology and Oceanography Letters, 3(3), 64-75.

Deng, Y. (1997). Formation of iron (III) hydroxides from homogeneous solutions. *Water Research*, *31*(6), 1347-1354.

Dinsmore, K. J., Billett, M. F., Skiba, U. M., Rees, R. M., Drewer, J., & Helfter, C. (2010). Role of the aquatic pathway in the carbon and greenhouse gas budgets of a peatland catchment. Global Change Biology, 16(10), 2750-2762.

Do, P. D. (2013). Quantifying organic carbon fluxes from upland peat.

Drozdova, O. Y., Aleshina, A. R., Tikhonov, V. V., Lapitskiy, S. A., & Pokrovsky, O. S. (2020). Coagulation of organo-mineral colloids and

formation of low molecular weight organic and metal complexes in boreal humic river water under UV-irradiation. Chemosphere, 250, 126216.

Eggleton, J., & Thomas, K. V. (2004). A review of factors affecting the release and bioavailability of contaminants during sediment disturbance events. Environment international, 30(7), 973-980.

Ekschmitt, K., Kandeler, E., Poll, C., Brune, A., Buscot, F., Friedrich, M., ... & Wolters, V. (2008). Soil-carbon preservation through habitat constraints and biological limitations on decomposer activity. Journal of Plant Nutrition and Soil Science, 171(1), 27-35.

Emmenegger, L., King, D. W., Sigg, L., & Sulzberger, B. (1998). Oxidation kinetics of Fe (II) in a eutrophic Swiss lake. Environmental science & technology, 32(19), 2990-2996.

Evans, M., & Warburton, J. (2011). Geomorphology of upland peat: erosion, form and landscape change. John Wiley & Sons.

Evans, M., Warburton, J., & Yang, J. (2006). Eroding blanket peat catchments: global and local implications of upland organic sediment budgets. Geomorphology, 79(1-2), 45-57.

Fan, L., Harris, J. L., Roddick, F. A., & Booker, N. A. (2001). Influence of the characteristics of natural organic matter on the fouling of microfiltration membranes. *Water Research*, *35*(18), 4455-4463.

Fellman, J. B., Hood, E., Edwards, R. T., & D'Amore, D. V. (2009). Changes in the concentration, biodegradability, and fluorescent properties of dissolved organic matter during stormflows in coastal temperate watersheds. Journal of Geophysical Research: Biogeosciences, 114(G1).

Filella, M. (2009). Freshwaters: which NOM matters?. Environmental chemistry letters, 7(1), 21-35.

Frauendorf, T. C., MacKenzie, R. A., Tingley III, R. W., Frazier, A. G., Riney, M. H., & El-Sabaawi, R. W. (2019). Evaluating ecosystem effects of climate change on tropical island streams using high spatial and temporal resolution sampling regimes. Global Change Biology, 25(4), 1344-1357.

Freeman, C., Fenner, N., Ostle, N. J., Kang, H., Dowrick, D. J., Reynolds, B., ... & Hudson, J. (2004). Export of dissolved organic carbon from peatlands under elevated carbon dioxide levels. *Nature*, *430*(6996), 195-198.

Fu, F., Dionysiou, D. D., & Liu, H. (2014). The use of zero-valent iron for

groundwater remediation and wastewater treatment: a review. *Journal of hazardous materials*, *267*, 194-205.

Gaffney, J. W., White, K. N., & Boult, S. (2008). Oxidation state and size of Fe controlled by organic matter in natural waters. *Environmental science & technology*, *42*(10), 3575-3581.

Gallego, S. M., Benavides, M. P., & Tomaro, M. L. (1996). Effect of heavy metal ion excess on sunflower leaves: evidence for involvement of oxidative stress. *Plant Science*, *121*(2), 151-159.

Garg, S., Ito, H., Rose, A. L., & Waite, T. D. (2013). Mechanism and kinetics of dark iron redox transformations in previously photolyzed acidic natural organic matter solutions. Environmental science & technology, 47(4), 1861-1869.

Garg, S., Jiang, C., & Waite, T. D. (2015). Mechanistic insights into iron redox transformations in the presence of natural organic matter: Impact of pH and light. Geochimica et Cosmochimica Acta, 165, 14-34.

Garg, S., Jiang, C., Miller, C. J., Rose, A. L., & Waite, T. D. (2013). Iron redox transformations in continuously photolyzed acidic solutions containing natural organic matter: Kinetic and mechanistic insights. Environmental science &

technology, 47(16), 9190-9197.

Gomes, T. F., Van de Broek, M., Govers, G., Silva, R. W., Moraes, J. M., Camargo, P. B., ... & Martinelli, L. A. (2019). Runoff, soil loss, and sources of particulate organic carbon delivered to streams by sugarcane and riparian areas: An isotopic approach. Catena, 181, 104083.

González A, Z. I., Krachler, M., Cheburkin, A. K., & Shotyk, W. (2006). Spatial distribution of natural enrichments of arsenic, selenium, and uranium in a minerotrophic peatland, Gola di Lago, Canton Ticino, Switzerland. Environmental science & technology, 40(21), 6568-6574.

Gorham, E. (1991). Northern peatlands: role in the carbon cycle and probable responses to climatic warming. Ecological applications, 1(2), 182-195.

Gorham, E., & Rochefort, L. (2003). Peatland restoration: a brief assessment with special reference to Sphagnum bogs. Wetlands Ecology and Management, 11(1), 109-119.

Günther, A., Böther, S., Couwenberg, J., Hüttel, S., & Jurasinski, G. (2018). Profitability of direct greenhouse gas measurements in carbon credit schemes of peatland rewetting. Ecological Economics, 146, 766-771.

Haag, I., Kern, U., & Westrich, B. (2001). Erosion investigation and sediment quality measurements for a comprehensive risk assessment of contaminated aquatic sediments. Science of the total environment, 266(1-3), 249-257.

Hand, V. L., Lloyd, J. R., Vaughan, D. J., Wilkins, M. J. & Boult, S. (2008). Experimental studies of the influence of grain size, oxygen availability and organic carbon availability on bioclogging in porous media. Environmental science & technology, 42(5), 1485-1491.

Harley, C. D., Randall Hughes, A., Hultgren, K. M., Miner, B. G., Sorte, C. J., Thornber, C. S., ... & Williams, S. L. (2006). The impacts of climate change in coastal marine systems. Ecology letters, 9(2), 228-241.

Harvey, C. F., Swartz, C. H., Badruzzaman, A. B. M., Keon-Blute, N., Yu, W., Ali, M. A., ... & Ahmed, M. F. (2002). Arsenic mobility and groundwater extraction in Bangladesh. Science, 298(5598), 1602-1606.

Hegan, A. F. (2012). The Occurrence and Mobility of Arsenic in Soils and Sediments: Assessing Environmental Controls. The University of Manchester (United Kingdom).

Hejzlar, J., Dubrovský, M., Buchtele, J., & Růžička, M. (2003). The apparent

and potential effects of climate change on the inferred concentration of dissolved organic matter in a temperate stream (the Malše River, South Bohemia). *Science of the Total Environment*, *310*(1-3), 143-152.

Héry, M., Gault, A. G., Rowland, H. A., Lear, G., Polya, D. A., & Lloyd, J. R. (2008). Molecular and cultivation-dependent analysis of metal-reducing bacteria implicated in arsenic mobilisation in south-east asian aquifers. Applied Geochemistry, 23(11), 3215-3223

Hook, A. M., & Yeakley, J. A. (2005). Stormflow dynamics of dissolved organic carbon and total dissolved nitrogen in a small urban watershed. Biogeochemistry, 75(3), 409-431

Hughes, M. F. (2002). Arsenic toxicity and potential mechanisms of action. Toxicology letters, 133(1), 1-16.

Hyung, H., & Kim, J. H. (2008). Natural organic matter (NOM) adsorption to multi-walled carbon nanotubes: effect of NOM characteristics and water quality parameters. *Environmental science & technology*, *42*(12), 4416-4421.

Jackson, A., Gaffney, J. W., & Boult, S. (2012). Subsurface interactions of Fe (II) with humic acid or landfill leachate do not control subsequent iron (III)(hydr)

oxide production at the surface. *Environmental science & technology*, *46*(14), 7543-7550.

Jansson, M. B. (1996). Estimating a sediment rating curve of the Reventazon river at Palomo using logged mean loads within discharge classes. Journal of Hydrology, 183(3-4), 227-241.

Jaouadi, M., Amdouni, N., & Duclaux, L. (2012). Characteristics of natural organic matter extracted from the waters of Medjerda dam (Tunisia). Desalination, 305, 64-71.

Jones, A. M., Collins, R. N., Rose, J., & Waite, T. D. (2009). The effect of silica and natural organic matter on the Fe (II)-catalysed transformation and reactivity of Fe (III) minerals. *Geochimica et Cosmochimica Acta*, *73*(15), 4409-4422.

Kerr, J. G., & Cooke, C. A. (2017). Erosion of the Alberta badlands produces highly variable and elevated heavy metal concentrations in the Red Deer River, Alberta. Science of the Total Environment, 596, 427-436.

Kim, H. B., Kim, S. H., Jeon, E. K., Kim, D. H., Tsang, D. C., Alessi, D. S., ... & Baek, K. (2018). Effect of dissolved organic carbon from sludge, Rice straw

and spent coffee ground biochar on the mobility of arsenic in soil. Science of the total environment, 636, 1241-1248.

Kim, H. C., & Yu, M. J. (2005). Characterization of natural organic matter in conventional water treatment processes for selection of treatment processes focused on DBPs control. *Water research*, *39*(19), 4779-4789.

Krachler, R., Krachler, R. F., Wallner, G., Steier, P., El Abiead, Y., Wiesinger, H., ... & Keppler, B. K. (2016). Sphagnum-dominated bog systems are highly effective yet variable sources of bio-available iron to marine waters. *Science of the Total Environment*, *556*, 53-62.

Krauss, K. W., Holm Jr, G. O., Perez, B. C., McWhorter, D. E., Cormier, N., Moss, R. F., ... & Raynie, R. C. (2016). Component greenhouse gas fluxes and radiative balance from two deltaic marshes in Louisiana: Pairing chamber techniques and eddy covariance. Journal of Geophysical Research: Biogeosciences, 121(6), 1503-1521.

Lal, R. (2003). Soil erosion and the global carbon budget. Environment international, 29(4), 437-450.

Leclerc, É., Venkiteswaran, J. J., Jasiak, I., Telford, J. V., Schultz, M. D., Wolfe,

B. B., ……. & Couture, R. M. (2021). Quantifying arsenic post-depositional mobility in lake sediments impacted by gold ore roasting in sub-arctic Canada using inverse diagenetic modelling. Environmental Pollution, 288, 117723.

Lee, J. A., & Tallis, J. H. (1973). Regional and historical aspects of lead pollution in Britain. Nature, 245(5422), 216-218.

Lee, T., Lim, H., Lee, Y., & Park, J. W. (2003). Use of waste iron metal for removal of Cr (VI) from water.*Chemosphere*, *53*(5), 479-485.

Liang, L., McNabb, J. A., Paulk, J. M., Gu, B., & McCarthy, J. F. (1993). Kinetics of iron (II) oxygenation at low partial pressure of oxygen in the presence of natural organic matter. *Environmental science & technology*, *27*(9), 1864-1870.

Liao, P., Li, W., Jiang, Y., Wu, J., Yuan, S., Fortner, J. D., & Giammar, D. E. (2017). Formation, aggregation, and deposition dynamics of NOM-iron colloids at anoxic–oxic interfaces. Environmental science & technology, 51(21), 12235-12245.

Ling, W., Xu, J., Gao, Y., & Wang, H. (2004). [influence of dissolved organic matter (dom) on environmental behaviors of organic pollutants in soils]. *Ying*

yong sheng tai xue bao = The journal of applied ecology,15(2), 326.

Liu, Y., Xu, F., & Liu, C. (2017). Coupled hydro-biogeochemical processes controlling cr reductive immobilization in Columbia River hyporheic zone. *Environmental science & technology*, *51*(3), 1508-1517.

Luan, H., & Vadas, T. M. (2015). Size characterization of dissolved metals and organic matter in source waters to streams in developed landscapes. Environmental Pollution, 197, 76-83.

Ma, W., Li, Z., Ding, K., Huang, J., Nie, X., Zeng, G., ... & Liu, G. (2014). Effect of soil erosion on dissolved organic carbon redistribution in subtropical red soil under rainfall simulation. Geomorphology, 226, 217-225.

Macrellis, H. M., Trick, C. G., Rue, E. L., Smith, G., & Bruland, K. W. (2001). Collection and detection of natural iron-binding ligands from seawater. *Marine Chemistry*, *76*(3), 175-187.

Mak, M. S., & Lo, I. M. (2011). Influences of redox transformation, metal complexation and aggregation of fulvic acid and humic acid on Cr (VI) and As (V) removal by zero-valent iron. *Chemosphere*, *84*(2), 234-240.

Matilainen, A., Gjessing, E. T., Lahtinen, T., Hed, L., Bhatnagar, A., & Sillanpää, M. (2011). An overview of the methods used in the characterisation of natural organic matter (NOM) in relation to drinking water treatment. *Chemosphere*, *83*(11), 1431-1442.

Matilainen, A., & Sillanpää, M. (2010). Removal of natural organic matter from drinking water by advanced oxidation processes. *Chemosphere*, *80*(4), 351-365.

Matilainen, A., Vepsäläinen, M., & Sillanpää, M. (2010). Natural organic matter removal by coagulation during drinking water treatment: a review. *Advances in colloid and interface science*, *159*(2), 189-197.

Ma, X., Zhao, C., & Zhu, J. (2021). Aggravated risk of soil erosion with global warming–A global meta-analysis. Catena, 200, 105129.

Mayes, W. M., Gozzard, E., Potter, H. A. B., & Jarvis, A. P. (2008). Quantifying the importance of diffuse minewater pollution in a historically heavily coal mined catchment. Environmental Pollution, 151(1), 165-175.

McLauchlan, K. K., & Hobbie, S. E. (2004). Comparison of labile soil organic matter fractionation techniques. Soil Science Society of America

Journal, 68(5), 1616-1625.

Miller, C. J., Rose, A. L., & Waite, T. D. (2009). Impact of natural organic matter on H2O2-mediated oxidation of Fe (II) in a simulated freshwater system. Geochimica et cosmochimica Acta, 73(10), 2758-2768.

Morel, B., Durand, P., Jaffrézic, A., Gruau, G., & Molenat, J. (2009). Sources of dissolved organic carbon during stormflow in a headwater agricultural catchment. Hydrological Processes: An International Journal, 23(20), 2888-2901.

Mueller, B., & Hug, S. J. (2018). Climatic variations and de-coupling between arsenic and iron in arsenic contaminated ground water in the lowlands of Nepal. Chemosphere, 210, 347-358.

Mulholland, P. J. (2003). Large-scale patterns in dissolved organic carbon concentration, flux, and sources. In Aquatic ecosystems (pp. 139-159). Academic Press.

Neubauer, E., von der Kammer, F., Knorr, K. H., Peiffer, S., Reichert, M., & Hofmann, T. (2013). Colloid-associated export of arsenic in stream water during stormflow events. Chemical Geology, 352, 81-91.

Ni, M., Li, S., Santos, I., Zhang, J., & Luo, J. (2020). Linking riverine partial pressure of carbon dioxide to dissolved organic matter optical properties in a Dry-hot Valley Region. *Science of The Total Environment*, *704*, 135353.

Oregon.gov. (2017). *Iron (Fe) and Manganese (Mn) in Groundwater*. [online] Available at: http://www.oregon.gov/oha/PH/HEALTHYENVIRONMENTS/DRINKINGWATER/SOURCEWATER/Documents/gw/FeMnInGroundwater.pdf [Accessed 17 Dec. 2017].

Owa, F. D. (2013). Water pollution: sources, effects, control and management. *Mediterranean journal of social sciences*, *4*(8), 65.

Panton, A., Couceiro, F., Fones, G. R., & Purdie, D. A. (2020). The impact of rainfall events, catchment characteristics and estuarine processes on the export of dissolved organic matter from two lowland rivers and their shared estuary. Science of the Total Environment, 735, 139481.

Parra, F. R. (2019). Characterising natural organic matter in runoff from upland peatlands (Doctoral dissertation, The University of Manchester).

Parry, L. E., Holden, J., & Chapman, P. J. (2014). Restoration of blanket peatlands. Journal of environmental management, 133, 193-205.

Pawson, R. R., Lord, D. R., Evans, M. G., & Allott, T. E. H. (2008). Fluvial organic carbon flux from an eroding peatland catchment, southern Pennines, UK. Hydrology and Earth System Sciences, 12(2), 625-634.

Pawson, R. R., Rothwell, J. J., Daniels, S., Lord, D. R., Evans, M. G. E., & Allott, T. E. H. (2007). Fluvial organic carbon flux from an eroding peatland catchment, southern Pennines, UK. Hydrology and Earth System Sciences Discussions, 4(2), 719-745

Penru, Y., Simon, F. X., Guastalli, A. R., Esplugas, S., Llorens, J., & Baig, S. (2013). Characterization of natural organic matter from Mediterranean coastal seawater. Journal of Water Supply: Research and Technology—AQUA, 62(1), 42-51.

Pimentel, D., Berger, B., Filiberto, D., Newton, M., Wolfe, B., Karabinakis, E., ... & Nandagopal, S. (2004). Water resources: agricultural and environmental issues. BioScience, 54(10), 909-918.

Ratnaike, R. N. (2003). Acute and chronic arsenic toxicity. Postgraduate medical journal, 79(933), 391-396.

Ritson, J. P., Graham, N. J. D., Templeton, M. R., Clark, J. M., Gough, R., & Freeman, C. (2014). The impact of climate change on the treatability of dissolved organic matter (DOM) in upland water supplies: a UK perspective. *Science of the Total Environment*, *473*, 714-730.

Rose, A. L., & Waite, T. D. (2003). Kinetics of iron complexation by dissolved natural organic matter in coastal waters. Marine chemistry, 84(1-2), 85-103.

Rose, J., Vilge, A., Olivie-Lauquet, G., Masion, A., Frechou, C., & Bottero, J. Y. (1998). Iron speciation in natural organic matter colloids. Colloids and Surfaces A: Physicochemical and Engineering Aspects, 136(1-2), 11-19.

Rothwell, J. J., Evans, M. G., Daniels, S. M., & Allott, T. E. H. (2007). Baseflow and stormflow metal concentrations in streams draining contaminated peat moorlands in the Peak District National Park (UK). Journal of Hydrology, 341(1-2), 90-104.

Rothwell, J. J., Taylor, K. G., Ander, E. L., Evans, M. G., Daniels, S. M., & Allott, T. E. H. (2009). Arsenic retention and release in ombrotrophic

peatlands. Science of the Total Environment, 407(4), 1405-1417.

Rothwell, J. J., Taylor, K. G., Chenery, S. R., Cundy, A. B., Evans, M. G., & Allott, T. E. (2010). Storage and behavior of As, Sb, Pb, and Cu in ombrotrophic peat bogs under contrasting water table conditions. Environmental science & technology, 44(22), 8497-8502.

Rothwell, J. J., Taylor, K. G., Evans, M. G., & Allott, T. E. (2011). Contrasting controls on arsenic and lead budgets for a degraded peatland catchment in Northern England. Environmental pollution, 159(10), 3129-3133.

Roulet, N. T. (2000). Peatlands, carbon storage, greenhouse gases, and the Kyoto Protocol: Prospects and significance for Canada. Wetlands, 20(4), 605-615.

Sarmiento, A. M., Caraballo, M. A., Sanchez-Rodas, D., Nieto, J. M., & Parviainen, A. (2012). Dissolved and particulate metals and arsenic species mobility along a stream affected by Acid Mine Drainage in the Iberian Pyrite Belt (SW Spain). Applied geochemistry, 27(10), 1944-1952.

Santana-Casiano, J. M., González-Dávila, M., & Millero, F. J. (2005). Oxidation of nanomolar levels of Fe (II) with oxygen in natural

waters. Environmental science & technology, 39(7), 2073-2079.

Schlesinger, W. H. (1984). Soil organic matter: a source of atmospheric CO2. The role of terrestrial vegetation in the global carbon cycle: Measurement by remote sensing, 111, 127.

Schreiber, M. E., Gotkowitz, M. B., Simo, J. A., & Freiberg, P. G. (2003). Mechanisms of arsenic release to ground water from naturally occurring sources, eastern Wisconsin. In Arsenic in ground water (pp. 259-280). Springer, Boston, MA.

Schwartz, L., & Seeley, K. (2002). Introduction to tangential flow filtration for laboratory and process development applications. *Pall Scientific & Technical Report, PN*, *33213*.

Science.uwaterloo.ca. (2017). *Natural water*. [online] Available at: http://www.science.uwaterloo.ca/~cchieh/cact/applychem/waternatural.html [Accessed 14 Dec. 2017].

Sharma, P., Rolle, M., Kocar, B., Fendorf, S., & Kappler, A. (2011). Influence of natural organic matter on As transport and retention. Environmental science & technology, 45(2), 546-553.

Shen, M. H., Yin, Y. G., Booth, A., & Liu, J. F. (2015). Effects of molecular weight-dependent physicochemical heterogeneity of natural organic matter on the aggregation of fullerene nanoparticles in mono-and di-valent electrolyte solutions. Water research, 71, 11-20.

Simonovic, S. P. (2002). World water dynamics: global modeling of water resources. *Journal of Environmental Management*, *66*(3), 249-267.

Smedley, P. L., & Kinniburgh, D. G. (2001). Source and behaviour of arsenic in natural waters. United Nations synthesis report on arsenic in drinking water. World Health Organization, Geneva, Switzerland. http://www. who. int/water_sanitation_health/dwq/arsenicun1. pdf, 1-61.

Smedley, P. L., & Kinniburgh, D. G. (2002). A review of the source, behaviour and distribution of arsenic in natural waters. Applied geochemistry, 17(5), 517-568.

Sobczak, W. V., & Findlay, S. (2002). Variation in bioavailability of dissolved organic carbon among stream hyporheic flowpaths. Ecology, 83(11), 3194-3209

Solaiman, A. R. M., Meharg, A. A., Gault, A. G., & Charnock, J. M. (2009). Arsenic mobilization from iron oxyhydroxides is regulated by organic matter carbon to nitrogen (C: N) ratio. Environment international, 35(3), 480-484.

Stookey, L. L. (1970). Ferrozine---a new spectrophotometric reagent for iron. Analytical chemistry, 42(7), 779-781.

Taujale, S., Baratta, L. R., Huang, J., & Zhang, H. (2016). Interactions in ternary mixtures of MnO2, Al2O3, and natural organic matter (NOM) and the impact on MnO2 oxidative reactivity. Environmental science & technology, 50(5), 2345-2353.

Templier, J., Derenne, S., Croué, J. P., & Largeau, C. (2005). Comparative study of two fractions of riverine dissolved organic matter using various analytical pyrolytic methods and a 13 C CP/MAS NMR approach. *Organic Geochemistry*, *36*(10), 1418-1442.

Theis, T. L., & Singer, P. C. (1974). Complexation of iron (II) by organic matter and its effect on iron (II) oxygenation.*Environmental Science & Technology*, *8*(6), 569-573.

Todman, M. (2005). Controls on Water Chemistry in an Upland Catchment.

The University of Manchester (United Kingdom).

Tranvik, L. J., Downing, J. A., Cotner, J. B., Loiselle, S. A., Striegl, R. G., Ballatore, T. J., ... & Weyhenmeyer, G. A. (2009). Lakes and reservoirs as regulators of carbon cycling and climate. Limnology and oceanography, 54(6part2), 2298-2314.

Tufekci, N., Demir, G., Ozgul, G., & Kinaci, C. (2003). The effect of organic matters on ferrous oxidation. *Fresenius Environmental Bulletin*, *12*(7), 771-775.

van de Wiel, H. J. (2003). Determination of elements by ICP-AES and ICP-MS. National Institute of Public Health and the Environment (RIVM). Bilthoven, The Netherlands, 1-19.

Vaughan, M. C., Bowden, W. B., Shanley, J. B., Vermilyea, A., & Schroth, A. W. (2019). Shining light on the storm: in-stream optics reveal hysteresis of dissolved organic matter character. Biogeochemistry, 143(3), 275-291.

Verma, P., Agarwal, A., & Singh, V. K. (2014). Arsenic removal from water through adsorption-A Review. Recent Research in Science and Technology, 6(1).

Vignati, D., & Dominik, J. (2003). The role of coarse colloids as a carrier phase for trace metals in riverine systems. Aquatic sciences, 65(2), 129-142.

Viollier, E., Inglett, P. W., Hunter, K., Roychoudhury, A. N., & Van Cappellen, P. (2000). The ferrozine method revisited: Fe (II)/Fe (III) determination in natural waters. *Applied geochemistry*, *15*(6), 785-790.

Volk, C., Wood, L., Johnson, B., Robinson, J., Zhu, H. W., & Kaplan, L. (2002). Monitoring dissolved organic carbon in surface and drinking waters. Journal of environmental monitoring, 4(1), 43-47.

Von Der Heyden, B. P., Hauser, E. J., Mishra, B., Martinez, G. A., Bowie, A. R., Tyliszczak, T., ... & Myneni, S. C. (2014). Ubiquitous presence of Fe (II) in aquatic colloids and its association with organic carbon. Environmental Science & Technology Letters, 1(10), 387-392.

Vosylienė, M. Z., & Mikalajūnė, A. (2006). Effect of heavy metal model mixture on rainbow trout biological parameters. *Ekologija*, (4), 12-17.

Vuori, K. M. (1995, January). Direct and indirect effects of iron on river ecosystems. In *Annales Zoologici Fennici* (pp. 317-329). Finnish Zoological and Botanical Publishing Board.

Waite, T. D., & Morel, F. M. (1984). Photoreductive dissolution of colloidal iron oxides in natural waters. Environmental science & technology, 18(11), 860-868.

Walling, D. E., & Webb, B. W. (1985). Estimating the discharge of contaminants to coastal waters by rivers: some cautionary comments. Marine Pollution Bulletin, 16(12), 488-492.

Wang, S., & Mulligan, C. N. (2006). Occurrence of arsenic contamination in Canada: sources, behavior and distribution. Science of the total Environment, 366(2-3), 701-721.

Wang, S., & Mulligan, C. N. (2009). Effect of natural organic matter on arsenic mobilization from mine tailings. Journal of Hazardous Materials, 168(2-3), 721-726.

Weber, T., Allard, T., & Benedetti, M. F. (2006). Iron speciation in interaction with organic matter: Modelling and experimental approach. *Journal of Geochemical Exploration*, *88*(1-3), 166-171.

Wen, L. S., Santschi, P., Gill, G., & Paternostro, C. (1999). Estuarine trace metal distributions in Galveston Bay: importance of colloidal forms in the

speciation of the dissolved phase. Marine Chemistry, 63(3-4), 185-212

WHO, G. (2011). Guidelines for drinking-water quality. World Health Organization, 216, 303-304.

Willey, J. D., Kieber, R. J., Eyman, M. S., & Avery Jr, G. B. (2000). Rainwater dissolved organic carbon: concentrations and global flux. Global Biogeochemical Cycles, 14(1), 139-148.

Wolthoorn, A., Temminghoff, E. J., Weng, L., & van Riemsdijk, W. H. (2004). Colloid formation in groundwater: effect of phosphate, manganese, silicate and dissolved organic matter on the dynamic heterogeneous oxidation of ferrous iron. *Applied Geochemistry*, *19*(4), 611-622.

Worrall, F., & Burt, T. (2005). Predicting the future DOC flux from upland peat catchments. Journal of Hydrology, 300(1-4), 126-139.

Worrall, F., Burt, T., Adamson, J., Reed, M., Warburton, J., Armstrong, A., & Evans, M. (2007). Predicting the future carbon budget of an upland peat catchment. Climatic Change, 85(1), 139-158.

Worrall, F., Burt, T. P., Jaeban, R. Y., Warburton, J., & Shedden, R. (2002).

Release of dissolved organic carbon from upland peat. Hydrological Processes, 16(17), 3487-3504.

Worrall, F., Rowson, J. G., Evans, M. G., Pawson, R., Daniels, S., & Bonn, A. (2011). Carbon fluxes from eroding peatlands–the carbon benefit of revegetation following wildfire. Earth Surface Processes and Landforms, 36(11), 1487-1498.

Wu, H., Xingkai, X., Cheng, W., & Lin, H. (2020). Dissolved organic matter and inorganic N jointly regulate greenhouse gases fluxes from forest soils with different moistures during a freeze-thaw period. *Soil Science and Plant Nutrition*, *66*(1), 163-176.

Yan, M., Korshin, G., Wang, D., & Cai, Z. (2012). Characterization of dissolved organic matter using high-performance liquid chromatography (HPLC)–size exclusion chromatography (SEC) with a multiple wavelength absorbance detector. Chemosphere, 87(8), 879-885.

Zhang, Y., Chen, Y., Westerhoff, P., & Crittenden, J. (2009). Impact of natural organic matter and divalent cations on the stability of aqueous nanoparticles. *Water research*, *43*(17), 4249-4257.

Zhang, Y., Zhang, X., Bi, Z., Yu, Y., Shi, P., Ren, L., & Shan, Z. (2020). The impact of land use changes and erosion process on heavy metal distribution in the hilly area of the Loess Plateau, China. Science of The Total Environment, 718, 137305

Zularisam, A. W., Ismail, A. F., & Salim, R. (2006). Behaviours of natural organic matter in membrane filtration for surface water treatment—a review. *Desalination*, *194*(1-3), 211-231.